NATIONAL ACADEMY OF SCIENCES OF UKRAINE
Palladin Institute of Biochemistry

BIOTECHNOLOGIA ACTA

2025
Vol. 18, no. 2

BIMONTHLY

Editorial address:
Palladin Institute of Biochemistry of the NAS of Ukraine, 9, Leontovich Street, Kyiv, 01054, Ukraine;
Tel.: +380 44 235 1472; ***E-mail:*** biotech@biochem.kiev.ua; ***Web-site*****:** www.biotechnology.kiev.ua

According to the resolution of the Presidium of the National Academy of Sciences of Ukraine from 27.05.2009 №1-05 / 2 as amended on 25.04.2013 number 463 Biotechnologia Acta has been included in High Attestation Certification Commission list of Ukraine for publishing dissertations on specialties "Biology" and "Technology".

Certificate of registration of print media КВ series №19650-9450ПР on 01.30.2013
Literary editor — H. **Shevchenko;** Computer-aided makeup — **O. Melezhyk**
Authorized for publishing 2025/04/30

NATIONAL ACADEMY OF SCIENCES OF UKRAINE
Palladin Institute of Biochemistry

BIOTECHNOLOGIA ACTA

Scientific journal

2025
Vol. 18, no. 2

International Conference of Young Scientists "CURRENT PROBLEMS OF BIOCHEMISTRY AND BIOTECHNOLOGY – 2025"

REVIEWS

EXPERIMENTAL WORKS

UDC 612.8:616.831-009.11:575.113 https://doi.org/10.15407/biotech18.02.007

HIPSC-DIFFERENTIATED DOPAMINERGIC NEURONS ARE A USEFUL TOOL FOR STUDYING THEIR NEUROPHYSIOLOGY AND MATURATION

O. PAVLOVA[1, 2], *L. VANDRIES*[2], *V. SEUTIN*[2]

[1]Palladin Institute of Biochemistry of the National Academy of Sciences of Ukraine, Kyiv
[2]Laboratory of Neurophysiology, GIGA-Neurosciences, University of Liege, Belgium

E-mail:aspavlova92@gmail.com

Received 2025/03/09
Revised 2025/03/13
Accepted 2025/04/30

Dopaminergic (DA) neurons play a crucial role in motor control, motivation, and cognition, with their degeneration in Parkinson's disease leading to severe motor deficits. While rodent models are widely used, species-specific differences necessitate human-relevant models.

Aim. This study investigates the functional maturation of DA neurons derived from human induced pluripotent stem cells (IPS).

Methods. DA differentiation was performed using a mCherry-based TH reporter iPS line. Immunocytochemistry confirmed neuronal identity, while patch-clamp recordings assessed electrophysiological properties, including firing rate, action potential duration, Ih current, and dopamine sensitivity.

Results. TH expression was detected from day 10, reaching 64% by day 30. Electrophysiological maturation followed a distinct timeline, with spontaneous activity emerging around day 20 and stable pacemaking developing by day 40, along with D2 receptor-mediated autoinhibition.

Conclusions. Our findings demonstrate that hIPSC-derived DA neurons attain an adult-like profile by day 40, making them a viable model for studying Parkinson's disease mechanisms and testing potential therapies. Further research will focus on slow pacemaking mechanisms in these neurons.

Keywords: Dopaminergic neurones, human induced pluripotent stem cells, electrophysiology, pacemaking, Parkinson's disease.

Dopaminergic (DA) neurons are essential for modulating motor control, motivation, and various cognitive functions. Predominantly located in the substantia nigra pars compacta and the ventral tegmental area, these neurons (at least part of them) undergo progressive degeneration in Parkinson's disease, resulting in severe motor deficits1. While rodent models are widely used to study DA neurobiology, species-specific differences limit the direct translation of findings to humans2. Consequently, investigating the electrophysiological and functional properties of DA

Citation: Pavlova, O., Vandries, L., Seutin, V. (2025). hIPSC-differentiated dopaminergic neurons are a useful tool for studying their neurophysiology and maturation. *Biotechnologia Acta*, 18(2), 7–9. https://doi.org/10.15407/biotech18.02.007

neurons derived from human induced pluripotent stem cells (IPS) represents a crucial strategy for advancing our understanding of their physiology and potential therapeutic interventions to prevent their degeneration.

Aim. This work aims to investigate the changes in the functional activity of human DA neurons in the process of its differentiation from hIPSC.

Methods. Differentiation of DA from mCherry-based human TH reporter iPS line was performed according to a published protocol 3 with minor changes. The DA profile of neurons in the process of maturation was confirmed by immunocytochemistry as described earlier 4 with the use of TH (Merck, AB152), βIII tubulin/ TUJ1 (BioLegend, MMS-435P) antibodies. For functional aspects, patch clamp recordings were performed, as described in Borgs et al.4 and Seutin, 20215. SNc DA neurons were identified and assessed based on their electrophysiological properties, including low frequency of firing (0.5–5 Hz), AP duration (width at half-amplitude > 1.35 ms), the presence of a strong hyperpolarization-activated inward current (Ih) and sensitivity to dopamine (100 µM) (hyperpolarization > 5 mV from -60 mV).

Results and Discussion. We found that cells that expressed βIII tubulin/ TUJ1 start expressing TH from day 10 of terminal differentiation (TD), and the percentage progressively increases to 64%

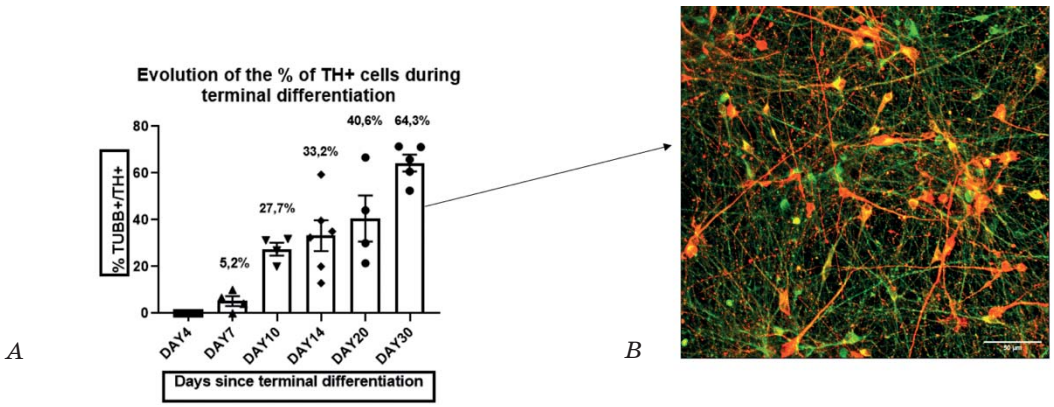

Fig. 1. **(*A*) Percentage of TUBB/TH ratio on day 4, 7, 10, 14, 20, 30 of terminal differentiation of dopaminergic neurons (*n* = 4). (*B*) — immunocytochemistry of neurons on day 30 of terminal differentiation TUBB(green)/TH(red)**

Bar = 50µm

by TD 30 (Fig. 1).

Regarding electrophysiological maturation, the ability to evoke action potentials appeared on days 10–14 of TD, as did the Ih current. After TD 20, cells demonstrated irregular spontaneous activity. At the same time, after TD 40, they had stable pacemaking activity both in the "on-cell" mode (Fig. 2) and in the "whole-cell" mode, which was reversibly blocked by 100 µM dopamine (Fig. 3), which indicates the presence of somatodendritic D2-type receptors. Activation of these receptors by dendritically released dopamine leads to a hyperpolarization mediated by GIRK-type K+ channels and is a hallmark of DA neurons. The coefficient of variation for firing was CV = 0.18; all together, this corresponds to a mature DA profile.

Conclusions. In this study, we characterized the maturation of dopaminergic neurons during their differentiation from human-induced stem cells. We obtained a relatively high percentage of

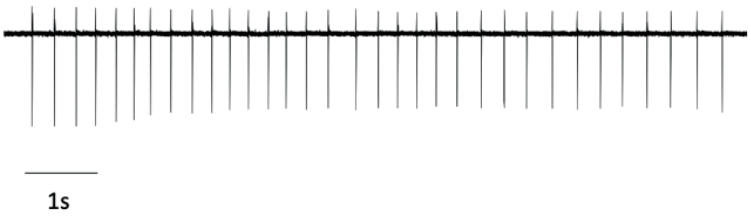

Fig. 2. **Representative cell-attached recording of a spontaneous firing dopaminergic neuron on day 49 of terminal differentiation**

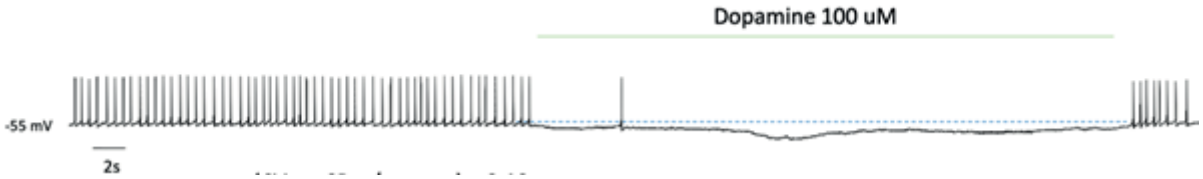

Fig. 3. **Representative recording showing that the firing of a DA neuron is reversibly inhibited by 100 µM dopamine**

TH-positive neurons. We showed that after day 40 of terminal differentiation, they have an adult profile (Ih current, stable regular pacemaking, and the presence of D2 receptors, which is confirmed by the reversible autoinhibition by 100 µM dopamine). Our results demonstrate that hIPS-induced dopaminergic neurons are a viable model for research and, in the future, may be used in a cellular model of Parkinson's disease both for understanding the mechanisms of pathology development and for finding preventive or therapeutic drugs. In addition, this model will be used to investigate further the mechanism of slow pacemaking of these cells, which is a current focus of the lab.

Authors' contribution

OP and LV worked on the cell culture; OP performed the electrophysiological recordings, LV performed ICC, and VS wrote the project and supervised the work. OP, LV, and VS analyzed the data.

Funding source

The work was supported by the FNRS ("Research Project") for project: "Identification of the generator of pacemaking in midbrain dopaminergic neurons and evaluation of its plasticity" 2022–2025 (contract T.0188.22 to VS) and grant from the University of Liège ("Crédits d'opportunit stratégique"), Project : "Vers l'identification du mécanisme de pacemaking lent dans les cellules excitables", 2025–26 (to VS)

REFERENCES

1. Michel, P. P., Hirsch, E. C., Hunot, S. (2016). Understanding Dopaminergic Cell Death Pathways in Parkinson Disease. *Neuron.*, 90(4), 675–691. https://doi.org/10.1016/j.neuron.2016.03.038
2. Potashkin, J. A., Blume, S. R., Runkle, N. K. (2011). Limitations of Animal Models of Parkinson's Disease. *Parkinsons Dis.*, 1–7. https://doi.org/10.4061/2011/658083
3. Stathakos, P., Jimenez-Moreno, N., Crompton, L., Nistor, P., Caldwell, M. A., Lane, J. D. (2019). Imaging Autophagy in hiPSC-Derived Midbrain Dopaminergic Neuronal Cultures for Parkinson's Disease Research. In: Ktistakis, N., Florey, O. (Eds.) Autophagy. *Methods in Molecular Biology*, 1880. Humana Press, New York, NY. 257–280. https://doi.org/10.1007/978-1-4939-8873-0_17
4. Borgs, L., Peyre, E., Alix, P., Hanon, K., Grobarczyk, B., Godin, J. D., Purnelle, A., Krusy, N., ..., Nguyen, L. (2016). Dopaminergic neurons differentiating from LRRK2 G2019S induced pluripotent stem cells show early neuritic branching defects. *Sci. Rep.*, 6(1), 33377. https://doi.org/10.1038/srep33377
5. Seutin, V. (2021). Electrophysiological Quality Control of Human Dopaminergic Neurons: Are We Doing Enough? *Front Cell Neurosci.*, 15. https://doi.org/10.3389/fncel.2021.715273

UDC 577.112.7:616 **https://doi.org/10.15407/biotech18.02.010**

THE MULTIFACETED ROLE OF ENDOPLASMIC RETICULUM STRESS IN THE REGULATION OF GENE EXPRESSION IN NORMAL ASTROCYTES AND GLIOBLASTOMA CELLS

O.V. RUDNYTSKA, M.Y. SLIUSAR, Y.V. KULISH

Palladin Institute of Biochemistry of NAS of Ukraine, Kyiv

E-mail: olga_rudnytska@ukr.net

Received 2025/03/04
Revised 2025/03/14
Accepted 2025/04/30

Aim. To determine the role of the endoplasmic reticulum (ER) in regulating gene expression in normal astrocytes and glioblastoma cells under the application of carbon nanoparticles as anti-tumor agents and inhibition of ERN1 (endoplasmic reticulum to nucleus signaling 1).

Methods. Aqueous dispersions of graphene oxide (GO) and aqueous suspensions of single-walled carbon nanotubes (SWCNTs) were used to study the impact of carbon nanoparticles. Experiments were conducted on regular human astrocytes line NHA/TS and U87MG glioblastoma cells. Two sublines of ERN1 knockdown cells were applied to determine the role of ERN1 in the control of gene expression. Quantitative RT-PCR detected the expression level of mRNA and microRNA.

Results. It was shown that GO and SWCNTs affect the expression of numerous regulatory genes in both normal human astrocytes and glioblastoma cells, but the effect was less pronounced in glioblastoma cells than in normal astrocytes and preferentially mediated by ERN1. The expression of serine biosynthesis genes is controlled by ERN1 protein kinase or endoribonuclease activity. Furthermore, the inhibition of functional activity of ERN1 modifies the effects of hypoxia on gene expression.

Conclusions. Thus, these results demonstrated that ER stress plays an essential role in controlling the expression of various regulatory genes in glioblastoma cells and that normal astrocytes are more sensitive to the effect of carbon nanoparticles than glioblastoma cells.

Keywords: ER stress, carbon nanoparticles, mRNA and microRNA expression, DNAJB9, serine synthesis genes, glioblastoma cells, normal astrocytes.

Endoplasmic reticulum (ER) stress is an essential factor in the development of many pathological conditions, including the growth of malignant tumors, as well as various complications due to the action of nanoparticles. Previous studies have shown that inhibition of ERN1 (endoplasmic reticulum to nucleus signaling 1), a key sensor in the ER stress response, suppressed glioma cell proliferation and decreased the effect of nanoparticles. The exact mechanisms of this influence remain poorly understood, but a possible pathway for their action may involve the recruitment of both protein kinase and endoribonuclease activity of ERN1 signaling protein. Moreover, ER stress is responsible for nanoparticle toxicity as well as for regulation of the expression of pro-oncogenic gene expression.

Aim. To investigate the comparative effects of carbon nanoparticles on the expression of key regulatory genes in normal astrocytes and glioblastoma cells and find out the molecular mechanism of regulation of serine synthesis gene expression in glioblastoma cells with different ERN1 knockdowns.

Methods. Experiments were conducted on U87MG glioblastoma cells and their sublines with different ERN1 knockdown and regular human astrocytes line NHA/TS. Aqueous dispersions of

Citation: Rudnytska, O. V., Sliusar, M. Y., Kulish, Y. V. (2025). The multifaceted role of endoplasmic reticulum stress in the regulation of gene expression in normal astrocytes and glioblastoma cells. *Biotechnologia Acta*, 18(2), 10–13. https://doi.org/10.15407/biotech18.02.010

graphene oxide (GO) and aqueous suspensions of single-walled carbon nanotubes (SWCNTs) were used to study the impact of carbon nanoparticles. The measurement of mRNA and microRNA expression levels was carried out using quantitative real-time polymerase chain reaction.

Results and Discussion. Our studies indicate that even small doses of graphene oxide (1 and 4 ng/mL) and SWCNTs (2 and 8 ng/mL) disrupt the expression of numerous regulatory genes in regular human astrocytes line NHA/TS [1–4]. Thus, the treatment of normal human astrocytes with GO nanoparticles in a dose of 1 ng/ml of medium) introduced a substantial increase in *DNAJB9* (heat shock protein family member B9 DnaJ) gene expression (by 126%, $P < 0.001$) as compared to the control [1]. A much stronger effect on the expression of *the DNAJB9* gene (203%, $P < 0.001$) was observed when using a bigger dose (1 ng/ml of medium) of these nanoparticles [1].

At the same time, the effect of GO nanoparticles on the expression of this gene was significantly lower (+41%, $P < 0.01$, and +82%, $P < 0.001$, respectively, for 1 and 4 ng/ml of nanoparticles) in glioblastoma cells with native ERN1 (Figure). It is interesting to note that the knocking down of ERN1 signaling protein in U87MG glioblastoma cells reduced the effect of these nanoparticles on *DNAJB9* gene expression close to a control level [1]. Similar results were shown for genes encoded transcription factors ATF3 and ATF4 [1]. These results demonstrated that the expression of different genes in normal astrocytes is more sensitive to GO nanoparticles than glioblastoma cells and that the effect of these nanoparticles is mainly mediated by ERN1 signaling protein, a major signaling pathway of ER stress. Thus, the impact of GO nanoparticles on different gene expressions is dose-dependent and gene-specific in both normal astrocytes and glioblastoma cells. Moreover, the gene specificity of the action of these nanoparticles is determined mainly by ER stress [1]. These carbon nanoparticles also affect microRNA expression levels, which have binding sites with target mRNAs, indicating the presence of post-transcriptional regulatory mechanisms for these genes [2].

It was also found that carbon nanotubes affect the expression of numerous genes in normal human astrocytes and glioblastoma cells. It was shown a more pronounced increase in the expression level of *BRCA1* (breast cancer type 1 susceptibility protein) and *DNAJB9* in normal cells [4]. Suppression of ERN1 signaling protein in glioblastoma cells decreased the effect of SWCNTs, thereby confirming the role of ER stress in affecting these gene expressions by carbon nanoparticles [4]. Furthermore, the treatment of normal human astrocytes with carbon nanotubes significantly affects the expression level of numerous microRNAs, which have binding sites with target mRNAs, indicating the possibility of a post-transcriptional mechanism for the regulation of studied gene expressions [3].

It has been shown that the expression level of genes responsible for serine synthesis was generally decreased in glioblastoma cells with inhibited both enzymatic activities of the ERN1, except *SHMT1* (serine hydroxymethyltransferase 1) gene, whose expression was sharply increased [5]. At the same time, the suppression of ERN1 endoribonuclease activity affects the expression of the *ATF4* (activating transcription factor 4) gene but does not significantly change the expression of *PHGDH* (phosphoglycerate dehydrogenase), *SHMT1*, and *SHMT2* genes. These results demonstrate that the expression of the *ATF4* gene is controlled by ERN1 endoribonuclease activity and that the expression of *PHGDH, SHMT1*, and *SHMT2* genes is regulated by ERN1 protein kinase activity [5]. It was also shown that silencing of XBP1 (X-box binding protein 1) by specific siRNA also suppresses only *ATF4* gene expression in glioblastoma cells. Still, silencing of ERN1 by specific siRNA decreases the expression of *PHGDH, SHMT2,* and *ATF4* genes. silencing of ERN1 by specific siRNA decreases the expression of *PHGDH, SHMT2,* and *ATF4* genes. At the same time, silencing of ERN1 strongly increases the expression of *SHMT1* [5].

The inhibition of ERN1 signaling protein also affects the expression of several microRNA expressions, which is responsible for post-transcriptional control of serine synthesis mRNA expressions in glioblastoma cells and possibly contributes to the suppression of these cell proliferation [5].

The significant results of analyzed data concerning the multifaceted role of ER stress in the regulation of gene expression in normal astrocytes and glioblastoma cells are summarized in Fig.

Conclusions. Changes in gene expression induced by graphene oxide nanoparticles and single-walled carbon nanotubes are mainly associated with the induction of ER stress and alterations in microRNA expression, which are key regulators of ER homeostasis and critical players in UPR (unfolded protein response) signaling. These changes are gene-specific and depend on ER stress because the inhibition of ERN1 significantly modifies the effects of carbon nanoparticles on the expression of studied genes. Meanwhile, normal human astrocytes are more sensitive to both graphene oxide nanoparticles and SWCNTs exposure compared to glioblastoma cells in a dose-

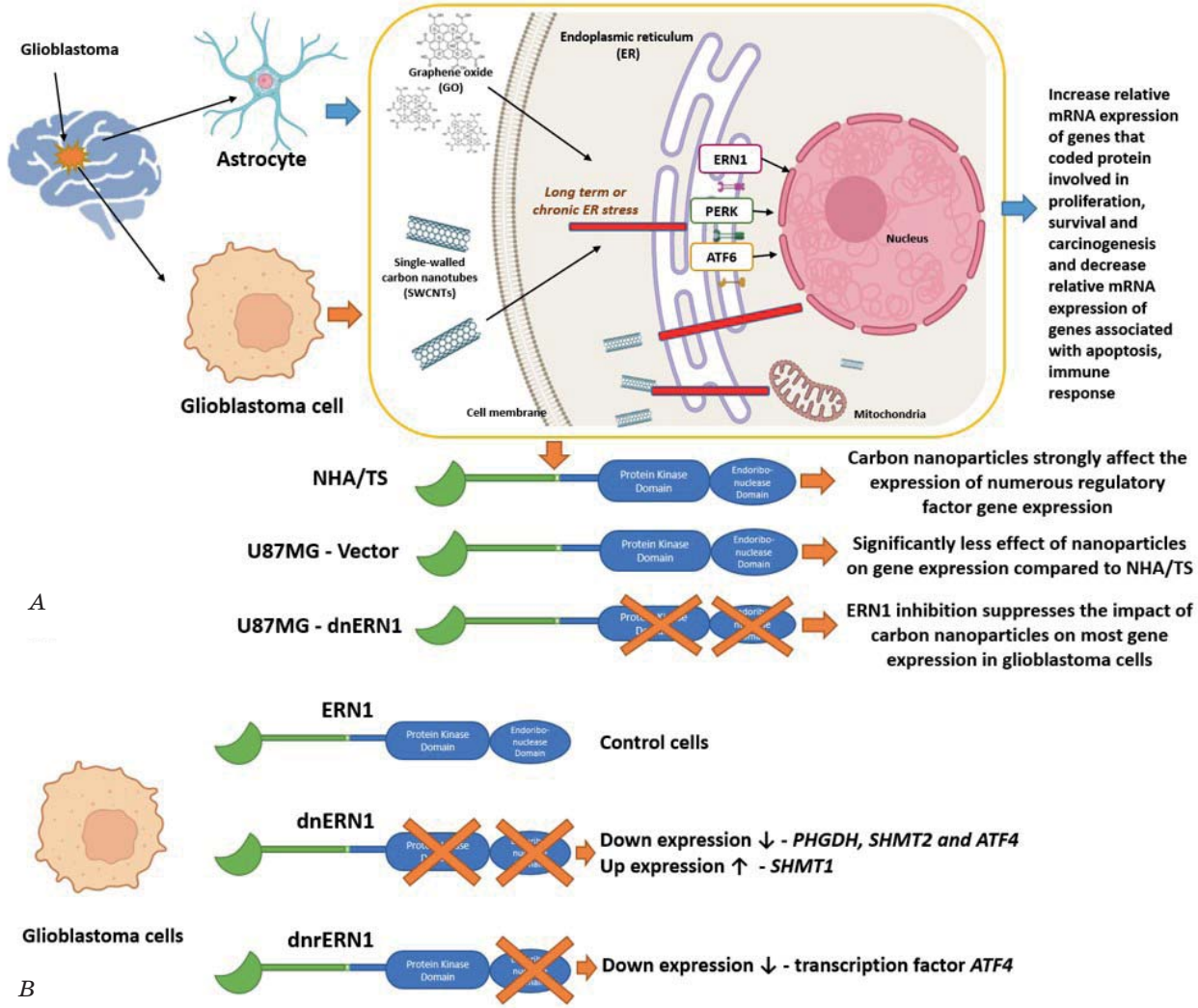

Figure. A — **Effect of ERN1 enzymatic activities on the expression level of genes in U87MG glioblastoma cells with suppressed both enzymatic activities (endoribonuclease and protein kinase) of ERN1 (dnERN1) and in cells without only endoribonuclease activity of ERN1 (dnrERN1) compared to control cells transfected with "empty" vector; *B* — Schematic representation of the effect of carbon nanoparticles on the expression level of genes associated with proliferation and survival processes in normal human astrocytes line NHA/TS, U87 glioblastoma cells transfected with a vector (U87-Vector) and cells with a dominant-negative ERN1 construct (U87-dnERN1)**

dependent manner, which is likely due to the tumor cell resistance to various external factors. This serves as a cautionary point regarding the biomedical applications of carbon nanoparticles. It has been established that the protein kinase activity of ERN1 is an essential regulator of serine biosynthesis gene expression, such as *PHGDH*, *SHMT1*, and *SHMT2* genes. At the same time, the ERN1 endoribonuclease activity controls the level of ATF4 gene expression.

Authors' Contribution
The authors contributed to the experimental work equally.

Funding source
The State Budget Program (Code: 6541030).

REFERENCES

1. Minchenko, O. H., Kulish, Y. V., Viletska, Y. M., Khita, O. O., Rudnytska, O. V., Kozynkevych, H. E., Minchenko, D. O. (2024). The expression of DNAJB9 in normal human astrocytes is more sensitive to nanographene oxide than in glioblastoma cells. *Endocr. Regul.*, 58(4), 242–251. https://doi.org/10.2478/enr-2024-0029.
2. Rudnytska, O. V., Kulish, Y. V., Khita, O. O., Minchenko, D. O., Tsymbal, D. O., Viletska, Y. M., Sliusar, M. Y., Trufanova, D. D., Minchenko, O. H. (2022). Exposure to nanographene oxide induces gene expression dysregulation in normal human astrocytes. *Endocr. Regul.*, 56(3), 216–226. https://doi.org/10.2478/enr-2022-0023.
3. Rudnytska, O. V., Khita, O. O., Minchenko, D. O., Tsymbal, D. O., Yefimova, Y. V., Sliusar, M. Y., Minchenko, O. (2021). The low doses of SWCNTs affect the expression of proliferation and apoptosis related genes in normal human astrocytes. *Current research in toxicology*, 2, 64–71. https://doi.org/10.1016/j.crtox.2021.02.001.
4. Minchenko, D. O., Rudnytska, O. V., Khita, O. O., Kulish, Y. V., Viletska, Y. M., Halkin, O. V., Danilovskyi, S. V., Ratushna, O. O., Minchenko, O. H. (2023). Expression of DNAJB9 and some other genes is more sensitive to SWCNTs in normal human astrocytes than glioblastoma cells. *Endocr. Regul.*, 57(1), 162–172. https://doi.org/10.2478/enr-2023-0020.
5. Minchenko, O. H., Sliusar, M. Y., Khikhlo, Y. P., Halkin, O. V., Viletska, Y. M., Khita, O. O., Minchenko, D. O. (2024). Knockdown of ERN1 disturbs the expression of phosphoserine aminotransferase 1 and related genes in glioblastoma cells. *Archives of biochemistry and biophysics*, 759, 110104. https://doi.org/10.1016/j.abb.2024.110104.

EXPERIMENTAL WORKS

UDC 615.471 https://doi.org/10.15407/biotech18.02.014

COLLAGEN MATRIX WITH INCREASED HEMOSTATIC PROPERTIES: COMPARATIVE ANALYSIS OF HEMOSTATIC EFFICACY

K.B. BAIDAKOVA[1, 2], *Y.P. KUCHERYAVYI*[1], *D.S. KOROLOVA*[1]

[1]Palladin Institute of Biochemistry of the National Academy of Sciences of Ukraine, Kyiv
[2] Educational and Scientific Center "Institute of Biology and Medicine" of Taras Shevchenko National University of Kyiv, Ukraine

E-mail: katrinbaidakova@gmail.com

Received 2025/02/21
Revised 2025/03/06
Accepted 2025/04/30

Aim. To develop collagen matrices with increased hemostatic properties and to evaluate their effectiveness in comparison with commercial products.

Methods. Collagen was obtained from calfskin by acid hydrolysis, identified by SDS-PAGE, and sterilized in an autoclave. The enzymatic clotting activator was purified from *Echis multisquamatis* venom by ion exchange chromatography. The activity of the activator was evaluated with the chromogenic substrate S2302. Ready-made modified matrices were obtained by lyophilization. Hemostatic efficacy was tested in the Wistar Han rat hepatic hemorrhage model, compared with commercial materials.

Results. Optimal concentrations of collagen (300 μg/cm^2) and enzyme activator (10 μg/cm^2) were selected for the manufacture of collagen matrices with increased hemostatic properties. Studies on the rat parenchymal bleeding model showed that these matrices provide faster bleeding control compared to commercial hemostatic materials. After the removal of collagen matrices, bleeding did not resume.

Conclusions. The developed collagen matrices with increased hemostatic properties demonstrate high efficiency, stable clot formation, and minimal risk of rebleeding, which confirms their prospects in surgery.

Keywords: collagen matrix, enzyme activator, haemostatic materials, comparison.

Uncontrolled bleeding remains one of the leading causes of trauma-related deaths in both military and civilian settings. A significant proportion of fatalities occur before patients arrive at the hospital or within the first hour of injury. This underscores the critical importance of effective hemostatic materials that can quickly stop bleeding and reduce the risk of complications [1]. Modern hemostatic agents such as coagulants, chemical agents, and physical barriers all have their advantages, but none of them is a one-size-fits-all solution.

Collagen matrices are a perspective material for stopping bleeding due to their biocompatibility and ability to stimulate platelet adhesion and promote blood clotting. However, standard collagen

Citation: Baidakova, K. B., Kucheryavyi, Y. P., Korolova, D. S. (2025). Collagen matrix with increased hemostatic properties: comparative analysis of hemostatic efficacy. *Biotechnologia Acta*, 18(2), 14–16. https://doi.org/10.15407/biotech18.02.014

matrices have certain limitations which necessitate their modification. One of the promising approaches is to add specific clotting activators to the matrices, which can accelerate clot formation and improve the material's effectiveness [2]. In this study, we used a prothrombin activator that acts exclusively on the final stage of blood clotting. This not only enhances the hemostatic effect of the material but also makes it more controlled and safer.

This study aimed to develop and comparatively analyze the effectiveness of collagen matrix with increased hemostatic properties with commercial hemostatic materials.

Methods. Collagen was isolated from calfskin by acid hydrolysis, characterized by SDS-PAGE, and sterilized by autoclaving (134 °C, 210 kPa, 35 minutes). The absence of gram-negative and gram-positive microorganisms and yeast assessed sterility. The enzymatic blood coagulation activator (EA) was purified from *Echis multisquamatis* venom by ion-exchange chromatography. The activity of the enzyme activator in combination with collagen matrices and the quality of immobilization was evaluated using the chromogenic substrate S2302 (HD-Pro-Phe-Arg-pNA×2HCl). Modified collagen matrices were prepared by lyophilization using the LyoQuest Telstar system. The hemostatic efficacy was assessed in a rat model of liver bleeding by comparing it with commercial hemostatic materials, including the hemostatic gelatin sponge 'CUTANPLAST Dental' (Mascia Brunelli, Italy) [3], corrugated hemostatic bandage 'HEMOSTATIC' (Senta Pharm, Ukraine) and hydrogel bandage 'HYDROBYNT №1' (V-CUBE, Ukraine) [4]. The comparison was performed by the time of stopping bleeding, the amount of blood loss, and the resumption of bleeding after the removal of the hemostatic agent. Local tolerability was assessed in Wistar Han rats by subcutaneous implantation in accordance with ISO 10993-6:2011.

Results. The study involved the development of collagen matrix with increased hemostatic properties, optimizing their composition to achieve maximum effectiveness. Several variants of collagen content were tested (100, 200, 300, 400 and 500 μg/cm^2). Analysis of the physicochemical properties showed that a concentration of 300 μg/cm^2 provides good mechanical strength, flexibility, and biodegradability. At lower concentrations, the structure of the matrices was too delicate, while higher values resulted in excessive density, which made it difficult to adapt them to the wound surface.

We also examined the effect of different concentrations of the enzyme activator (4, 8, 10 and 16 μg/cm^2). The optimization of the concentration of the enzyme activator allowed us to establish that the most effective value was 10 μg/cm^2. Lower concentrations did not provide sufficient activation of prothrombin, which slowed down the process of blood clot formation. At the same time, no significant improvement in efficacy was observed when the concentration exceeded 10 μg/unit. Still, there was a risk of excessive release of the activator into the general bloodstream.

The study of the stability of the activator immobilization showed that in the buffer solution, the release of the enzyme from the matrices was less than 10%. In the blood plasma, its diffusion from the clot was less than 5%. This indicates the effective immobilization of the activator in the collagen structure and its controlled release at the site of injury.

Collagen matrices 3×3 cm in size and weighing 3 mg were prepared and modified with the enzyme activator. Microbiological testing confirmed their sterility, and subcutaneous implantation testing showed good local tolerance.

We compared the hemostatic effectiveness of collagen matrix with increased hemostatic properties with the hemostatic gelatin sponge 'CUTANPLAST Dental', corrugated hemostatic bandage 'HEMOSTATIC,' and hydrogel bandage 'HYDROBYNT №1' in a rat parenchymal liver bleeding model (Fig.). The study included a comparison of the bleeding time after the usage of different hemostatic agents, measurement of blood loss, and whether bleeding resumed after the removal of the hemostatic material from the wound surface.

Experimental results have shown that collagen matrices modified with an enzyme activator provide bleeding control in an average of 20 seconds. This is faster than when using 'CUTANPLAST Dental,' 'HYDROBYNT No 1', and 'HEMOSTATIC,' for which the stopping time was longer. In all cases of use of modified collagen matrices, there was no rebleeding after their removal.

Discussion. The developed collagen matrix with increased hemostatic properties has a significant potential for use in clinical practice. The combination of biocompatibility, biodegradability, and active influence on the blood coagulation system makes them a promising solution for local hemostasis. Their use can be particularly useful in surgery, traumatology, and emergency medicine, where fast and reliable bleeding control is critical.

Unlike many traditional hemostatic materials, collagen matrices modified with an enzyme activator not only create a physical barrier to blood but also directly affect the clotting process,

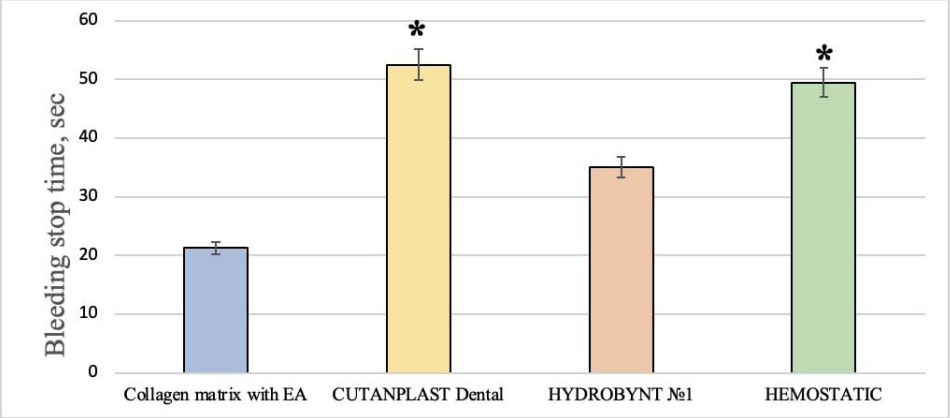

Figure. **Comparison of the bleeding stop time of the collagen matrix with increased hemostatic properties with the 'CUTANPLAST Dental' (Mascia Brunelli, Italy), 'HYDROBYNT №1' (V-CUBE, Ukraine), and 'HEMOSTATIC' (Senta Pharm, Ukraine)**
* $P \leq 0.05$ compared to collagen matrix modified with enzyme activator

promoting the rapid formation of a stable clot. This can provide better results in patients with a disrupted coagulation system, where passive hemostatic methods may not be effective enough.

Conclusions. We have developed collagen matrices with increased hemostatic properties that have demonstrated high efficiency compared to commercial hemostatic agents. They provide rapid and stable clot formation, significantly reducing the time to stop bleeding. The results confirm the prospects of their use as an effective hemostatic material with a minimal risk of bleeding reopening after removal.

Authors' contribution

KB was involved in the manufacture of collagen matrices with increased hemostatic properties; YP performed the in vivo experiments in a rat parenchymal liver bleeding model; DK supported and organized the research.

Funding source

The research was financed by the project No. 0124U000251, "Research and search for ways to regulate molecular mechanisms of intravascular and extravascular thrombosis" (2024–2028).

Acknowledgment

The authors gratefully thank the Ukrainian Armed Forces for such an opportunity to live and work in a peaceful Kyiv.

REFERENCES

1. Peng, H. T. (2020). Hemostatic agents for prehospital hemorrhage control: a narrative review. *Military Medical Research*, 7(1), 13. https://doi.org/10.1186/s40779-020-00241-z
2. Yu, P., Zhong, W. (2021). Hemostatic materials in wound care. *Burns Trauma*, 9, tkab019. https://doi.org/10.1093/burnst/tkab019
3. Cho, K. S., Park, C. H., Hong, S. L., Kim, M. J., Kim, J. Y., Kim, Y. W., Koo, S. K., Roh, H. J. (2015). Comparative analysis of Cutanplast and Spongostan nasal packing after endoscopic sinus surgery: a prospective, randomized, multicenter study. *Eur. Arch. Otorhinolaryngol.*, 272(7), 1699–1705. https://doi.org/10.1007/s00405-014-3264-3
4. Neimash, V. B. (2022). Radiation Technology for the Manufacture of Medical Products with Nanosilver: from Development to Commercialization. *Science and Innovation,* 18(5), 69–84. https://doi.org/10.15407/scine18.05.069

UDC 577.15, 543.272.8, 621.314 **https://doi.org/10.15407/biotech18.02.017**

DEVELOPING A NEW ELECTROCHEMICAL ENZYME BIOSENSOR FOR HIGHLY SENSITIVE DETERMINATION OF HEAVY METAL IONS

V. A. BAKHMAT[1, 2], *O.O. SOLDATKIN*[1, 2], *S.V. DZYADEVYCH*[1, 2], *V.M. PYESHKOVA*[1, 2, 3]

[1]Institute of Molecular Biology and Genetics of the National Academy of Sciences of Ukraine, Kyiv
[2]Taras Shevchenko National University of Kyiv, Ukraine
[3]School of Engineering and Innovation, The Open University, Milton Keynes, MK7 6AA, United Kingdom

E-mail: veronikab2406@gmail.com

Received 2025/03/21
Revised 2025/03/27
Accepted 2025/04/30

Aim. This work was purposed to develop a new electrochemical enzyme biosensor for the highly sensitive determination of heavy metal ions.

Methods. The electrochemical transducers consisted of two pairs of gold-interdigitated electrodes that connected to the impedimetric measuring device. Urease was immobilized with glutaraldehyde on one electrode pair, while a reference membrane with BSA was prepared similarly. Measurements were conducted in 5 mM PBS (pH 7.35) using differential mode to compensate for non-specific signal variations.

Results. The biosensor detected multiple HMIs with high sensitivity and showed high work reproducibility (RSD = 2.28%). EDTA treatment successfully restored enzyme activity, allowing various reuses. The sensor retained 85% activity after 18 months at 4 °C, confirming its long-term stability.

Conclusions. This biosensor provides a cost-effective, sensitive, and reusable platform for sensitive HMIs detection in wastewater, offering an alternative to conventional analytical techniques.

Keywords: biosensor, enzyme inhibition, urease, heavy metal ions.

Heavy metal ion (HMIs) contamination is a serious environmental issue, especially in industrial wastewater. Textile production is one of the significant sources of HMIs such as silver (Ag), cobalt (Co), cadmium (Cd), nickel (Ni), zinc (Zn), copper (Cu), and lead (Pb). These metals accumulate in the environment and pose significant risks to human health [1]. Traditional detection methods, such as inductively coupled plasma optical emission spectrometry and atomic absorption spectroscopy, are highly sensitive but require expensive equipment and trained personnel and are not suitable for real-time monitoring [2, 3]. Therefore, there is a need for cost-effective, rapid, and portable methods for HMIs detection.

Biosensors based on enzyme inhibition offer a promising alternative due to their high specificity, sensitivity, and ability to provide continuous monitoring. In this study, an impedimetric biosensor based on urease inhibition was developed and tested for detecting HMIs in textile wastewater before and after treatment.

Aim. This work was purposed to develop a new electrochemical enzyme biosensor for the highly sensitive determination of HMIs.

Citation: Bakhmat, V. A., Soldatkin, O. O., Dzyadevych, S. V., Pyeshkova, V. M. (2025). Developing a new electrochemical enzyme biosensor for highly sensitive determination of heavy metal ions. *Biotechnologia Acta*, 18(2), 17–19. https://doi.org/10.15407/biotech18.02.017

Methods. The electrochemical transducers consist of two identical pairs of gold interdigitated electrodes obtained by gold sputtering onto a ceramic plate. The sensitive surface of each electrode pair was approximately 1.0–1.5 mm. The transducers were connected to the portable measuring device. The immobilization procedure was performed as follows. The enzyme solution was prepared by dissolving 5% urease (EC 3.5.1.5, E. coli (115 U/mg)) in 20 mM phosphate buffer solution (PBS), pH 6.5, containing 10% bovine serum albumin (BSA) and 10% glycerol. The mixture for the reference membrane was prepared by the same procedure using BSA instead of enzymes. The solutions were mixed with 1% aqueous solution of glutaraldehyde (GA) in a 1:1 ratio and were deposited on the electrodes. Then, the membranes were dried in open air at room temperature. Before starting the experiments, the electrodes with membranes were washed out in excess of unbound components using PBS. Measurements were carried out at room temperature in an open cell filled with five mM PBS, pH 7.35. Non-specific changes in the output signal associated with fluctuations in temperature, medium pH, and electrical noise were compensated by using the differential mode of measurement. At least three series of experiments were performed.

The HMIs measurement procedure (Fig. 1) involves recording the initial biosensor response (A_0) to 2 mM urea, followed by 30 min incubation in the sample with HMIs. The response (A_i) is then measured again, with inhibition reducing the signal. Residual activity (R%) and inhibition level (L%) are calculated as $R\% = (A_i/A_0)\times100$ and $L\% = [(A_0 - A_i)/A_0]\times100$. For reuse, the biosensor is reactivated by 30 min incubation in 5 mM EDTA, and the response (A_r) is measured to assess reactivation efficiency.

Results and Discussion. The biosensor showed high sensitivity to HMIs, detecting Ag, Co, Cd, Ni, Zn, Cu, and Pb (Fig. 2). Based on the obtained results, the sensitivity of the biosensor enables the detection of HMIs concentrations exceeding the maximum permissible limits in water. The response was stable, with a relative standard deviation (RSD) of 2.28%, indicating high reproducibility. The optimal incubation time in the solution containing HMIs was determined to be 20–30 minutes. After inhibition, the biosensor was successfully reactivated using EDTA, allowing multiple uses. The reactivation efficiency depended on the reactivation time (the optimal regeneration time using EDTA was established at 30 minutes) and the concentration of chelating agents. The biosensor retained 85% of its initial activity after 18 months of storage at 4 °C, demonstrating excellent long-term stability.

Conclusions. A new electrochemical enzyme biosensor for highly sensitive determination of HMIs was developed. The biosensor exhibited high sensitivity, excellent reproducibility, and long-term stability. The possibility of multiple reuses after EDTA reactivation was demonstrated.

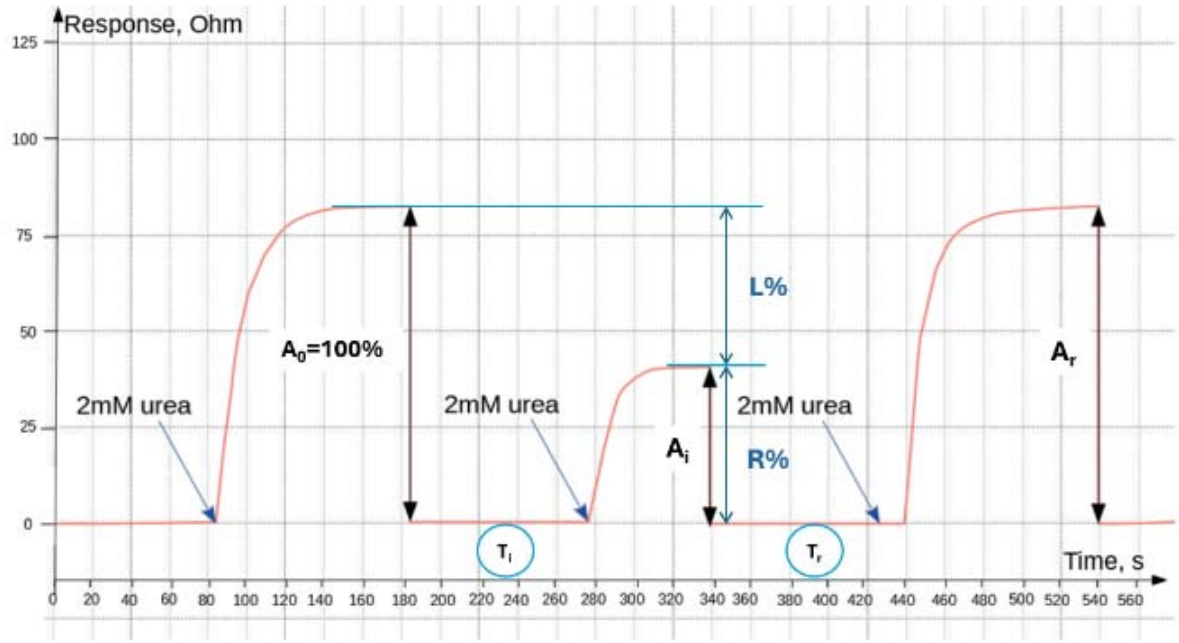

Fig. 1. **Inhibitory determination of heavy metal ions by biosensor:**
A_0 — response before inhibition; A_i — response after inhibition; A_r — response after reactivation; T_i — inhibition time (30 min); T_r — reactivation time (30 min)

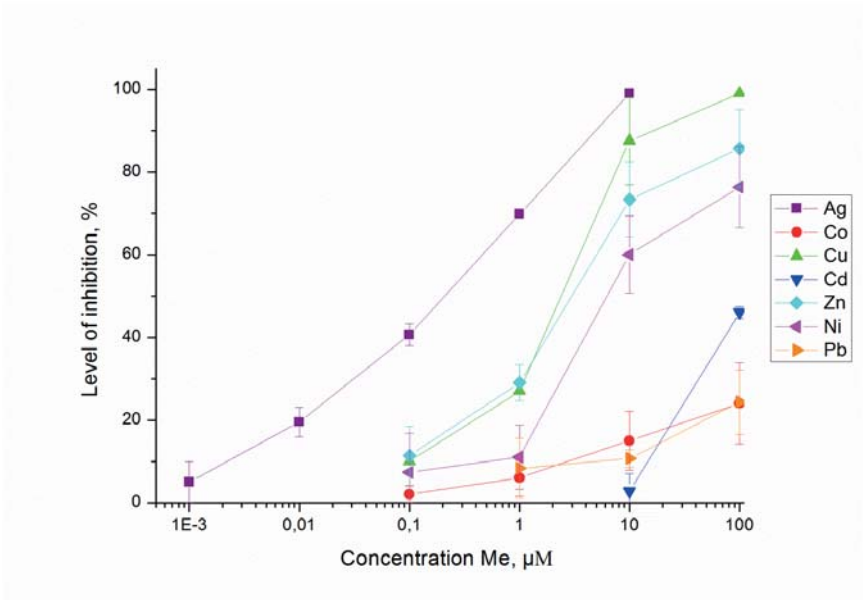

Fig. 2. **Dependence of inhibition level of urease-based biosensors on different concentrations of HMIs Measurements were carried out in 5 mM phosphate buffer solution, pH 7.35; concentration of urea 2.0 mM.** All measurements were performed with a minimum of three replicates

This biosensor provides a practical and efficient solution for environmental monitoring, offering a valuable alternative to conventional methods.

Authors' contribution

VAB performed experiments, data analysis, and presentation; OOS aimed for data analysis; SVD aimed for data analysis; and VMP managed the project and developed a plan of experiments.

Funding source

This work is supported by CARA (the Council for At-Risk Academics) and the National Academy of Sciences of Ukraine: "Smart sensor devices of a new generation based on modern materials and technologies." Furthermore, this study is part of a project that has received funding from the European Union's Horizon 2020 research and innovation program under the grant agreement No 958491, Project Waste2Fresh.

REFERENCES

1. Singh, R., Gautam, N., Mishra, A., Gupta, R. (2011). Heavy metals and living systems: an overview. *Indian J. Pharmacol.*, 43(3), 246–253. https://doi.org/10.4103/0253-7613.81505
2. Abrham, F., Gholap, A. V. (2021). Analysis of heavy metal concentration in some vegetables using atomic absorption spectroscopy. *Pollution*, 7(1), 205–216. https://doi.org/10.22059/POLL.2020.308766.877
3. Mitrano, D. M., Lesher, E. K., Bednar, A., Monserud, J., Higgins, C. P., Ranville, J. F. (2012). Detecting nanoparticulate silver using single-particle inductively coupled plasma–mass spectrometry. *Environ. Toxicol. Chem.*, 31(1), 115–121. https://doi.org/10.1002/etc.719

UDC 543.553+577.151 **https://doi.org/10.15407/biotech18.02.020**

DEVELOPMENT AND ADAPTATION OF A BIOSENSOR BASED ON LACTATE OXIDASE AND POLY-M-PHENYLENEDIAMINE FOR THE DETERMINATION OF L-LACTATE IN REAL BIOLOGICAL SAMPLES

K.O. BERKETA[1, 2], *A.V. BUZHAK*[1, 2], *Y.R. VAKHOVSKIY*[1, 2], *A.S. SVERSTIUK*[3, 4], *O.V. SOLDATKINA*[5], *O.Y. LYUBOVYCH*[6], *S.V. DZYADEVYCH*[1, 2], *O.O. SOLDATKIN*[1, 7]

[1]Institute of Molecular Biology and Genetics, NAS of Ukraine, Kyiv
[2]Shevchenko National University of Kyiv, Kyiv, Ukraine
[3]Horbachevsky Ternopil National Medical University, Ternopil
[4]Ternopil National Ivan Puluj Technical University, Ternopil
[5]Ternopil Regional Clinical Hospital, Ternopil
[6]Odesa Regional Pediatric Clinical Hospital, Odesa
[7]National Technical University of Ukraine "Igor Sikorsky Kyiv Polytechnic Institute", Kyiv

E-mail: ksenya.berketa.10@gmail.com

Received 2025/03/24
Revised 2025/04/27
Accepted 2025/04/30

Aim. Development and optimization of an amperometric biosensor based on lactate oxidase with a poly-meta-phenylenediamine membrane for the accurate measurement of L-lactate in blood serum.

Material and Methods. The biosensor was based on a platinum disk amperometric transducer modified with a PPD membrane with immobilized LOx. Measurements were performed in a three-electrode amperometric system at a potential of +0.6 V. The real sample results were verified spectrophotometrically and by an electrochemical analyzer.

Results. The biosensor demonstrated a wide linear range (7–1000 μM), a low detection limit (7 μM), and high selectivity. The standard addition method showed a high correlation (0.982) with reference methods.

Conclusions. The developed biosensor is promising for clinical diagnostics of blood lactate levels.

Keywords: amperometric biosensor, lactate oxidase, real sample analysis, enzyme.

Biosensors as a new generation of analytical devices are rapidly gaining popularity due to their significant advantages over traditional measurement methods. They are easy to use, portable and characterized by a low cost per analysis, which makes them ideal for use in clinical diagnostics, for example, for monitoring the levels of vital substances in biological fluids. In particular, among the important biomarkers that can be measured by the biosensor method, lactate — the anion of lactic acid, has an extremely important physiological value, because it can be used as biomarker of a number of diseases of the cardiovascular system, hypoxia, diabetes (types 1 and 2), and a number of others. Traditionally, lactate levels have been determined using methods such as colorimetry [1],

Citation: Berketa, K. O., Buzhak, A. V., Vakhovskiy, Y. R., Sverstiuk, A. S., Soldatkina, O. V., Lyubovych, O. Y., Dzyadevych, S. V., Soldatkin, O. O. (2025). Development and adaptation of a biosensor based on lactate oxidase and poly-m-phenylenediamine for the determination of l-lactate in real biological samples. reticulum stress in the regulation of gene expression in normal astrocytes and glioblastoma cells. *Biotechnologia Acta*, 18(2), 20–23. https://doi.org/10.15407/biotech18.02.020

spectrophotometry [2], fluorimetry, liquid chromatography [3], nuclear magnetic resonance (NMR) [4], and enzymatic assays [5]. While these techniques are known for their accuracy and reliability, they are often hindered by complex procedures, the requirement for costly and bulky instrumentation, and limited potential for miniaturization. These drawbacks have stimulated interest in biosensor-based approaches for lactate detection. Biosensors offer several advantages — they are user-friendly, portable, cost-effective, and suitable for on-site and real-time analysis. Currently, a variety of lactate biosensors have been developed, including electrochemical, optical, and enzymatic types. However, despite their growing popularity, many still face challenges such as limited stability, sensitivity to environmental factors, and relatively short operational lifetimes. These limitations highlight the need for continued innovation in biosensor design and materials.

Aim. Due to the importance of lactate as a biomarker for a number of serious diseases, we decided to create an amperometric biosensor for measuring lactate based on lactate oxidase using an additional semipermeable membrane based on poly-meta-phenylenediamine.

Methods. Biosensors were created using platinum disk amperometric transducers. A poly-meta-

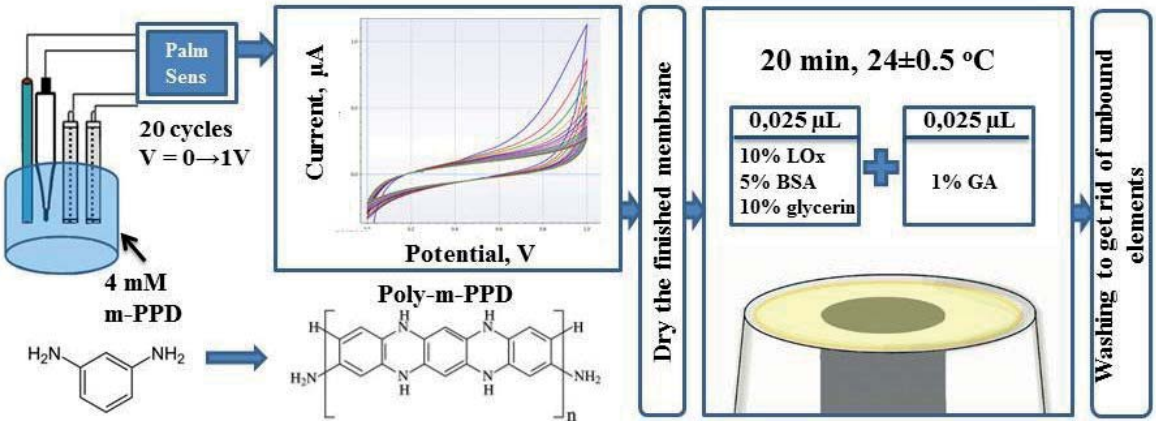

Fig. 1. **Scheme biosensor bioselective element preparation**

phenylenediamine membrane was applied to their surface by electropolymerization, after which the electrode surface was dried, and a mixture of enzyme gel based on 10% lactate oxidase mixed with 1% glutaraldehyde (1:1) was applied. The enzyme was immobilized on the surface of the transducer by covalent binding using glutaraldehyde for 30 minutes at a temperature of 24±1.5 °C in the open air. After that, the biosensor was washed for 5 minutes from unbound membrane elements, changing the buffer solution in the measuring cell several times. The scheme for creating a bioselective element of the biosensor is presented in Fig. 1.

The measurements were performed in an open measuring cell with a volume of 2 ml using a classical three-electrode amperometric system using working, reference, and additional electrodes at an applied potential of +0.6 V.

The spectrophotometric method and a commercial electrochemical analyzer were used as reference methods for measuring real samples.

To process the experimental data obtained in the course of the work, standard methods of variational statistics were used. The study was carried out in at least 5-9 repetitions. When statistically processing the results, the arithmetic mean and its standard deviation were determined,and the data were considered reliable at $P < 0.05$. Data processing and calculations were performed using the OriginLab graphic editor (OriginPro version 8.5).

Results and Discussion. In the course of our work, we developed and optimized an amperometric biosensor based on lactate oxidase and a polymetaphenylenediamine (PPD) membrane. This involved a series of experiments to assess the influence of the main parameters of the working solution on the functioning of the sensor. Studies have shown that the presence of a PPD membrane reduces the impact of ionic strength on the sensor response, although at high concentrations of salts (e.g., NaCl) a decrease in the signal was still observed. However, given that biological samples are diluted before measurement, the effect of this factor is insignificant when measuring real samples of biological fluids.

A study of the buffer capacity of the working solution indicated that the optimal concentration of HEPES salt in the buffer was 25 mM since it is under these conditions that the most extensive linear measurement range and high sensitivity to lactate are ensured. Similarly, the influence of protein concentration on the functioning of the biosensor was analyzed since biological fluids usually contain a significant amount of proteins. The PPD membrane was shown to significantly reduce the influence of protein (BSA) significantly, minimizing mechanical membrane fouling and signal loss.

One of the key characteristics of the biosensor was its selectivity towards potential interferents. Studies have shown that without the PPD membrane, the sensor responded significantly to ascorbic acid and some amino acids. In contrast, in the presence of the membrane, these effects were almost eliminated. This is because larger molecules cannot penetrate the pores of the PPD membrane, which prevents signal distortion and provides a high level of selectivity towards possible interferents.

Analyzing the analytical characteristics, we determined that the biosensor has a wide linear operating range, high sensitivity, and a low detection limit. The total analysis time was 8 minutes, which is fast enough for practical use.

Final testing of the biosensor on real blood serum samples confirmed its effectiveness. The standard addition method was found to be the most accurate and stable, demonstrating a high correlation with the reference results from an electrochemical analyzer. At the same time, the results of spectrophotometric analysis differed in some cases, which may be due to the peculiarities of sample transportation or serum heterogeneity. The measurement results of real samples are shown in Fig. 2.

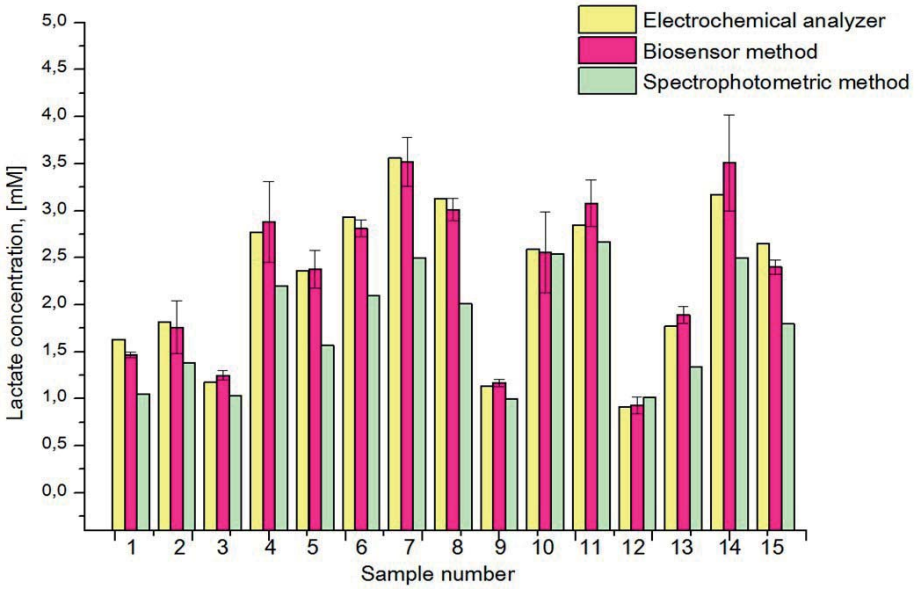

Fig. 2. **Comparison of serum lactate concentrations measured by biosensor (n = 9) and reference methods**

Conclusions. Thus, in the course of the work, an amperometric biosensor with a semipermeable PPD membrane and immobilized LOx was developed and optimized for the rapid and accurate determination of L-lactate in blood serum. The PPD membrane minimizes biological and solvent interferences, ensuring high accuracy of the analysis. The biosensor has a wide linear range (7–1000 μM), a low detection limit (7 μM) and a short analysis time.

The biosensor method of standard additions showed the best correlation with the reference methods (0.982 and 0.914), and the repeatability of measurements was high (deviation of 2.9% and 6.7% for model solutions and real blood serum samples, respectively). The device remained stable after 5 days of continuous use (signal decrease of 3–5%).

Thus, it can be concluded that a biosensor based on lactate oxidase and PPD can be considered promising for clinical and laboratory diagnostics of blood lactate levels.

Authors' contribution

KOB, AVB and YRV performed the main biosensor measurements related to the development and optimization of the biosensor. OVS performed the analysis of blood serum samples by

spectrophotometric method, OYL — by electrochemical analyzer method. ASS provided samples and assisted with experiments. OOS and SVD were the project supervisors and provided the material base for the research.

Funding source

In frame of Joint Call 'Ukrainian-Swiss Joint Research Projects: Call for Proposals 2023' (project No 225067).

REFERENCES

1. Suman, S., Singhal, R., Sharma, A. L., Malthotra, B. D., Pundir, C. S. (2005). Development of a lactate biosensor based on conducting copolymer bound lactate oxidase. *Sensors and Actuators B: Chemical*, 107(2), 768–772. https://doi.org/10.1016/j.snb.2004.11.050
2. Brandt, R. B., Siegel, S. A., Waters, M. G., Bloch, M. H. (1980). Spectrophotometric assay for D-(–)-lactate in plasma. *Anal. Biochem.*, 102(1), 39–46. https://doi.org/10.1016/0003-2697(80)90105-4
3. Wasek, B., Arning, E. (2022). Quantitation of lactate in cerebrospinal fluid using liquid chromatography–electrospray-tandem mass spectrometry. In: *Clinical Applications of Mass Spectrometry in Biomolecular Analysis: Methods and Protocols*. New York, NY: Springer US, 253–260. https://doi.org/10.1007/978-1-0716-2317-9_19
4. Lloyd, S. G., Zeng, H., Wang, P., Chatham, J. C. (2004). Lactate isotopomer analysis by 1H NMR spectroscopy: consideration of long-range nuclear spin–spin interactions. *Magn. Reson. Med.*, 51(6), 1279–1282. https://doi.org/10.1002/mrm.20092
5. Rodriguez, F. A., Banquells, M., Pons, V., Drobnic, F., Galilea, P. A. (1992). A comparative study of blood lactate analytic methods. *Int. J. Sports Med.*, 13(6),462–466. https://doi.org/10.1055/s-2007-1021304

UDC 547.56:615.322:582.734.4 **https://doi.org/10.15407/biotech18.02.024**

CHERRY LAUREL (*Prunus laurocerasus*) EXTRACT AND LIPOSOME ENCAPSULATION

ESMA NUR BULUT[1], *CAN ALI AĞCA*[2], *NILGÜN ERTAŞ*[3]

[1]Department of Food Technology, Food Agriculture and Livestock Vocational School, Bingöl University, Türkiye
[2]Department of Molecular Biology and Genetics, Bingöl University, Türkiye
[3]Department of Food Engineering, Engineering Faculty, Necmettin Erbakan University, Koyceğiz Campus, Konya, Türkiye

E-mail: enbulut@bingol.edu.tr

Received 2025/03/21
Revised 2025/03/27
Accepted 2025/04/30

Aim. The study aimed to determine the antioxidant activity and the number of phenolic substances of cherry laurel fruit and to reveal the usability of the fruit for other studies.

Methods. Cherry laurel fruit was separated from the seeds and pureed. The fruit was extracted by ultrasonic extraction. Ethanol was used as a solvent. The fruit was extracted by acidic and ethanol extraction. The solvent was removed in a rotary evaporator at 50–60 °C. For liposome production, lecithin solution was first prepared. Chitosan solution was added to the resulting reduced-size liposome and mixed overnight. Liposomes with and without extracts were prepared.

Results. The DPPH value of the acidic fruit extract was determined as 66.399 mg TEAA/kg KM, the CUPRAC analysis result was 42.424,84 mg/kg KM, and the total phenolic content was 3.895,34 mg GAE/kg KM.

Conclusion. The data obtained from this study show that cherry laurel fruit has good antioxidant activity and phenolic substance content and that the fruit can be a raw material for anticancer studies in this field.

Keywords: antioxidant and phenolic, cherry laurel, encapsulation, liposome.

Cherry laurel (*Laurocerasus officinalis* Roem.) is a red-purple fruit belonging to the Rosaceae family, also known locally as “taflan and laz cherry.” In Turkey, it is generally cultivated in the Eastern Black Sea region and is also produced in the Balkans, Iran, Western Europe, Southern and Western Caucasus, and some Mediterranean countries [1–3]. Wild-grown cherry laurel fruits are astringent, while specially grown fruits have a sweet taste. The fruit is consumed fresh, dried, roasted, or in forms such as jam, pickle, and marmalade [3–5]. Cherry laurel can be consumed as food as well as for the treatment of some diseases among the people. Among these diseases are stomach ulcers, bronchitis, digestive system disorders, eczema, and hemorrhoids [6, 7]. Phenolic acids such as chlorogenic, vanillic, syringic, caffeic, p-coumaric, and p-hydroxybenzoic in the structure of cherry laurel make the fruit a good source of antioxidants [7, 8]. Fruits and vegetables have a significant place in human nutrition. This importance of fruits and vegetables is due to the antioxidant and phenolic compounds they contain. These compounds especially protect against cancer and cardiovascular diseases [9, 10]. The use of natural compounds in the treatment of diseases is becoming increasingly popular.

Citation: Bulut, E. N., Ağca, C. A., Ertaş, N. (2025). Cherry laurel (*Prunus laurocerasus*) extract and liposome encapsulation. *Biotechnologia Acta*, 18(2), 24–27. https://doi.org/10.15407/biotech18.02.024

Due to this, researchers have focused on the extraction of phenolic compounds from natural sources in recent years. Extraction is a method used to extract the desired bioactive compounds from plant, animal, and microbial tissues with special solvents. Various techniques are used for this purpose. Ultrasonically assisted extraction is one of these methods [11–13]. The extraction process, which takes hours with conventional extraction, can be performed in minutes with ultrasound-assisted extraction. This extraction method has advantages such as reducing time, being environmentally friendly, inexpensive, and increasing extract yield [13–15]. Encapsulation enables an active ingredient to be coated with a specific coating material to maintain its stability and release at the desired dose. There are different encapsulation techniques in the literature. Liposome formation is one of them and has been a popular research topic in recent years. Liposomes are small vesicular spheres with a lipid bilayer containing hydrophilic and hydrophobic substances together. Liposomal encapsulation also has benefits, such as increasing the bioavailability of active compounds and ensuring stability and controlled release. Therefore, it is a preferred encapsulation method for phenolic compounds [16].

Aim. The objectives of this study were to perform ultrasonically assisted extraction of cherry laurel fruit, to compare the antioxidant activity and total phenolic content of acidic and non-acidic extracts, and to form extract-containing/plain liposomes.

Methods. Blackcurrant fruit was separated from the seeds and pureed with the help of a blender. 100 g of fruit was mixed with 1000 ml ethanol and 1% formic acid. Only ethanol was used in the acid-free extraction. Extraction was performed in an ultrasonicator at 40 °C for 40 min. At the end of the time, the mixture was filtered with coarse filter paper (Fig. 1). The solvent was evaporated in a rotary evaporator at 60 °C. °Brixs value of the extract was measured by hand refractometer. The method of Demircan et al. was modified and used for liposome formation. First, lecithin solution was prepared for liposome production. Chitosan solution was added to the resulting size-reduced liposome and mixed overnight. 0.8% w/v chitosan solution was added to the solution to ensure the stability of the liposomes formed. Liposomes with and without extracts were prepared [17].

Results and Discussion. The antioxidant activity content of cherry laurel fruit was determined by DPPH (2-2-Diphenyl-2-picrylhydrazyl) and CUPRAC analysis [18, 19]. Total phenolic content was determined by total phenolic matter analysis according to the Folin Ciocalteau method [20]. The results of the extract analysis are given in Table 1. The DPPH value of the acidic fruit extract was determined as 66.399 mg TEAA/kg KM, the CUPRAC analysis result was 42.424,84 mg/kg KM, and the total phenolic content was 3.895,34 mg GAE/kg KM. According to the results of the acid-free extract, the DPPH value of the fruit was 52.696 mg TEAA/kg KM, the amount of phenolic matter was 3.383,97 mg/kg KM, and the CUPRAC value was 63.898,63 mg/kg KM. The water-soluble matter content of the extract was determined as 83°Brix, and the results were given over this dry matter.

According to Table 1, acidic extraction increased the amount of antioxidant and phenolic substances in the fruit. DPPH and CUPRAC assays are two separate antioxidant assays. In the DPPH method, the reduction of the free radical DPPH by antioxidants is measured, while in the CUPRAC analysis, the reduction of copper (Cu) ions is measured. These two values differ from each other according to the type of antioxidant compounds. The CUPRAC value of the acid-free extract was lower than the acid extract. This indicates that the acid-free extract releases more copper-binding compounds. The use of acid in the extraction increased the amount of DPPH and total phenolic content (TFM). Acidic media increase the extraction efficiency of phenolic compounds due to their

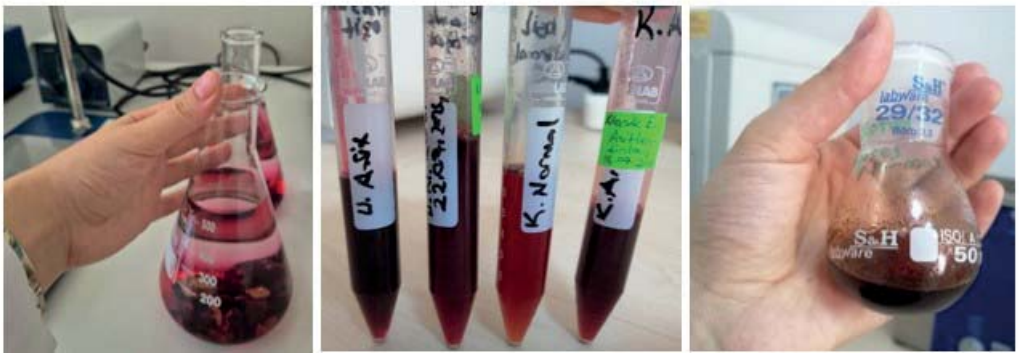

Fig. 1. **Extraction of cherry laurel**

Table 1. **Cherry laurel extract analysis results**

	DPPH TEAA mg/kg KM	CUPRAC mg/kg KM	TFM mg/kg KM
Ultrasonic-Acid	66.399	42.424,84	3.895,34
Ultrasonic-Acid-Free	52.696	63.898,63	3.383,97

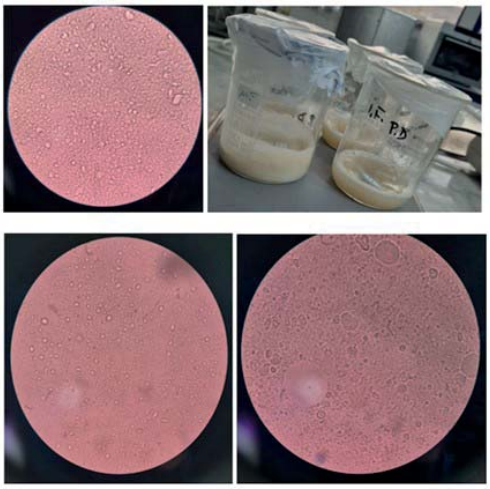

Fig. 2. **Liposome formation and microscope view**
(Images were obtained at 100× magnification under a light microscope)

effects, such as increasing the solubility of the compounds and disintegration of the cell wall [21]. The results given in Table 1 also show this. Extract-loaded and empty liposome samples are presented in Fig. 2.

Conclusions. The data obtained from this study show that cherry laurel fruit has good antioxidant activity and phenolic substance content and that the fruit can be a raw material for anticancer studies in this field.

Authors' contribution

E. N. Bulut — analysis, thesis writing; C.A. Ağca — giving ideas, guiding the study, supporting the laboratory environment, providing materials; N. Ertaş — goal setting, laboratory environment support, material and analysis support, evaluation of research results

Funding Source

This study was financially supported by Necmettin Erbakan University, Scientific Research Projects (BAP — 24DR19006).

REFERENCES

1. Ayaz, F., Kadiog, A., Reunanen, M. (1997). Sugar composition in fruits oflaurocerasus officinalis roem. and its three cultivars. *Journal of Food Composition and Analysis*. 10, 82–86.
2. Kolayli, S., Küçük M., Duran, C., Candan, F., Dinçer, B. (2003). Chemical and antioxidant properties of Laurocerasus officinalis Roem.(cherry laurel) fruit grown in the Black Sea region. *Journal of Agricultural and Food Chemistry*, 51, 7489–7494.
3. Karataş, E., Uçar, A. Karayemiş'in Sağlık Üzerine, Etkisi. (2018). *Sağlık Bilimleri Dergisi*, 27, 70–75.
4. Çalışır, S., Aydın, C. (2004). Some physico-mechanic proper ties of cherry laurel *(Prunus lauracerasus* L.) fruits. *Journal of Food Engineering,* 65, 145–150.
5. İslam, A. (2002). Kiraz'cherry laurel (Prunus laurocerasus). *Journal of Crop and Horticultural Science*, 30, 301–302.
6. Baytop, T. (2001). *Therapy with medicinal plants in Turkey* (past and present), 1st ed. Istanbul University: Istanbul, Turkey. P. 178–249.
7. Talih, M. (2018). Dondurarak Kurutma Yöntemi İle Taflan (Karayemiş) (*Prunus laurocerasus* L.) Meyvesinin Kurutulması ve Örnek Gıda Sisteminde Denenmesi. *Master Thesis, EÜ Institute of Science and Technology*. İzmir.

8. Yaylacı-Karahalil, F., Şahin, H. (2011). Phenolic composition and antioxidant capacity of Cherry laurel (*Laurocerasus officinalis* Roem.) sampled from Trabzon region. *Biotechnology,* 10(72), 16293–16299.
9. Uğurlu, S., Bakkalbaşı, E. (2023). Elma kabuğundan fenolik maddelerin ultrases destekli ekstraksiyonu. *Food and Health*. 9(4), 341–349. https://doi.org/10.3153/FH23031.
10. Wolfe, K. L., Liu, R. H. (2003). Apple Peels as a Value-Ad ded Food Ingredient. *Journal of Agricultural and Food Chemistry*, 51, 1676–1683. https://doi.org/10.1021/jf025916z
11. Roohinejad, S., Koubaa, M., Barba, F. J., Greiner, R., Orlien, V., Lebovka, N. I. (2016). Negative pressure cavitation extraction: A novel method for extraction of food bioactive compounds from plant materials. *Trends in Food Science and Technology*, 52, 98–108.
12. Topdaş, E. F., Şengül, M. (2019). Katı-sıvı Ekstraksiyonunda kullanılan modern Teknikler ve bu Teknikler arasında ultrason Yardımlı Ekstrak siyonun yeri. *Atatürk Üniversitesi Ziraat Fakültesi Dergisi*. 201–216.
13. Taşkıran, Z. G., Dündar, A., Yıldız, H. (2023). Bitkisel materyallerdeki biyoaktif bileşenlerin ekstraksiyonunda kullanılan konvansiyonel ve yeni nesil ekstraksiyon yöntemleri. *Food Science and Engineering Research*, 2(2), 50–58.
14. Picó, Y. (2013). Ultrasound-assisted extraction for food and environmen tal samples. *TrAC Trends in Analytical Chemistry*, 43, 84–99.
15. Siddiqui, H., Sultan, Z., Yousuf, O., Malik, M., Younis, K. (2023). A review of the health benefits, functional properties, and ultrasound-assisted dietary fiber extraction. *Bioactive Carbohydrates and Dietary Fibre*, 30, 100356.
16. Allen, T. M., Cullis, P. R. (2013). Liposomal drug delivery systems: From concept to clinical applications. *Advanced Drug Delivery Reviews*, 65(1), 36–48.
17. Demircan, E. (2016). Elma Kabuklarından Elde Edilen Bileşiklerin Lipozom ile Enkapsülasyonu. *Istanbul Technical University, Institute of Science and Technology. İstanbul*.
18. Beta, T., Nam, S., Dexter, J. E., Sapirstein, H. D. (2005). Phenolic content and antioxidant activitiy of pearled wheat and roller-milled fractions. *Cereal Chemistry*, 82(4), 390–393.
19. Gyamfi, M. A., Yonamine, M., Aniya, Y. (1999). Free radical scavenging action of medical herbs from ghane: thonningia sanguinea on experimentally-induced liver injuries. *General Pharma*, 32(6), 661–667.
20. Maurya, S., Singh, D. (2010). Quantitative analysis of total phenolic content in *Adhatoda vasica* Nees extracts. *International Journal of PharmTechonology Research*, 2(4), 2403–2406.
21. Stalikas, C.D. (2007). Determination of phenolic compounds in olive oils: A review. *Food Chemistry*, 100(4), 1329–1336.

UDC 577.1:615.277.3:612.017.1 **https://doi.org/10.15407/biotech18.02.028**

VIRTUAL SCREENING STRATEGY FOR IDENTIFYING NEW SMALL-MOLECULE ANTAGONISTS OF INTEGRIN αIIBβ3

O.A. CHUK

Palladin Institute of Biochemistry of NAS of Ukraine, Kyiv.

E-mail: oleksiy.chook@gmail.com

Received 2025/03/21
Revised 2025/04/17
Accepted 2025/04/30

Aim. To develop an optimal strategy for identifying new small-molecule antagonists of integrin αIIbβ3 using virtual screening.

Methods. Molecular modeling.

Results. The 7TMZ-based model demonstrated high classification accuracy (receiver operating characteristic area under the curve (ROC AUC): 84.285) and pose reproducibility (root mean square deviation (RMSD): 0.326 Å). The 3T3M-based model demonstrated high pose reproducibility (RMSD of 0.218 Å for RUC2 and 0.254 Å for RUC1).

Conclusions. Two virtual screening models were developed to identify integrin αIIbβ3 antagonists that do not induce receptor unfolding. Preliminary evaluation suggests their strong potential in selecting active compounds.

Keywords: virtual screening, small-molecule antagonists, integrin αIIbβ3, glycoprotein IIb/IIIa.

Integrin αIIbβ3 antagonists inhibit platelet-fibrinogen binding, preventing blood clotting. They are used to reduce thrombosis related to certain medical conditions and procedures [1].

Clinically used αIIbβ3 antagonists include the αIIbβ3-specific antibody abciximab, the cyclic heptapeptide eptifibatide, which contains a KGD (Lys-Gly-Asp) sequence, and the peptidomimetic tirofiban, which mimics the RGD (Arg-Gly-Asp) sequence [2]. Despite their anticoagulant effect, these drugs are associated with the development of thrombocytopenia [3]. A conformational change may cause this side effect, the unfolding of integrin αIIbβ3 on the platelet surface upon interaction with antagonists. It is assumed that the unfolding of integrin makes the immunogenic site on the surface of integrin accessible, which leads to an immune response, which in turn leads to the development of thrombocytopenia [4]. Such unfolding may also lead to a high level of active platelets after a decrease in the antagonist concentration in the blood plasma, which may be the reason why a number of other RGD peptidomimetics failed to receive regulatory approval [5, 6].

However, some small-molecule inhibitors are able to exert an antagonistic effect without inducing αIIbβ3 integrin unfolding. Among them are both stabilizing RGD peptidomimetics and conformationally neutral compounds of another type of binding — the RUC family. Lin, Fu-Yang, et al. proposed that stabilization of the closed integrin conformation is mediated by a specific water molecule in the fibrinogen binding site. Displacement of this water leads to Ser123-Mg^{2+} contact, causing integrin unfolding [7]. Therefore, RGD peptidomimetics that stabilize this key water molecule may not have those mentioned above adverse clinical effects. And since the dominant conformation of integrin in the body is closed, the family of conformationally neutral RUC compounds is also promising.

Thus, the search for new low-molecular antagonists of integrin αIIbβ3 that don't induce receptor unfolding can result in a significant contribution to the direction of platelet aggregation inhibition.

Citation: Chuk, O. A. (2025). Virtual screening strategy for identifying new small-molecule antagonists of integrin αIIbβ3. *Biotechnologia Acta*, 18(2), 28–30. https://doi.org/10.15407/biotech18.02.028

For this purpose, the use of the method of virtual screening based on molecular docking is promising. Virtual screening can be divided into two parts: the search for RGD peptidomimetics that stabilize the closed conformation of integrin and the search for antagonists that have the binding type of compounds of the RUC family. Two models were created for this purpose.

Aim. To develop an optimal strategy for identifying new small-molecule antagonists of integrin αIIbβ3 using virtual screening.

Methods. To identify RGD peptidomimetics that stabilize the closed conformation, a model was created based on the crystal structure of the integrin αIIbβ3 complex with the stabilizing ligand BMS4 (PDB ID: 7TMZ). This model includes the water molecule essential for stabilization and two additional molecules that interact with the Mg^{2+}.

To identify antagonists that have the binding type of RUC family compounds, a model was created based on the crystal structure of the RUC2-integrin αIIbβ3 complex (PDB ID: 3T3M). This model includes two molecules that mediate the hydrogen bond of the ligand with residue D232. The construction and evaluation of the models were carried out using the ICM-Pro software (Molsoft LLC, USA). The dudes module of the Tldr's Ligand Discovery Resource service (UCSF, USA) was utilized to generate the test set of compounds [8].

Results and Discussion. The model for identifying RGD peptidomimetics that stabilize the closed conformation demonstrated high classification accuracy and pose reproducibility for active compounds. The model achieved an ROC AUC of 84.285 (Fig. 1). The RMSD between the pose of the ligand from the 7TMZ (redocking), and the model prediction was 0.326 Å. The average RMSD between the poses of similar stabilizing RGD peptidomimetics from the crystal structures 7UCY, 7TCT, 7UJE, 7U9F, 7U9V, 7UDH, 7UBR, and the predicted ones was 0.326 Å.

The model for identifying antagonists that have RUC family binding type demonstrated relatively high pose reproducibility, with an RMSD of 0.218 Å for RUC2 (redocking) and 0.254 Å for RUC1.

The determined classification accuracy of the RGD peptidomimetic screening model may be underestimated since the list of active compounds in the test set included all compounds from the ChEMBL database with a pChEMBL value ≥ 6, regardless of interaction type. Still, the model was optimized for the selection of integrin-stabilizing compounds.

Assessing the relevant classification accuracy of the RUC family antagonist screening model is challenging due to the limited number of documented active compounds with sufficiently high activity (pChEMBL value ≥ 6).

Conclusions. As the result of the development of an optimal virtual screening strategy for identifying small-molecule integrin αIIbβ3 antagonists, two virtual models were created and tested. Each model is optimized for the selection of one of two types of antagonists that do not induce integrin unfolding, which can cause adverse clinical effects. Preliminary evaluation suggests that these models have strong potential for identifying suitable active compounds.

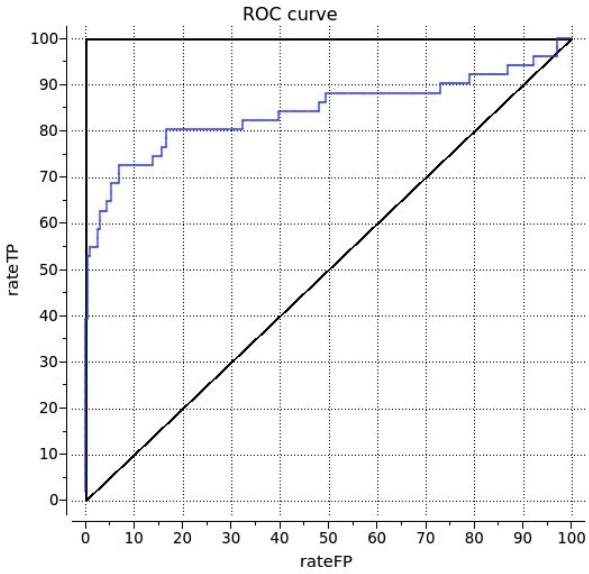

Fig. 1. **Receiver operating characteristic curve for the 7TMZ-based model:** rateFP — false positive rate; rateTP — actual positive rate

The determined classification accuracy of the RGD peptidomimetic screening model may be underestimated since the list of active compounds in the test set included all compounds from the ChEMBL database with a ChEMBL act value ≥ 6, regardless of interaction type. Still, the model was optimized for the selection of integrin-stabilizing compounds.

Assessing the relevant classification accuracy of the RUC family antagonist screening model is challenging due to the limited number of documented active compounds with sufficiently high activity (ChEMBL act ≥ 6).

Author's contribution

OC developed the virtual screening strategy, built and analyzed the virtual models, and prepared the manuscript.

Funding source

The research was financed by project No. 0124U000251, "Research and search for ways to regulate molecular mechanisms of intravascular and extravascular thrombosis" (2024–2028).

REFERENCES

1. Antoniucci, D. (2007). Differences among GP IIb/IIIa inhibitors: different clinical benefits in non-ST-segment elevation acute coronary syndrome percutaneous coronary intervention patients. *European Heart Journal Supplements*, 9 (suppl_A), A32–A36. https://doi.org/10.1093/eurheartj/sul069
2. Hagemeyer, C. E., Peter, K. (2010). Targeting the platelet Integrin GPIIB/IIIA. *Current Pharmaceutical Design*, 16(37), 4119–4133. https://doi.org/10.2174/138161210794519255
3. McClure, M. W., Berkowitz, S. D., Sparapani, R., Tuttle, R., Kleiman, N. S., Berdan, L. G., Lincoff, A. M., Deckers, J., ..., Harrington, R. A. (1999). Clinical significance of thrombocytopenia during a Non–ST-Elevation acute Coronary Syndrome. *Circulation,* 99(22), 2892–2900. https://doi.org/10.1161/01.cir.99.22.2892
4. Bougie, D. W., Rasmussen, M., Zhu, J., Aster, R. H. (2012). Antibodies causing thrombocytopenia in patients treated with RGD-mimetic platelet inhibitors recognize ligand-specific conformers of αIIb/β3 integrin. *Blood*. 119(26), 6317–6325. https://doi.org/10.1182/blood-2012-01-406322
5. Cox, D. (2004). Oral GPIIB/IIIA antagonists: What went wrong? *Current Pharmaceutical Design*. 10(14), 1587–1596. https://doi.org/10.2174/1381612043384673
6. Chew, D. P., Bhatt, D. L., Topol, E. J. (2001). Oral glycoprotein IIB/IIIA inhibitors. *American Journal of Cardiovascular Drugs,* 1(6), 421–428. https://doi.org/10.2165/00129784-200101060-00002
7. Lin, F., Li, J., Xie, Y., Zhu, J., Nguyen, T. T. H., Zhang, Y., Zhu, J., Springer, T. A. (2022). A general chemical principle for creating closure-stabilizing integrin inhibitors. *Cell*, 185(19), 3533–3550.e27. https://doi.org/10.1016/j.cell.2022.08.008
8. Irwin, J. J., Shoichet, B. K., Mysinger, M. M., Huang, N., Colizzi, F., Wassam, P., Cao, Y. (2009). Automated Docking Screens: A Feasibility study. *Journal of Medicinal Chemistry,* 52(18), 5712–5720. https://doi.org/10.1021/jm9006966

UDC 577.332.4 **https://doi.org/10.15407/biotech18.02.031**

CALIX[4]ARENE C-715 MODULATES MITOCHONDRIAL FUNCTIONING AND CONTRACTILE ACTIVITY OF UTERINE SMOOTH MUSCLE

I.S. FORYS[1], *O.V. TSYMBALYUK*[2], *R.V. RODIK*[3], *M.V. RUDNYTSKA*[1], *H.V. DANYLOVYCH*[1], *Yu.V. DANYLOVYCH*[1]

[1]Palladin Institute of Biochemistry of the National Academy of Sciences of Ukraine, Kyiv
[2]Educational Scientific Institute of High Technologies, Taras Shevchenko National University of Kyiv
[3]Institute of Organic Chemistry of the National Academy of Sciences of Ukraine, Kyiv

E-mail: illia.forys@ukr.net

Received 2025/03/24
Revised 2025/03/03
Accepted 2025/04/30

Aim. To elucidate the effects of calix[4]arene C-715 on the contractile activity of myometrial strips and the Ca^{2+}-dependent functional activity of mitochondria.

Materials and Methods. Confocal imaging was performed on Wistar rats myocytes using MitoTracker Orange CM-H_2TMRos and FITC-labeled compound C-1308. NADH autofluorescence, energy-dependent Ca^{2+} accumulation, and NO generation in the isolated mitochondria were measured by spectrofluorimetry and flow cytometry. The contractile activity of rat's myometrium was recorded in the isometric mode. The hydrodynamic diameter of myocytes was assessed by laser correlation spectroscopy.

Results. C-1308 accumulates in myocytes and colocalizes with MitoTracker, confirming the ability of C-715 to interact with mitochondria. A mechano-kinetic analysis showed that C-715 at 30 μM enhances the amplitude, frequency, force, temporal, and impulse parameters of spontaneous contractions while reducing the velocity. C-715 at 30 μM inhibited NO synthesis in intact myocytes and mitochondria; at 10–30 μM suppressed NADH oxidation and energy-dependent Ca^{2+} accumulation, which correlate with the contractility increase and the decrease in the hydrodynamic diameter of myocytes.

Conclusions. The action of C-715 is directed at reducing Ca^{2+} transport activity and Ca^{2+}-dependent processes in mitochondria, resulting in an enhancement of myometrial contractility.

Key words: calix[4]arenes, Ca^{2+}, myometrium, contractile activity, mitochondria.

Mitochondria are crucial for both Ca^{2+} signaling and homeostasis, and smooth muscle contraction. At the same time, disruptions in inner mitochondrial membrane Ca^{2+} transport systems can lead to dysfunction, including ROS overproduction and contractile impairments [1]. Given the link between myometrial contractility and labor complications, identifying non-toxic compounds that modulate mitochondrial Ca^{2+}-transport systems and Ca^{2+}-dependent processes is a relevant medical challenge. The basis of the smooth muscle cell contraction-relaxation process lies in the coordinated functioning of systems that regulate changes in Ca^{2+} concentration within the myoplasm [2]. It has been demonstrated that polyphenolic macrocyclic compounds calix[4]arenes effectively modulate

Citation: Forys, I. S., Tsymbalyuk, O. V., Rodik, R. V., Rudnytska, M. V., Danylovych, H. V., Danylovych, Yu. V. (2025). Calix[4]arene C-715 modulates mitochondrial functioning and contractile activity of uterine smooth muscle. *Biotechnologia Acta*, 18(2), 31–34. https://doi.org/10.15407/biotech18.02.031

the activity of ATP-hydrolyzing Ca^{2+}-transporting systems of the plasma membrane, sarcoplasmic reticulum, and mitochondria in uterine smooth muscle (myometrium) [3]. The aforementioned energy-dependent Ca^{2+} transport systems of the plasmalemma and reticulum, as well as the ATPase activity of the myosin head, exhibit low sensitivity to the action of calix[4]arene C-715 (5,17-di(trifluoro)acetamido-11,23-di-*tert*-butyl-26,28-dihydroxy-25,27-dipropoxycalix[4]arene) (Fig. 1), suggesting a specific effect of this compound on mitochondrial Ca^{2+}-transporting systems.

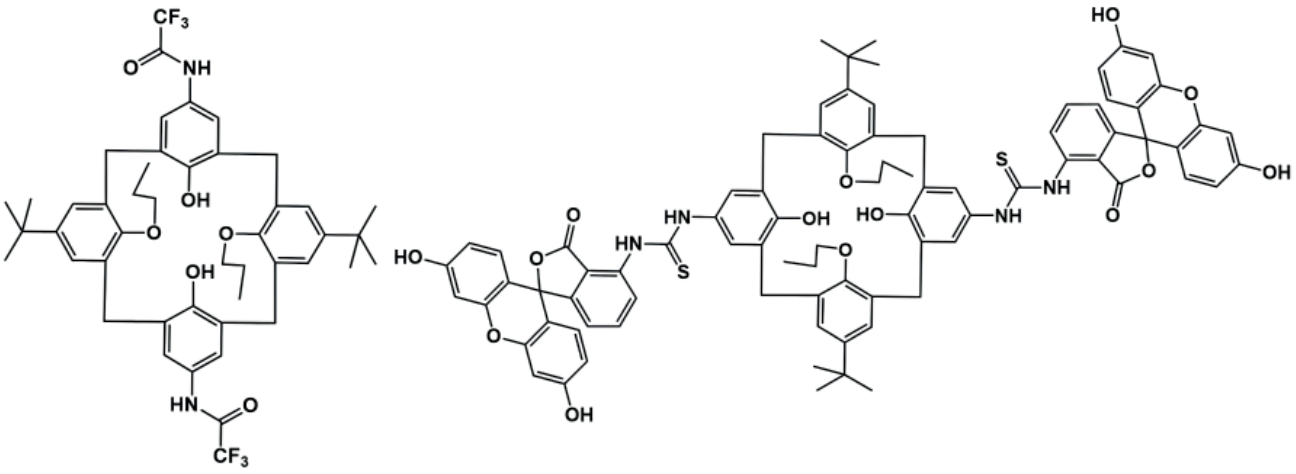

Fig. 1. **Structural formulas of calix[4]arenes C-715 and C-1308**

Aim. The study purposed to elucidate the effects of calix[4]arene C-715 on the contractile activity of myometrial strips and the Ca^{2+}-dependent functional activity of isolated mitochondria.

Methods. Studies were conducted on isolated myometrial mitochondria, cell suspensions, and strips from non-pregnant Wistar rats. Confocal imaging was performed on freshly isolated myocytes using MitoTracker Orange CM-H_2TMRos and FITC-labeled analog of calix[4]arene C-715 — compound C-1308 (Fig. 1). Measurement of changes in NADH autofluorescence, as well as the energy-dependent Ca^{2+} accumulation (using the Ca^{2+}-specific probe Fluo-4 AM), and NO generation (using the NO-specific probe DAF-FM) in the isolated mitochondria was carried out by spectrofluorimetry and flow cytometry (for NO production in myocytes). The spontaneous contractile activity of longitudinal smooth muscle preparations of rat uterus was recorded in the isometric mode under a constant load of 10 mN. Changes in the hydrodynamic diameter of myocytes in suspension were assessed using laser (photon) correlation spectroscopy. Data are presented as means ± SE based on the numbers of determinations. Differences between data sets from fluorometric experiments were analyzed using unpaired Student's *t*-tests in Microsoft Excel.

Results and Discussion. It was demonstrated that the FITC-labeled analog of calix[4]arene C-715 effectively accumulates in myocytes and colocalizes with MitoTracker Orange CM-H_2TMRos, confirming the ability of compound C-715 to interact with mitochondria (Fig. 2).

It was shown that calix[4]arene C-715 at 30 μM, both the amplitude and frequency increased while a decrease in basal tension was observed (Fig. 3). A comprehensive mechano-kinetic analysis [4] revealed that C-715 at 30 μM significantly increased the force at which the maximum velocity of the relaxation phase occurred, whereas a similar parameter for the contraction phase only showed a tendency to increase. Additionally, C-715 at 30 μM increased certain temporal and impulse parameters of myometrial contractile activity while reducing the velocity of spontaneous contractions relative to the control.

A series of biochemical and biophysical studies were conducted to elucidate the underlying mechanisms of these effects. In particular, it was shown that calix[4]arene C-715 at 30 μM inhibited NO synthesis in intact myocytes and isolated mitochondria. Additionally, C-715 (10–30 μM) suppressed NADH oxidation in mitochondria and reduced the efficiency of energy-dependent Ca^{2+} accumulation in these subcellular structures. These effects may explain the stimulatory effect of the studied compound on myometrial strips' contractile activity. In

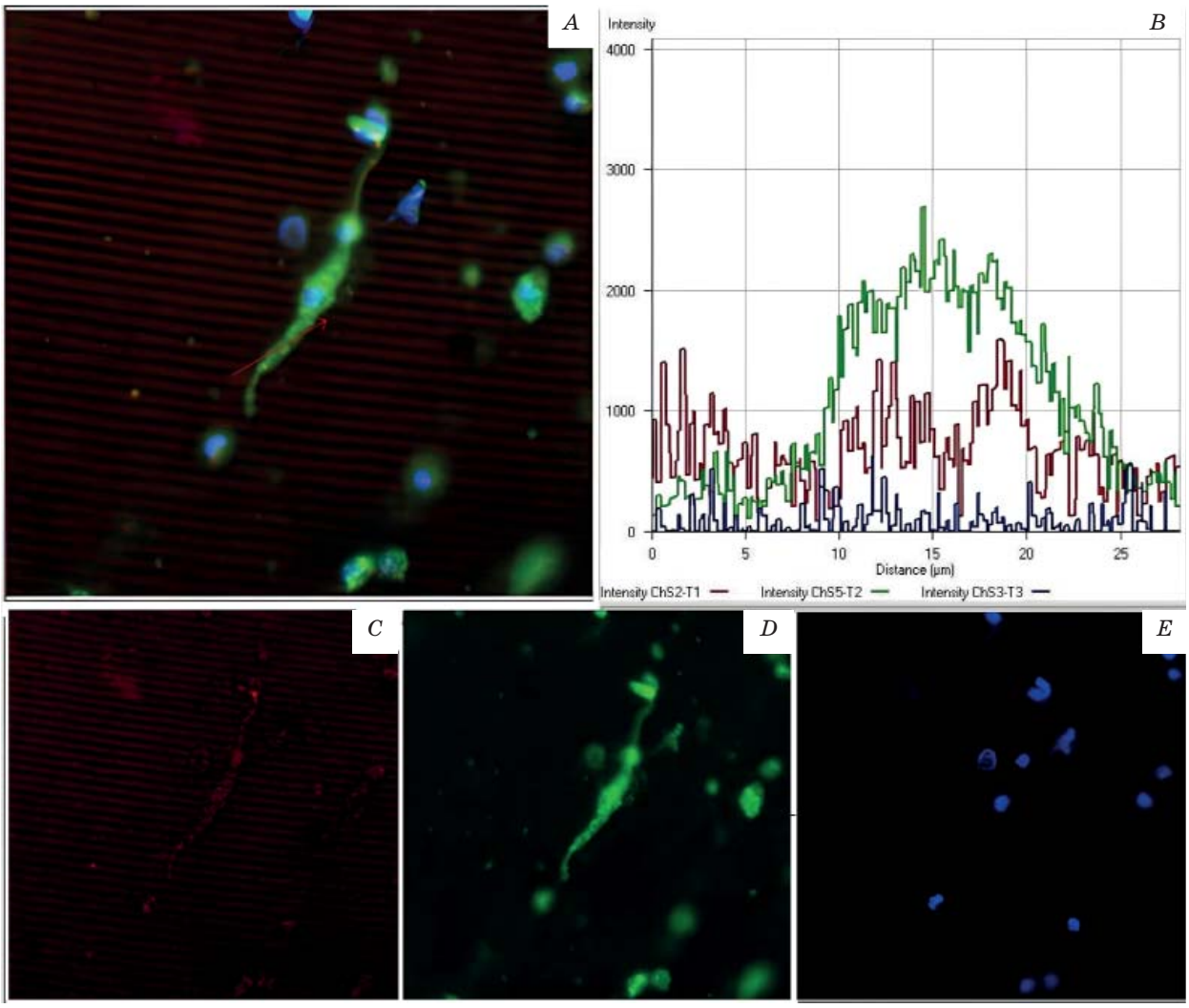

Fig. 2. **Evidence of calix[4]arenes' penetration in uterine smooth muscle cell**
Example of colocalization of fluorescent probes FITC-labeled calix[4]arene C-1308 (10 µM, green) and MitoTracker Orange CM-H2TMRos (200 nM, red) in myocytes (*A, B*). The computer analysis of the fluorescent dyes distribution profiles (*C–E*). Blue color — specific to the nucleus dye Hoechst 33342 (50 nM)

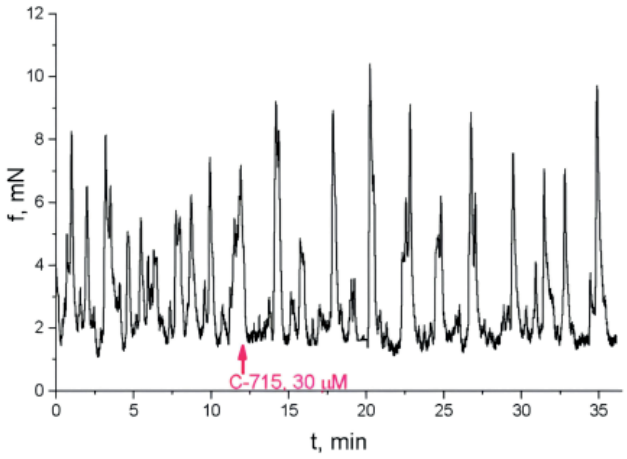

Fig. 3. **Typical mechanogram of the modulation of spontaneous contractions in the longitudinal smooth muscles of rat fallopian tubes and under the action of calix[4]arene C-715 (30 µM)**
The arrow indicates the moment of the compound adding to the normal Krebs solution

particular, inhibiting the electron transport chain under the influence of C-715 results in a decrease in the electrical potential on the inner mitochondrial membrane and a corresponding suppression of Ca^{2+} accumulation. These data also correlate with our results on the decrease in myocytes' hydrodynamic diameter (characteristic size) obtained by photon correlation spectroscopy. At 30 μM, this decrease reaches 30%, comparable to the similar effect of oxytocin at 10 μM.

Conclusions. Thus, the action of calix[4]arene C-715 on uterine smooth muscle cells is directed at reducing Ca^{2+} transport activity and Ca^{2+}-dependent processes in mitochondria, particularly electron transport chain activity and NO synthesis, which enhances myometrial contractile activity. The obtained data suggest the potential use of the studied calix[4]arene for targeted modulation of mitochondrial functional activity and, prospectively, as a uterotonic agent.

Authors' contribution

ISF performed both preparation of biological objects and solutions, executed spectrofluorimetric studies, and wrote the article; OVT carried out contractile activity studies including mechanokinetic analysis; RVR synthesized the studied compounds; MVR performed flow cytometry and laser correlation spectroscopy experiments; HVD carried out confocal imaging and statistical processing of results; YuVD guided the conception of the research and analyzed the results.

Funding source

This work was supported by grant funding for Palladin Institute of Biochemistry, National Academy of Sciences of Ukraine: "Creation of Modern Calixaren Regulators of Biochemical Processes for Medicine and Biotechnology" (State registration number 0123U100894), "Study of Molecular and Membrane Mechanisms of Calcium Signal Regulation in Smooth Muscle Cells" (State registration number 0124U000224).

Acknowledgment

The authors gratefully acknowledge PhD S.O. Karakhim for technical support in working with the laser confocal microscope and PhD O.Yu. Chunikhin for technical support in working with the laser correlation spectrometer.

REFERENCES

1. Matuz-Mares, D., González-Andrade, M., Araiza-Villanueva, M. G., Vilchis-Landeros, M. M., Vázquez-Meza, H.(2022). Mitochondrial calcium: effects of its imbalance in disease. *Antioxidants*, 11(5), 801. https://doi.org/10.3390/antiox11050801
2. Wray, S., Prendergast, C. (2019). The myometrium: from excitation to contractions and labour. *Adv. Exp. Med. Biol.,* 1124, 233–263. https://doi.org/10.1007/978-981-13-5895-1_10
3. Kosterin, S. O., Kalchenko, V. I., Veklich, T. O., Babich, L. G., Shlykov, S. G. (2019). Calixarenes as modulators of ATP-hydrolyzing systems of smooth muscles. Kyiv. 256 p.
4. Kosterin, S. O., Tsymbalyuk, O. V. (2022). Mechanokinetics of visceral smooth muscle and its modulation by nanomaterials. Kyiv. 232–247.

UDC: 612.33+577.1 https://doi.org/10.15407/biotech18.02.035

METABOLIC CHARACTERISTICS OF GASTRIC CONTENTS UNDER CONDITIONS OF NEUROMUSCULAR DYSFUNCTION OF THE ESOPHAGOGASTRIC JUNCTION

A.M. HALINSKA[1, 2], *O.V. SEVERYNOVSKA*[2], *O.O. HALINSKYI*[1]

[1]SI "Institute of Gastroenterology of the National Academy of Medical Sciences of Ukraine"
[2]Oles Honchar Dnipro National University, Dnipro

E-mail:biolog.anastasia@gmail.com

Received 2025/03/04
Revised 2025/03/26
Accepted 2025/04/30

Neuromuscular dysregulation at the esophagogastric junction, characteristic of achalasia cardia, leads to alterations in the metabolic composition of gastric contents, particularly in acidity, pepsin concentration, bile acids, and protective mucosal factors. Investigating these changes is essential for understanding the pathophysiological mechanisms underlying motor-secretory dysfunction and the development of esophageal and gastric disorders. The relevance of such research is underscored by the limited available data on the biochemical composition of gastric juice in the context of esophageal dysfunction, especially achalasia cardia, thereby highlighting the need for further investigations in this area.

Aim. The work was purposed to determine the biochemical characteristics of gastric contents in neuromuscular dysfunction of the esophagogastric junction.

Materials and Methods. In total of 69 patients with achalasia of the cardia and 26 control subjects were examined. The following parameters were assessed: pH, pepsin, cholic acid, NOx, calcium, glycoproteins, fucose, glycosaminoglycans, and sialic acid.

Results. Patients demonstrated increased gastric content volume (2.9 times), cholic acid (1.8 times), and sialic acid (2.4 times), as well as elevated NOx (68.2%) and calcium (31.6%) levels. Glycoproteins (85.7%), fucose (73.0%), and glycosaminoglycans (35.5%) were significantly decreased.

Conclusions. Neuromuscular dysfunction is associated with alterations in the composition of gastric juice, weakening of protective factors, and accumulation of aggressive metabolites, indicating local homeostatic disruption.

Keywords: achalasia of the cardia, gastric juice, mucosal protection, biochemical markers.

Neuromuscular dysregulation of the lower esophageal sphincter leads to alterations in the motor-secretory function of the esophagogastric junction, a hallmark feature of Achalasia cardia. This dysfunction is accompanied by delayed gastric content clearance, changes in acidity, and qualitative transformation of gastric secretions, all of which are essential contributors to disease progression. Various studies have highlighted the significance of specific biochemical parameters of gastric juice, including pH, concentrations of pepsin, and bile acids [1], as well as mucosal protective markers and molecules involved in local homeostasis, such as mucins [2]. The investigation of these changes offers insights into the mechanisms underlying altered gastric composition and reveals potential metabolic shifts associated with esophageal dysfunction [3–5].

Citation: Halinska, A. M., Severynovska, O. V., Halinskyi, O. O. (2025). Metabolic characteristics of gastric contents under conditions of neuromuscular dysfunction of the esophagogastric junction. *Biotechnologia Acta*, 18(2), 35–37. https://doi.org/10.15407/biotech18.02.035

A review of the current literature indicates that, despite several relevant studies, the biochemical alterations in gastric secretions in the context of esophageal dysfunction remain insufficiently explored, underscoring the need for further targeted research in this domain.

Aim. The work purposed to determine the physicochemical and biochemical characteristics of gastric contents in neuromuscular dysfunction of the esophagogastric junction.

Methods. Gastric juice samples from 69 patients with symptoms of impaired lower esophageal sphincter relaxation were analyzed; samples were collected during diagnostic video gastroscopy (achalasia of the cardia, ICD-10 K22.0). The examinations were conducted at the Department of Mini-Invasive Endoscopy, SI "IGNAMSU". The control group included 26 apparently healthy volunteers without gastrointestinal pathology. The following parameters were assessed: pH, concentrations of pepsin, bile acids, sialic acid, fucose, and glycosaminoglycans [6]. Calcium was determined using the "Filisit-Diagnostics" reagent kit. NOx levels were measured using nitrate reduction followed by diazotization. The study was conducted in accordance with ethical standards. Statistical analysis was performed using Microsoft Excel. Data are presented as Me (Q1; Q3); group comparisons were performed using the Mann–Whitney U test; $P < 0.05$ was considered statistically significant.

Results and Discussion. Significant changes in the physicochemical and biochemical composition of gastric contents were identified in patients with achalasia of the cardia compared to the control group. The gastric content volume in patients was 7.65 (5.08; 10.08) mL, which was 2.9 times higher than that in controls 2.60 (2.10; 4.70) mL ($P < 0.001$). The pH level in patients was elevated by 6.0% — 3.08 (2.18; 4.55) versus 2.90 (2.45; 3.58); however, this difference did not reach statistical significance ($P = 0.58$). Pepsin concentration showed a decreasing trend of 0.50 (0.08; 0.80) mg/mL in patients versus 0.92 (0.70; 1.21) mg/mL in the control group (45.8%; $P = 0.055$). Glycoprotein concentration was significantly reduced by 85.7% in patients with 0.09 (0.06; 0.16) mmol/L compared to 0.63 (0.36; 0.80) mmol/L in controls ($P = 0.001$). Cholic acid levels increased 1.8 times — 211 (140; 404) μmol/L versus 118 (113; 121) μmol/L in the control group ($P < 0.001$).

Total calcium concentration was elevated by 31.6% — 1.27 (1.08; 1.52) compared to 0.97 (0.76; 1.21) ($P = 0.045$). NOx levels were 68.2% higher in patients — 52.21 (21.69; 119.49) μmol/L compared to 31.03 (24.39; 36.63) μmol/L in controls ($P = 0.017$). The level of sialic acid in patients was 2.4 times higher — 0.18 (0.08; 0.28) mmol/L versus 0.08 (0.04; 0.08) mmol/L ($P = 0.007$). Fucose concentration was reduced by 73.0% — 0.30 (0.18; 0.58) mmol/L compared to 1.12 (0.41; 1.12) mmol/L in controls ($P = 0.001$). Glycosaminoglycans were decreased by 35.5% — 0.52 (0.30; 0.73) mmol/L versus 0.80 (0.55; 0.93) mmol/L in the control group ($P = 0.009$).

Analysis of the physicochemical and biochemical composition of gastric contents in achalasia revealed significant changes compared to the control group, as shown in Table 1.

The observed changes in the composition of gastric contents indicate a marked impairment of mucosal function, reduced protective capacity, and activation of aggressive metabolites [7]. The increase in volume, cholic acid, NOx, and sialic acid, combined with decreased levels of pepsin [8] and

Table 1. **Biochemical parameters of gastric juice**

Parameter	Control group ($n = 26$) Me (Q1;Q3)	Achalasia of the cardia ($n = 69$) Me (Q1;Q3);	*P*-value
Volume, mL	2.60 (2.10; 4.70)	7.65 (5.08;10.08)	< 0.001
pH	2.90 (2.45;3.58)	3.08 (2.18;4.55)	0.58
Pepsin, mg/mL	0.92 (0.7;1.21)	0.50 (0.08;0.80)	0.055
Glycoproteins, mmol/L	0.63 (0.36;0.80)	0.09 (0.06;0.16)	0.001
Cholic acid, μmol/L	118 (113;121)	211 (140;404)	< 0.001
Total calcium mmol/L	0.97 (0.76;1.21)	1.27 (1.08;1.52)	0.045
NOx, μmol/L	31.03 (24.39;36.63)	52.21 (21.69;119.49)	0.017
Sialic acid, mmol/L	0.08 (0.04;0.08)	0.18 (0.08;0.28)	0.007
Fucose, mmol/L	1.12 (0.41;1.12)	0.30 (0.18;0.58)	0.001
Glycosaminoglycans, mmol/L	0.80 (0.55;0.93)	0.52 (0.30;0.73)	0.009

mucus components, suggests destabilization of local homeostasis in achalasia. This area of research requires further development, as current literature lacks sufficient data specifically addressing the biochemical parameters associated with neuromuscular dysregulation of the lower esophageal sphincter.

Conclusions. In patients with achalasia of the cardia, significant alterations in the biochemical composition of gastric contents were identified, indicating impaired secretory and protective functions. An increase in gastric volume was observed along with stable pH and reduced pepsin levels, as well as decreased concentrations of glycoproteins, fucose, and glycosaminoglycans, suggesting a compromised mucosal barrier. Elevated levels of cholic acid, calcium, and NOx may reflect duodenogastric reflux and impaired motor regulation, while increased sialic acid may indicate mucus degradation. These changes may play a key role in the pathogenesis of the condition, justifying further investigation and the search for relevant biomarkers.

Authors' contribution

AMH performed biochemical analysis, primary statistical processing, and writing the abstract; OVS reviewed the manuscript and participated in data analysis; OOH designed the tables and statistical analysis.

Funding source

This research was carried out as part of the state-funded project at the SI "Institute of Gastroenterology of the NAMS of Ukraine" (2023–2024, No. 0119U102471).

Acknowledgment

The authors express their gratitude to the SI "IGNAMSU" for the opportunity to conduct the study and for scientific and methodological support. Special thanks are extended to Doctor of Medical Sciences N.V. Prolom for participation in the collection of gastric juice samples during video gastroscopy.

REFERENCES

1. Sharma, P., Yadlapati, R. (2021). Pathophysiology and treatment options for gastroesophageal reflux disease: looking beyond acid. *Ann. N. Y. Acad. Sci.*, 1486(1), 3–14. https://doi.org/10.1111/nyas.14501
2. Vllahu, M., Voli, A., Licursi, V., Zagami, C., D'Amore, A., Traulsen, J., Woelffling, S., Schmid, M., Crickley, R., Lisle, R., Link, A., Tosco, A., Meyer, T. F., Boccellato, F. (2024). Inflammation promotes stomach epithelial defense by stimulating the secretion of antimicrobial peptides in the mucus. *Gut. Microbes.*, 16(1), 2390680. https://doi.org/10.1080/19490976.2024.2390680
3. Ates, F., Vaezi, M. F. (2015). The pathogenesis and management of achalasia: current status and future directions. *Gut Liver.,* 9(4), 449–463. https://doi.org/10.5009/gnl14446
4. Ergun, P., Kipcak, S., Dettmar, P. W., Fisher, J., Woodcock, A. D., Bor, S. (2022). Pepsin and pH of gastric juice in patients with gastrointestinal reflux disease and subgroups. *J. Clin. Gastroenterol.,* 56(6), 512–517. https://doi.org/10.1097/MCG.0000000000001560
5. Martinsen, T. C., Fossmark, R., Waldum, H. L. (2019). The Phylogeny and biological function of gastric juice-microbiological consequences of removing gastric acid. *Int. J. Mol. Sci.,* 20(23), 6031. https://doi.org/10.3390/ijms20236031
6. Rudenko, A. I., Maykova, T. V., Mosiychuk, L. M., Ponomarenko, O. A., Tolstykova, T. M., Syrotenko, A. S. (2004). *Clinical and laboratory assessment of the functional state of the secretory glands of the stomach.* Kyiv. 1–23.
7. Mittal, R., Vaezi, M. F. (2020). Esophageal motility disorders and gastroesophageal reflux disease. *N. Engl. J. Med.,* 383(20), 1961–1972. https://doi.org/10.1056/NEJMra2000328
8. da Rocha, J. R., Ribeiro, U., Cecconello, I., Sallum, R. A., Takeda, F., Nasi, A., Szachnowicz, S. (2009). Gastric secretory and hormonal patterns in end-stage chagasic achalasia. *Dis. Esophagus.,* 22(7), 606–610. https://doi.org/10.1111/j.1442-2050.2009.00961.x

UDC 577.218+616-006 **https://doi.org/10.15407/biotech18.02.038**

ADAPTOR PROTEIN CIN85 POTENTIATES THE MOTILITY OF OSTEOSARCOMA CELLS

I. HORAK[1, 2], *T. SKATERNA*[2], *M. PŘIKRYL*[1], *J. NAVRÁTILOVÁ*[1, 3], *J. ŠMARDA*[1], *L. DROBOT*[2], *P. BENEŠ*[1, 3], *L. KNOPFOVÁ*[1, 3]

[1]Department of Experimental Biology, Faculty of Science, Masaryk University, Brno, Czech Republic
[2]Department of Cell Signaling, Palladin Institute of Biochemistry, National Academy of Sciences of Ukraine, Kyiv, Ukraine
[3]International Clinical Research Center, Brno, Czech Republic

E-mail: iryna.horak@gmail.com

Received 2025/03/27
Revised 2025/03/06
Accepted 2025/04/30

Osteosarcoma (OSA) is the most common primary malignant bone tumor in children and adolescents, characterized by high metastatic potential and poor prognosis. The adaptor protein CIN85 is known to be upregulated in various cancers and is involved in cell motility and invasion.

Aim. This study was purposed to investigate the role of CIN85 in the migration of osteosarcoma cells.

Methods. *In vitro*, scratch assay, xCELLigence, and Transwell assay were used to evaluate cell migration, while RNA-seq, qPCR, and Western blotting assessed gene expression.

Results. Public datasets revealed elevated CIN85/*SH3KBP1* expression in OSA tissues compared to normal bone, with even higher levels observed in metastases. Functional studies using CIN85-overexpressing and CIN85-silenced HOS and SAOS-2 osteosarcoma cells demonstrated that CIN85 promotes OSA cell migration and invasion in both 2D and 3D models. RNA-seq analysis identified differentially expressed genes and enriched pathways related to migration, extracellular matrix, adhesion, and cell signaling. CIN85-driven motility was shown to depend on the expression of *COL3A1* and *MMP2*, Akt/mTOR signaling, and NOX activity.

Conclusion. These findings support CIN85 as a potential biomarker and therapeutic target in osteosarcoma.

Keywords: osteosarcoma, migration, metastasis, CIN85.

Osteosarcoma (OSA) represents the most prevalent primary malignant tumor of the bone, primarily affecting children and adolescents. It accounts for approximately 8.9% of all cancer-related deaths in the pediatric population. The disease most frequently arises in long bones such as the femur, tibia, and humerus, while less commonly observed in the skull, mandible, pelvis, and ribs. One of the most concerning aspects of OSA is its aggressive metastatic behavior, particularly to the lungs and, less frequently, to other bones. At the time of diagnosis, around 20% of patients already present with metastases, which significantly worsens prognosis. The 5-year survival rate for patients with metastatic OSA remains low — approximately 30%. Current treatment regimens typically involve surgical removal of the tumor in combination with multi-agent chemotherapy, which includes drugs like methotrexate, doxorubicin, and

Citation: Horak, I., Skaterna, T., Přikryl, M., Navrátilová, J., Šmarda, J., Drobot, L., Beneš, P., Knopfová, L. (2025). Adaptor protein CIN85 potentiates the motility of osteosarcoma cells. *Biotechnologia Acta*, 18(2), 38–40. https://doi.org/10.15407/biotech18.02.038

cisplatin. In some cases, immunotherapy is also being explored as an adjunct treatment. Despite these efforts, outcomes remain unsatisfactory, particularly for those with metastatic disease, making the identification of reliable prognostic biomarkers essential for advancing personalized therapeutic approaches [1].

High-grade OSA is characterized by a variety of genetic mutations and disruptions in several cellular signaling and metabolic pathways that control proliferation, survival, and motility. Among the most commonly observed molecular alterations are mutations in the tumor suppressor gene TP53, along with enhanced activity in pathways such as IGF1R, PI3K/Akt, and MAPK. Additionally, OSA cells exhibit metabolic reprogramming regulated by signaling cascades, including PI3K/Akt/mTOR, HIF-1, Wnt, Hippo, NF-κB, and MAPK, which contribute to the aggressive nature of the disease [1, 2].

One protein of emerging interest in cancer biology is CIN85, an adaptor protein encoded by the SH3KBP1 gene and a member of the CIN85/CMS family. CIN85 has been found to be upregulated in multiple tumor types, such as breast, prostate, cervical, colon, and esophageal cancers, as well as gliomas. Its overexpression is frequently associated with poor patient outcomes. CIN85 is known to participate in processes such as vesicle trafficking, cell adhesion, motility, and invasion. It exerts its effects through interaction with a wide range of signaling proteins (according to the BioGRID database, there are about 150 binding partners identified). In cancerous and normal cells, CIN85 is involved in multiple signaling pathways, including HIF1α, TGFβ, Src, EGFR, MAPK, PI3K-Akt, and TNF [3, 4], and in this manner affects cell behavior and gene expression.

Given these diverse roles, CIN85 is considered a significant contributor to tumor progression and a potential prognostic biomarker. Nevertheless, little is known about the specific function of CIN85 in non-epithelial tumors like osteosarcoma. Consequently, the current study aimed to examine CIN85 expression levels in OSA and to explore its functional relevance, particularly regarding the migratory behavior of osteosarcoma cells.

Methods. Public databases (TNMplot, GEO, Human Protein Atlas) were used to analyze *SH3KBP1* expression in OSA tissues and cell lines. HOS and SAOS-2 cells were transfected with pRc/CMV2-Rukl plasmid (upCIN85) or *SH3KBP1*-targeting siRNA (siCIN85). Migration was assessed using an xCELLigence real-time system, scratch assay, and collagen-embedded spheroids. The invasion was evaluated via collagen Transwell assay. The CEITEC facility at Masaryk University performed RNA-seq and DEG analysis. Statistical analysis was conducted using Origin; $P < 0.05$ was considered significant.

Results and Discussion. SH3KBP1 expression was significantly elevated in OSA vs. normal bone (TNMplot) and higher in metastases than in primary tumors (GEO datasets GSE220538, GSE237033, GSE87624, GSE32981). It was shown that a high level of CIN85 expression was associated with enhanced OSA cell motility in 2D and 3D assays.

Transcriptomic analysis identified hundreds of differentially expressed genes dependent on CIN85. Eight genes (*HCLS1, PLPP2, ETS1, ESM1, DHRS2, ARHGDIB, ADAM19, PHLDA2*) were inversely regulated between upCIN85 and siCIN85 cells. Enrichment analysis revealed involvement in proliferation, apoptosis, adhesion, ECM remodeling, and migration. Key pathways included NF-κB, TNF, MAPK, Wnt, PI3K/Akt/mTOR, TGF, and VEGF.

Functional assays confirmed that CIN85-driven migration involves the expression of *COL3A1* and *MMP2* genes, Akt/mTOR signaling, and NADPH oxidase (NOX) activity.

This study highlights the adaptor protein CIN85 as a key regulator of osteosarcoma (OSA) cell migration and collagen invasion. Elevated expression of CIN85 has previously been observed in several cancers and is frequently linked to poor clinical outcomes. Consistent with these findings, our analysis shows that CIN85 is significantly upregulated in osteosarcoma tissues compared to normal bone and in metastasis compared to primary tumors. Furthermore, CIN85 upregulation leads to increased migration and invasiveness of osteosarcoma cells. The main highlights of this study are shown in Fig. 1.

Conclusion. Our results demonstrate that CIN85 is overexpressed in osteosarcoma and is associated with increased metastatic potential. Functional studies confirmed that CIN85 promotes cell migration and invasion in 2D and 3D conditions. Notably, CIN85-induced motility depends on *COL3A1* and *MMP2* expression, as well as on activation of the Akt/mTOR signaling and NOX. These findings provide a basis for further investigation of CIN85 as a potential prognostic marker and therapeutic target in OSA.

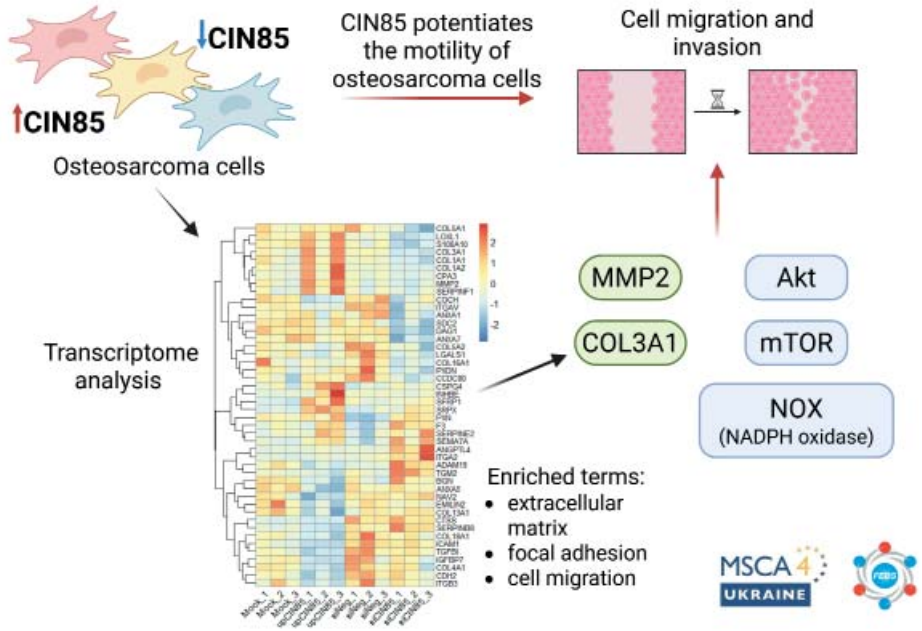

Fig. 1. **Adaptor protein CIN85 potentiated the motility of osteosarcoma cells**
Image created with BioRender [https://www.biorender.com]

Authors' contribution

IH performed migration/invasion assays, RNA isolation, transcriptomic analysis, and statistical analysis. TS studied the effect of Apocynin on cell motility. MP and JN contributed to 3D spheroid assays. IH, LK, PB, JS, and LB conceptualized the study. All authors contributed to manuscript preparation and revision.

Funding source

This project has received funding through the MSCA4Ukraine project, which the European Union funds. Views and opinions expressed are, however, those of the author(s) only and do not necessarily reflect those of the European Union. Neither the European Union nor the MSCA4Ukraine Consortium as a whole nor any individual member institutions of the MSCA4Ukraine Consortium can be held responsible for them.

The FEBS Ukrainian Short-Term Fellowship supported this research.

REFERENCES

1. Smeland, S., Bielack, S. S., Whelan, J., Bernstein, M., Hogendoorn, P., Krailo, M. D., Gorlick, R., Janeway, K. A., …, Marina, N. (2019). Survival and prognosis with osteosarcoma: outcomes in more than 2000 patients in the EURAMOS-1 (European and American Osteosarcoma Study) cohort. *Eur. J. Cancer,* 109, 36–50. https://doi.org/10.1016/j.ejca.2018.11.027
2. An, F., Chang, W., Song, J., Zhang, J., Li, Z., Gao, P., Wang, Y., Xiao, Z., Yan C. (2024). Reprogramming of glucose metabolism: Metabolic alterations in the progression of osteosarcoma. *J. Bone Oncol.,* 44, 100521. https://doi.org/10.1016/j.jbo.2024.100521
3. Samoylenko, A., Vynnytska-Myronovska, B., Byts, N., Kozlova, N., Basaraba, O., Pasichnyk, G., Palyvoda, K., , Yaroslav Bobak, Y., …, Drobot, L. (2012). Increased levels of the HER1 adaptor protein Rukl/CIN85 contribute to breast cancer malignancy. *Carcinogenesis*, 33, 1976–84. https://doi.org/10.1093/carcin/bgs228
4. Havrylov, S., Jolanta Redowicz, M., Buchman, V. L. (2010). Emerging Roles of Ruk/CIN85 in Vesicle-Mediated Transport, Adhesion, Migration and Malignancy. *Traffic,* 11. 721–31. https://doi.org/10.1111/j.1600-0854.2010.01061.x.

UDC 582.66: 602 **https://doi.org/10.15407/biotech18.02.041**

OBTAINING IN VITRO CALLUS BIOMASS OF AMARANTH VARIETY "LERA"

K.I. HUTSKO, R.O. PETRINA

Lviv Polytechnic National University, Lviv

E-mail: kateryna.i.hutsko@lpnu.ua

Received 2025/03/07
Revised 2025/03/13
Accepted 2025/04/30

Aim. To obtain callus biomass of the amaranth variety "Lera" *in vitro* and determine the optimal concentration of growth regulators in the nutrient medium for maximum callus formation.

Methods. The study was conducted using in vitro cell culture. Cultivation was performed on a modified Murashige-Skoog medium supplemented with benzylaminopurine and naphthylacetic acid at various concentrations. Experimental conditions: photoperiod 16/8 h (light/darkness), temperature 20±1 °C, illumination 2000 lux, relative humidity 70%. The total cultivation duration was 56 days.

Results. The seed sterilization method used resulted in a 52% yield of viable explants. Callusogenesis was studied on media containing 3 mg/L BAP in combination with NAA at concentrations ranging from 0.25 to 1.25 mg/L. A total of 61 explants were introduced into each medium. On the 28th day, the explants were subcultured onto a fresh medium of identical composition. The frequency of callus induction was 15–38% on the 28th day and 50–77% on the 56th day, depending on the medium composition.

Conclusions. The optimal medium for obtaining callus culture of the amaranth variety "Lera" is Murashige-Skoog medium supplemented with 3 mg/L BAP and 0.5 mg/L NAA, which provides the highest frequency of callus induction.

Keywords: *Amaranthus hypochondriacus*, cell culture method, callus biomass, frequency of callus induction.

Amaranthus spp. are significant plants with great importance in the food, cosmetic, and pharmaceutical industries. Amaranthus is known for its valuable nutritional properties, including proteins, fats, fibers, and minerals [1], and it contains various metabolites such as flavonoids, carotenoids, squalane, and betalains [2, 3].

The *Amaranthus hypochondriacus* variety "Lera" is an early-ripening cultivar. It has a red inflorescence measuring 50–55 cm, green stems and leaves with red veins, and white grains, while the plant itself reaches a height of 200–220 cm [4]. The ethanol extract of *A. hypochondriacus* leaves and seeds contains numerous metabolites, including flavonoids, polyphenolic compounds, and essential amino acids [5].

Plant biomass obtained through cell culture methods provides a continuous and reliable source of metabolites year-round. The efficiency of *in vitro* callus formation depends on the plant genotype, the composition of the culture medium, and the presence of appropriate concentrations of growth regulators [1].

To obtain callus biomass of *Amaranthus,* a modified Murashige-Skoog (MS) medium supplemented with 3.0 mg/L 6-benzylaminopurine (BAP) and 0.5 mg/L 2,4-dichlorophenoxyacetic acid (2,4-D) or 1-naphthaleneacetic acid (NAA) has been used. Studies have shown that this

Citation: Hutsko, K. I., Petrina, R. O. (2025). Obtaining in vitro callus biomass of Amaranth variety "Lera". *Biotechnologia Acta*, 18(2), 41–44. https://doi.org/10.15407/biotech18.02.041

combination can promote callus formation and growth within 20 days, though the callus induction rate varies by variety, ranging from 50% to 95% [1].

For *Amaranthus tricolor* callus biomass production, it is recommended to use MS medium with either 1 mg/L BAP and 10 mg/L NAA or 1.0 mg/L BAP and 0.5 mg/L 2,4-D [6].

Aim. To obtain callus biomass of amaranth from seeds of the "Lera" variety using the *in vitro* cell culture method and to determine the optimal concentration and ratio of growth regulators in a modified MS medium for maximum biomass production.

Methods. The object of the study was environmentally friendly amaranth seeds of the "Lera" variety from "Amarant Bio" (Cherkasy, Ukraine). To improve germination, the seeds were soaked in water for 72 hours. They were then sterilized with a 30% hydrogen peroxide solution for 20 minutes and washed three times with sterilized distilled water.

The sterilized seeds were transferred to Petri dishes containing a hormone-free MS medium and incubated under the following conditions: photoperiod 16/8 h (light/dark), temperature 20±1 °C, illumination 2000 lux, and relative humidity 70%. After 9 days, sprouts measuring 1.3±0.2 cm were obtained and transferred to a modified MS medium.

The modified MS medium was supplemented with BAP and NAA at various concentrations. Glucose (30 g/L) served as the carbon source. Cultivation was conducted for 28 days under the same conditions: photoperiod 16/8 h (light/dark), temperature 20±1 °C, illumination 2000 lux, and relative humidity 70%. After this period, subculturing was performed using a nutrient medium of identical composition.

The frequency of callus induction was determined as the ratio of explants with callus to the total number of explants. All experiments were performed in triplicate. The results were statistically analyzed using Microsoft Excel 2010 software, with the arithmetic mean and standard error calculated.[1, 7].

Results and Discussion. The yield of viable explants was 52%, with a sterilization efficiency of 100% when using the proposed seed sterilization method.

Aseptically grown whole amaranth sprouts were used for further cultivation. Cultivation was conducted on MS medium supplemented with BAP in combination with varying concentrations of NAA. Variants of the MS nutrient medium with different concentrations of growth regulators are presented in Table 1. A total of 61 explants were introduced into each medium.

Cultivation was conducted for 28 days. Some explants exhibited thickening, particularly noticeable in the apical meristem, along with an increase in callus mass. Infected explants were discarded and excluded from further experiments. During cultivation on different nutrient media, variations in the intensity of callus formation were observed. The callus formation frequency of *Amaranthus hypochondriacus* cultivated on the studied modified nutrient media (MS1– MS4) on the 28^{th} day of cultivation is presented in Fig. 1.

On the 28^{th} day of cultivation, the explants were subcultured onto a fresh modified medium of identical composition. Cultivation was continued for another 28 days. Infected explants were discarded and excluded from further experiments. The frequency of callus induction of *Amaranthus hypochondriacus* cultivated on the studied modified nutrient media (MS1– MS4) on the 56^{th} day of cultivation is presented in Fig. 2.

The lowest frequency of callus induction was observed in the callus culture of *Amaranthus hypochondriacus* cultivated on the nutrient medium MS1, supplemented with 3.0 mg/L BAP and 0.25 mg/L NAA. It was found that the optimal medium among those tested was MS2 (3.0 mg/L BAP and 0.5 mg/L NAA), which showed the highest frequency of callus induction on both the 28^{th} and 56^{th} days.

Table 1. **Composition of modified MS medium for cultivation of *Amaranthus hypochondriacus***

Modified MS medium	Concentration of growth regulators, mg/ L	
	BAP	NAA
MS1	3	0.25
MS2	3	0.50
MS3	3	1
MS4	3	1.25

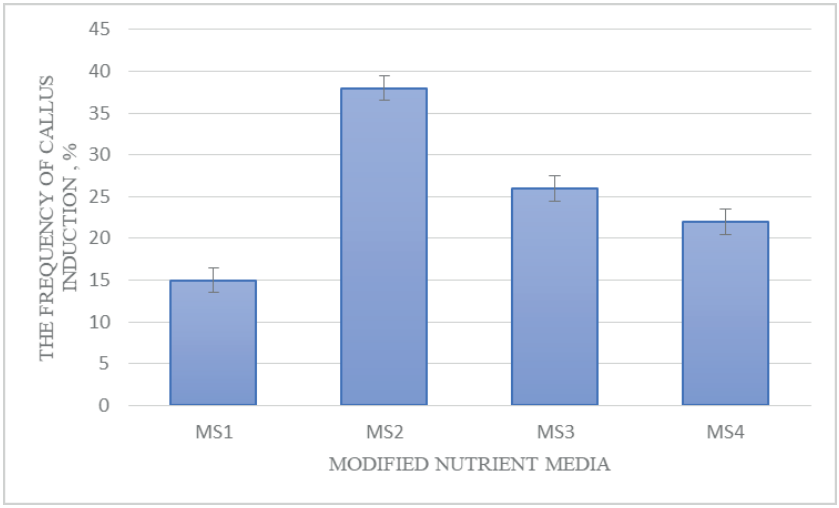

Fig. 1. **The frequency of callus induction of Amaranthus hypochondriacus on the 28th day of cultivation on modified nutrient media MS1–MS4 (mean ± standard error, *n* = 3)**

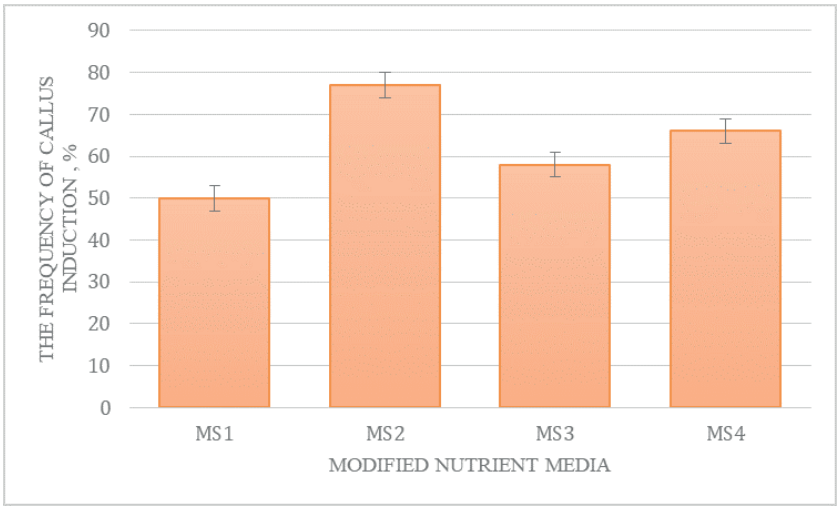

Fig. 2. **The frequency of callus induction of *Amaranthus hypochondriacus* on the 56th day of cultivation on modified nutrient media MS1–MS4 (mean ± standard error, *n* = 3)**

Conclusions. It was established that the optimal nutrient medium for cultivating the callus culture of *Amaranthus hypochondriacus* is Murashige–Skoog, supplemented with 3 mg/L BAP and 0.5 mg/L NAA, at a temperature of 20±1°C, illumination of 2000 lux, and relative humidity of 70%, on which the highest frequency of callus induction was observed.

Authors' Contribution

K. I. Hutsko — goal setting, conducting research stages: preparation of nutrient medium, seed germination, introduction of explants into the medium, subculturing, analysis of results, writing the thesis. R.O. Petrina– methodology search, control of cultivation conditions, analysis of results, writing the thesis.

Funding source

The present research was conducted without any external financial support.

REFERENCES

1. Hadidi, M., Aghababaei, F., Mahfouz,i M., Zhang, W., Julian, McClements D. (2024). Amaranth proteins: From extraction to application as nanoparticle-based delivery systems for bioactive compounds. *Food chemistry*, 439. https://doi.org/10.1016/j.foodchem.2023.138164
2. Xuan, Y., Liu, S., Xie, L., Pan, J. (2023). Establishment of *Amaranthus* spp. calluses and cell suspension culture, and the effect of plant growth regulators on total flavonoid content. *Tropical Plants,* 2, 15. https://doi.org/10.48130/TP-2023-0015
3. Hutsko, K. I., Petrina, R. O. (2024). Amaranthus as a source of polyphenolic compounds and flavonoids for use in medicine. *Biotechnologia Acta*, 17(2), 46–48. https://doi.org/10.15407/biotech17.02.046
4. Lyubych, V. V., Manzii, O. P., Voitovska, V. I., Klymovych, N. M. (2023). Physicochemical properties of amaranth grain depending on variety and moisture content. *Novitni ahrotekhnolohiyi,* 11(1). https://doi.org/10.47414/na.11.1.2023.275736
5. Barba de la Rosa, A. P., de León-Rodríguez, A., Laursen, B., Fomsgaard, I. (2019). Influence of the growing conditions on the flavonoids and phenolic acids accumulation in amaranth *(Amaranthus hypochondriacus L.)* leaves. *REVISTA TERRA LATINOAMERICANA,* 37(4), 449–457. https://doi.org/10.28940/terra.v37i4.541
6. Comia-Yebron, R., Aspuria, E. T., Bernardo, E. L. (2017). Callus induction in Amaranthus tricolor and Amaranthus spinosus. *Journal of the International Society for Southeast Asian Agricultural Sciences*, 23, 12–23.
7. Zagorodnya, D. S., Hutsko, K. I., Petrina, R. O. (2021). Investigation of the influence of growth regulators on the growth of callula biomass *Carlina acaulis. Vcheni zapysky TNU imeni V.I. Vernadskoho. Seriya: Tekhnichni nauky,* 6(71), 161–166. https://doi.org/10.32838/2663-5941/2021.6/26

UDC 577.47: 504.054 **https://doi.org/10.15407/biotech18.02.045**

INDICATION OF THE BIOCHEMICAL TARGETS OF RARE EARTH ELEMENTS IN BIVALVE MOLLUSCS UNDER MULTIPLE EXPOSURE

V. KHOMA[1], *K. YUNKO*[2], *V. MARTYNIUK*[3], *M. ZARIAN*[4], *V. HAVRYSHKIV*[2]

[1]Ternopil Scientific Research Forensic Center of the Ministry of Internal Affairs of Ukraine, Ternopil
[2]Ternopil Volodymyr Hnatiuk National Pedagogical University, Ternopil
[3]Ternopil Ivan Puluj National Technical University, Ternopil
[4]Nature Research Centre, Vilnius, Lietuvos Respublika

E-mail: khomav@tnpu.edu.ua

Received 2025/03/05
Revised 2025/03/11
Accepted 2025/04/30

Rare earth elements (REE) are considered the pollutants of priority, and biological effects are studied poorly.

Aim. Our study was devoted to the elucidation of suspected biochemical effects of two representative REEs, gadolinium (Gd) and yttrium (Y), individually and in a mixture with Ca-channel blocker nifedipine (Nfd), using the freshwater bivalve *Unio tumidus* as a model organism.

Materials and Methods. The specimens of swollen river mussel *Unio tumidus* were treated with GdCl3, 30 nM, YCl3, 30 nM, or their mixture with Nfd (10 µM) for 14 days. The set of metal-binding, reductive state, biotransformation activities, and toxicity in the digestive gland of mussels was selected.

Results. All exposures caused the elevation of the ratio of reduced and oxidized forms of nicotinamide adenine dinucleotide ($NADH/NAD^+$ ratio) and increase of the levels of reduced and oxidized glutathione (GSH and GSSG), the total level of cysteine-rich protein metallothionein (MTSH) in the Gd- and Y- groups and non-metalated MTSH in all exposures. The effects on the transformation of Phase I and Phase II enzymes were exposure-dependent. Dynamin-related GTP-ase activity increased in all exposures. The lysosomal membrane integrity and apoptotic activity decreased only in the Gd-group.

Conclusion. REEs in low concentrations cause adaptive metabolic responses in the mussels. The changes in the Zn distribution within the cells and Zn-dependent functions were indicated, confirming the impact of REEs on the functionality of the essential metal. In the combined exposure of REEs with a Ca-channel blocker, a cumulative effect was detected.

Keywords: Gadolinium, Yttrium, multiple exposure, mussels, stress.

Rare earth elements (REE) are considered “strategic elements” [6]. Consequently, the rising of their entry into the surface waters from anthropogenic sources can be expected. Knowledge about the biological role of REEs is currently fragmentary [1]. The REEs can disrupt ion regulation [4]. Therefore, the combined exposure to REEs and Ca-channel blocker nifedipine (Nfd) can elucidate this regularity.

Citation: Khoma, V., Yunko, K., Martyniuk, V., Zarian, M., Havryshkiv, V. (2025). Identification of biochemical targets of rare earth elements in bivalve mollusks under multiple exposure. *Biotechnologia Acta*, 18(2), 45–47. https://doi.org/10.15407/biotech18.02.045

Aim. The assessment of the impact of two representative REEs, gadolinium (Gd) and yttrium (Y), individually and in a mixture with Nfd, on the metal-related functions and stress response in the bivalve *Unio tumidus*.

Methods. The specimens of swollen river mussel *U. tumidus* from the pristine area were distributed randomly to four groups: untreated mussels (C) and treated with GdCl3, 30 nM, YCl3, 30 nM, or their mixture with Nfd (10 μM) during 14 days. The digestive gland was utilized. The applied methods are described thoroughly in our previous work [7]. Briefly, reduced and oxidized forms of nicotinamide coenzymes (NADH and NAD+) were determined according to the enzymatic cycling assay based on the oxidation of ethanol to acetaldehyde with the reduction of NAD+. Reduced and oxidized glutathione (GSH and GSSG) were quantified by the glutathione reductase recycling assay using 5,5-dithiobis-2-nitrobenzoate (DTNB) for thiols quantification. Metallothionein protein (MTSH) concentration was determined after the ethanol/chloroform extraction utilizing DTNB. For the determination of Zn bound to metallothioneins (ZnMT), these heat-denaturated proteins were isolated by chromatography on a Sephadex G-50. The concentration of Zn in the tissue (Zn t) and ZnMT were measured utilizing the reaction of the complexation of Zn(II) with 5-Br-PAPS. For the evaluation of biotransformation activities, we analyzed the activities of cytochrome P450 (CYP450) related ethoxy resorufin *O-demethylase* (EROD) by indicating the formation of resorufin in the presence of reduced form nicotinamide adenine dinucleotide phosphate (NADPH), glutathione *S*-transferase (GST), using GSH and 1-chloro-2,4-dinitrobenzene as the substrate, and GTPase dynamin utilizing guanosine triphosphate (GTP) as the substrate and malachite green for the determining of the released inorganic phosphate. The caspase-3-related activity assay was based on the cleavage of peptide acetyl-Asp-Glu-Val-Asp p-nitroanilide (Ac-DEVD-pNA). The loss of lysosomal membrane integrity was analyzed utilizing the Neutral Red Retention (NRR) assay. The IBM SPSS Statistics version 26 software for Windows was used for calculations.

Results and Discussion. The responses of reductive shift belong to almost unified responses to stress in facultative anaerobes like bivalve mollusks [7]. The present study confirms these previous findings. Indeed, all exposures caused the elevation of the NADH/NAD+ ratio from 0.56 to 1.03-1.15, particularly in the Mix-group. The level of GSH and GSSG increased simultaneously in all exposures, particularly in the Gd-group (GSH about five times), resulting in the relatively stable rate of GSH/GSSG ratio (Fig. 1). The level of cysteine-rich protein MTSH increased in the Gd- and Y-groups but was corresponding to control value in the Mix-group. The part of ZnMT changed not so prominently, and, consequently, in all treated groups, the part of non-metallated protein increased, promoting the redox state of SH-groups [7]. The Zn t increased in all exposures by 15-32%, leading to a rise of Zn partitioning among other than ZnMT cellular targets. The biotransformation manifestations were more particular depending on the exposure (Fig. 1).

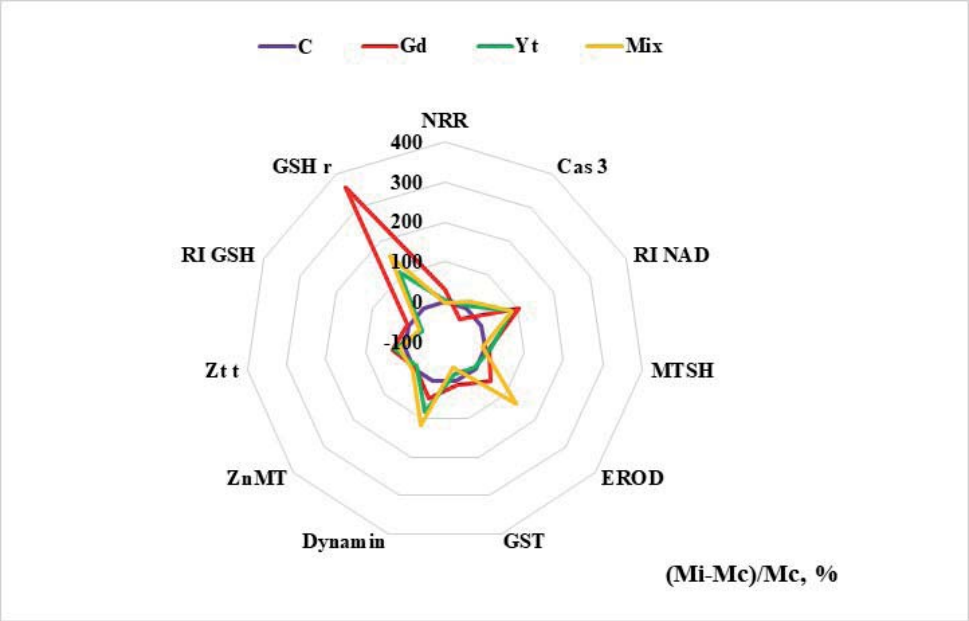

Fig. 1. **Graphical presentation of relative to control (C) responses of biomarkers in the exposures of *Unio tumidus* to the Gadolinium (Gd), Yttrium (Y), and their mixture with nifedipine (Mix)**

EROD activity increased in the Gd- and, particularly, in the Mix-groups, whereas GST was activated by Gd and depressed by Y and Mix. Significantly, dynamin-related GTPase activity increased in all exposures (up to two times in the Mix-group). The lysosomal membrane integrity decreased only in the Gd-group (by 32%). The caspase-3 activity was oppressed in the Gd-group, probably due to the highest level of unbound to MT Zn, its inhibitor [5], but increased by Mix.

The comparison of the reactions indicated, in most cases, the higher limits of responses in the Gd-group. Lifting of biotransformation and apoptotic activities demonstrated the cumulative effect in the presence of Nfd [2, 3].

Conclusion. Low nM concentrations of REEs cause adaptive metabolic responses in the mussels. The dependence on the Zn distribution within the cells was indicated, confirming the interaction between REEs and essential metals activities and its distorting in the multiple exposures with Ca-channel blocker.

Authors' contribution

VK: data analysis, presentation, analysis, interpretation, drafted manuscript; KY: sampling, biochemical and data analysis, presentation; VM: biochemical analysis, sampling, data analysis; MZ: biochemical and data analysis; VH: biochemical analysis, sampling.

Funding source

The work was supported by the bilateral Ukraine-Lithuania scientific project of the Ministry of Education and Science of Ukraine (M/48-2024, M/48-2025) and Project No S-LU-24-13 under the Lithuanian-Ukrainian Cooperation Program.

Acknowledgment

We are grateful to the supervisors of the projects, Prof O. Stoliar, Dr. L. Manusadžianas, and staff Dr. L. Gnatyshyna, PhD R. Karitonas, and PhD B. Gylytė for their professional guidance and valuable support of this study.

REFERENCES

1. Banaee, M., Mossotto, C., Maganza, A., Azizi, P., Prearo, M., Pastorino, P., Faggio, C. (2025). Rare earth elements on aquatic organisms: Toxicity, detoxification, and ecological implications. *Emerging Contaminants*, 11(1), 100457. https://doi.org/10.1016/j.emcon.2024.100457
2. Khoma, V., Gnatyshyna, L., Martinyuk, V., Mackiv, T., Mishchenko, L., Manusadzïanas, L., Stoliar, O. (2021). Common and particular biochemical responses of *Unio tumidus* to herbicide, pharmaceuticals and their combined exposure with heating. *Ecotoxicol. Environ. Saf.*, 208, 111695. https://doi.org/10.1016/j.ecoenv.2020.111695
3. Khoma, V. V., Gnatyshyna, L. L., Martinyuk, V. V., Mackiv, T. R., Mishchuk, N. Y., Stoliar, O. B. (2020). Metallothioneins contribution to the response of bivalve mollusk to xenobiotics. *Ukr. Biochem. J.*, 92(5), 87–96. https://doi.org/10.15407/ubj92.05.087 Q4
4. Lachaux, N., Otero-Fariña, A., Minguez, L., Sohm, B., Rétif, J., Châtel, A., Poirier, L., Devin, S., Pain-Devin, S., Gross, E. M., Giamberini, L. (2023). Fate, subcellular distribution and biological effects of rare earth elements in a freshwater bivalve under complex exposure. *The Science of the total environment*, 905, 167302. https://doi.org/10.1016/j.scitotenv.2023.167302
5. Lambert, J. C., Wang, G. W., Kang, Y. J. (2001). Zinc inhibition of caspase-3 activation does not protect HeLa cells from apoptotic cell death. *Toxicology and applied pharmacology*, 175(1), 89–93. https://doi.org/10.1006/taap.2001.9239
6. Malhotra, N., Hsu, H. S., Liang, S. T., Roldan, M. J. M., Lee, J. S., Ger, T. R., Hsiao, C. D. (2020). An updated review of toxicity effect of the rare earth elements (REEs) on aquatic organisms. *Animals (Basel)*, 10(9), 1663. https://doi.org/10.3390/ani10091663
7. Martyniuk, V., Matskiv, T., Yunko, K., Khoma, V., Gnatyshyna, L., Faggio, C., Stoliar, O. (2024). Reductive stress and cytotoxicity in the swollen river mussel (*Unio tumidus)* exposed to microplastics and salinomycin. *Environ Pollut.*, 350, 123724. https://doi.org/10.1016/j.envpol.2024.123724

UDC 602.4+604+663.1 **https://doi.org/10.15407/biotech18.02.048**

EFFECT OF B VITAMIN ADDITION ON THE BIOSYNTHESIS OF LACTIC ACID BY *Lactobacillus delbrueckii*

D.I. KIIV, S.V. VASYLYUK

Lviv Polytechnic National University

E-mail: dimakiiv@gmail.com

Received 2025/03/15
Revised 2025/03/21
Accepted 2025/04/30

Aim. The main objective of this work is to investigate the effect of B vitamins on the biosynthesis of lactic acid (LA) by the *Lactobacillus delbrueckii* UY-2/13 strain when using corn-steep liquor as the sole nitrogen source.

Methods. The influence of B vitamins was assessed using a one-factor experimental design. The lactic acid concentration in the culture broth at the end of fermentation was determined using high-performance liquid chromatography, while reducing sugars were analyzed by the modified Bertrand method.

Results. The study revealed that riboflavin (B_2) at a concentration of 1 mg/L increased lactic acid production by approximately 6%, whereas calcium pantothenate (B_5) reduced it by about 4%. Other vitamins (PP, B_9, B_1, B_6, H) had no significant effect on LA biosynthesis.

Conclusions. Vitamins B_2 and B_5 have a specific effect on the biosynthesis of lactic acid by *L. delbrueckii* UY-2/13. Other B vitamins (PP, B_9, B_1, B_6, and H) do not significantly influence the biosynthesis of lactic acid.

Keywords: *Lactobacillus delbrueckii*, lactic acid biosynthesis, B vitamins, cofactor supplementation, vitamin influence.

Lactic acid, also known as hydroxypropanoic acid, is an industrially significant organic acid primarily produced through biotechnological processes. Lactic acid bacteria (LAB) are the leading microbial producers of lactic acid; however, their cultivation requires complex nutrients that must be incorporated into the fermentation medium [1]. One of the most commonly used components is yeast extract, which can account for up to 38% of the total production costs, making large-scale lactic acid manufacturing economically challenging [2].

To reduce costs, alternative low-cost nitrogen sources can be used instead of yeast extract. However, such substitutions often lead to a significant decrease in process efficiency. The critical role of yeast extract in LA biosynthesis is attributed to its composition, particularly its content of purine and pyrimidine bases, as well as B vitamins [3]. These vitamins are essential cofactors in metabolic pathways responsible for carbohydrate conversion into lactic acid [4].

Thus, the complete or partial replacement of yeast extract with more affordable nitrogen sources, supplemented with B vitamins, may help sustain high lactic acid concentrations while substantially reducing fermentation costs.

Aim. The main objective of this work was to investigate the effect of B vitamin supplementation on LA biosynthesis by *Lactobacillus delbrueckii* UY-2/13 when using corn-steep liquor as the sole nitrogen source.

Citation: Kiiv, D. I., Vasylyuk, S. V. (2025). Effect of B vitamin addition on the biosynthesis of lactic acid by *Lactobacillus delbrueckii*. *Biotechnologia Acta*, 18(2), 48–50. https://doi.org/10.15407/biotech18.02.048

Methods. Microorganism. L. delbrueckii UY-2/13 was obtained from the industrial collection of production strains (DE "Enzym", Ladyzhyn, Ukraine). *Cultivation.* The seed culture was grown in MRS medium (De Man, Rogosa, and Sharpe, 1960) in test tubes and flasks at 40±2 °C for 16 hours. Lactic acid biosynthesis was conducted in 300 mL-Erlenmeyer flasks containing 150 mL of medium (glucose — 180 g/L, corn steep liquor — 60 g/L, $CaCO_3$ — 10 g/L). The media were sterilized at 112 °C for 20 minutes. Fermentation was performed at 40±2 °C without stirring, with an inoculum volume of 10%, and a total process duration of 96 hours. The pH was maintained between 4.5 and 6.5 by adding a 10% $Ca(OH)_2$. *Preparation of vitamin solutions*. Sterile vitamin solutions were obtained by filtration through a 0.2 µm cellulose acetate membrane (Sartorius Corporation, New York, USA) and added after medium sterilization. The tested vitamins and their concentrations were as follows: PP (10 mg/L), B_5 (6 mg/L), B_2 (1 mg/L), B_9 (500 µg/L), B_1 (500 µg/L), B_6 (400 µg/L), and H (30 µg/L).

Analysis. The LA concentration was determined using high-performance liquid chromatography (Shimadzu® LC-40D; Shimadzu Corporation, Kyoto, Japan). The concentration of reducing sugars was measured using the modified Bertrand method. The lactic acid yield was calculated considering the dilution factor of the culture fluid with a 10% $Ca(OH)_2$.

Results and Discussion. The selection of vitamin concentrations for the fermentation medium was based on literature data [2, 4] and an approximate calculation of their content in yeast extract at a concentration of 30 g/L. The influence of vitamins was assessed using a one-factor experimental design.

As shown in Figure, riboflavin (B_2) exhibited a positive effect on lactic acid biosynthesis, increasing its concentration by approximately 6%. In contrast, calcium pantothenate (B_5) reduced LA production by approximately 4% (Fig.). Other tested vitamins (PP, B_9, B_1, B_6, H) had no significant impact on lactic acid biosynthesis under the given experimental conditions. According to the results obtained, vitamins B_2 and B_5 in the described concentrations have a specific effect on the biosynthesis of LA.

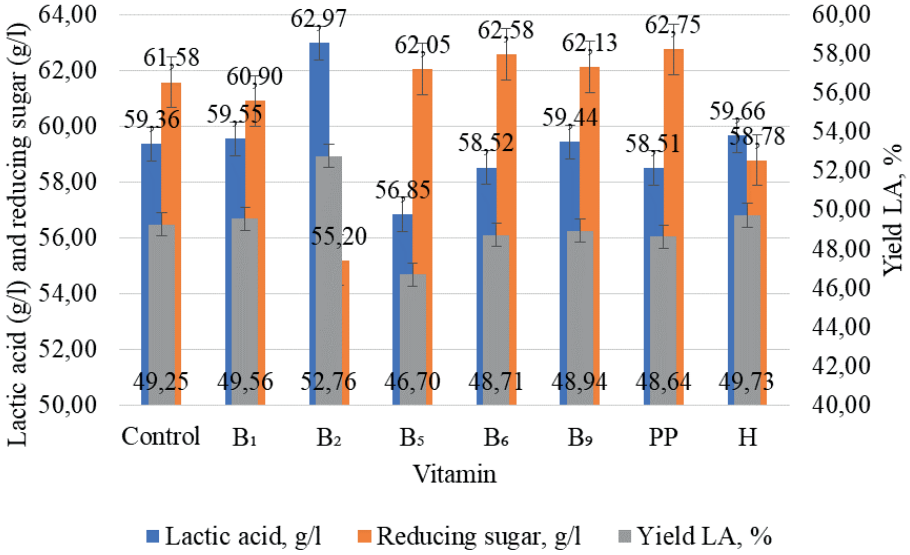

Figure. **Study of the effect of B vitamins on the biosynthesis of lactic acid by strain *L. delbrueckii* UY-2/13**
Control — without the addition of vitamins

Conclusions. Vitamins B_2 and B_5 have a specific effect on the biosynthesis of lactic acid by *L. delbrueckii* UY-2/13. Other B vitamins (PP, B_9, B_1, B_6, and H) do not significantly influence the biosynthesis of lactic acid.

Authors' contribution

Dmytro Kiiv conducted the literature review, performed the experimental studies and data analysis, and drafted the manuscript. Sofia Vasylyuk provided critical input throughout the research, data analysis, and manuscript preparation. All authors have read and approved the final version of the manuscript.

Acknowledgment

The authors express their gratitude to the CEO of DE "Enzim" Valeriy Volodymyrovych Skorokhod, Head of the R&D Laboratory Natalia Borysivna Martyniuk, and the staff of DE "Enzim" (24321, Ladyzhyn, Khlibozavodska St., 2, Vinnytsia region) for providing the *L. delbrueckii* UY-2/13 strain, research facilities, and initial data for this study.

REFERENCES

1. Kiiv, D., Vasylyuk, S., Lubenets, V. (2024). Lactic acid: Industrial synthesis, microorganisms-producers and substrates: A review. *Chemistry & Chemical Technology*. 18(2), 157–169. https://doi.org/10.23939/chcht18.02.157
2. Ma, K., Cui, Y., Zhao, K., Yang, Y., Wang, Y., Hu, G., He, M. (2022). D-Lactic acid production from agricultural residues by membrane integrated continuous fermentation coupled with B vitamin supplementation. *Biotechnology for Biofuels and Bioproducts*. 15(1). https://doi.org/10.1186/s13068-022-02124-y
3. Yu, L., Lei, T., Ren, X., Pei, X., Feng, Y. (2008). Response surface optimization of l-(+)-lactic acid production using corn steep liquor as an alternative nitrogen source by Lactobacillus rhamnosus CGMCC 1466. *Biochemical Engineering Journal*. 39(3), 496–502. https://doi.org/10.1016/j.bej.2007.11.008
4. Xu, G.-Q., Chu, J., Zhuang, Y.-P., Wang, Y.-H., Zhang, S.-L. (2008). Effects of vitamins on the lactic acid biosynthesis of Lactobacillus paracasei NERCB 0401. *Biochemical Engineering Journal*. 38(2), 189–197. https://doi.org/10.1016/j.bej.2007.07.003

UDC 581.1:615.322:577.2 **https://doi.org/10.15407/biotech18.02.051**

"HAIRY" ROOT CULTURE OF *Scutellaria altissima* L. FOR HIGH-LEVEL FLAVONOID PRODUCTION

K.S. KOSHCHAVKO

Institute of Biology and Medicine of Taras Shevchenko National University of Kyiv, Ukraine

E-mail: kseniako05@gmail.com

Received 2025/03/13
Revised 2025/03/19
Accepted 2025/04/30

The study is devoted to the obtaining of *Scutellaria* "hairy" root culture and the analysis of the level of accumulation of pharmacologically valuable substances in *Scutellaria* plants.

The aim was to obtain the transgenic root culture of *Scutellaria altissima* L. and *Scutellaria albida* L. via *Agrobacterium rhizogenes*-mediated transformation and to compare the level of flavonoid accumulation in the obtained cultures.

Methods: surface sterilization of seeds, *A. rhizogenes*-mediated genetic transformation, polymerase chain reaction, spectrophotometric method for determination of flavonoids by rutin.

As a result of *Agrobacterium*-mediated transformation we obtained the "hairy" root cultures of these plants, and PCR-analysis proved the transgenic nature of the obtained cultures. A significantly higher flavonoid content was shown for *Ri*-root culture compared to the roots of plants grown *in vitro* plants and came up to ±0,12 mg/g and ±0,09 mg/g respectively.

Conclusions. The transgenic root culture of *Scutellaria altissima* was characterized by a high content of flavonoids and can be considered a pharmacologically promising material.

Keywords: *Scutellaria* L., genetic transformation, *Agrobacterium rhizogenes*, hairy root culture, flavonoids, antioxidant activity.

The modern pharmaceutical industry offers a wide range of chemical-based medicines that are characterized by their rapid effect on the human body. Still, at the same time, they are known for their side effects and contraindications. The search for herbal medicines that would be effective and have no side effects is becoming increasingly important.

Recent studies of the antibacterial and antioxidant effects of *Scutellaria altissima* extracts have shown these mechanisms being based on the effect of the flavonoid substances (scutellarin, vogonin, baikalin, and baikalein) [1, 2]. These substances were shown to accumulate mainly in the root tissues of these plants. Therefore, the obtaining of hairy root culture, which is known for its relatively low-cost cultivation and hormone-free rapid growth, is promising. This way, *A. rhizogenes*-meadiated genetic transformation can be used in order to obtain "hairy" root cultures of *S. altissima* and *S. albida*, which are considered promising producers of compounds with antioxidant and antiviral properties [3]. However, the problem of genetic transformation's effect on the accumulation levels of biologically active compounds in plants remains unstudied.

Our study aimed to obtain *Scutellaria* transgenic root culture and compare the level of accumulation of biologically active compounds for the obtained transgenic root and intact root cultures.

All the studies were carried out at the Institute of Cell Biology and Genetic Engineering NAS of Ukraine.

Citation: Koshchavko, K. S. (2025). "Hairy" root culture of *Scutellaria altissima* L. for high-level flavonoid production. *Biotechnologia Acta*, 18(2), 51–53. https://doi.org/10.15407/biotech18.02.051

Scutellaria plants were introduced into *in vitro* culture by surface sterilization of seeds of two *Scutellaria* L. species (*S. albida*, *S. altissima*) by rinsing them in 70% ethanol solution for 1 minute and in 25% hydrogen peroxide solution for 20 minutes. The plants were cultivated on Murashige-Skoog medium [4] at 18–20 °C, 16-hour photoperiod. We used 6–12-week plants for further genetic transformation. The overnight bacterial suspension culture (*Agrobacterium rhizogenes* A4 strain) was sedimented by centrifugation for 10 min. (4000 rpm), then, the precipitate was resuspended in a liquid MS medium. The plant (*S. albida* and *S. altissima*) explants were cultivated with bacterial suspension in an orbital shaker (150 rpm) for 48 hours at 28 °C. Subsequently, the explants were transferred to an MS agar medium with the addition of 400 mg/L of antibiotic cefotaxime for bacteria elimination.

To confirm the transgenic nature of the obtained root cultures, we performed PCR analysis for the presence of *Agrobacterium rolB* gene (fragment size 780 bp, nucleotide sequence of primers: *5′-atggatcccaaattgctattccttccacga-3′*, *5′-ttaggcttctttcttcaggtttactgcagc-3′*). The amplification was carried out under the following conditions: denaturation 94 °C/ 5 min, 30 cycles (denaturation 94 °C/ 30 s, annealing 55 °C/ 30 s, synthesis 72 °C/ 50 s), final synthesis 72 °C/ 5 min. The reaction products were separated by electrophoresis in a 1.5% agarose gel in a TAE buffer system.

The plant material was weighed, homogenized in 96% ethanol, and centrifuged, and then the supernatant was used for biochemical analysis. In order to analyze the flavonoid content in the transgenic root culture and intact root lines, we used the spectrophotometric method (wavelength = 510 nm) based on the property of flavonoids to form a colored complex with an alcoholic solution of aluminum chloride [5]. The study was performed three times, and the t-test was used to analyze the significance of the difference in the obtained results.

We carried out *A. rhizogenes*-mediated genetic transformation for *S. altissima* and *S. albida* plants. The initiation of root culture was observed on *S. altissima* and *S. albida* plant explants three weeks after transformation. The obtained roots were characterized by *Ri*-phenotype (such as rapid growth, hairness, and lack of geotropism) (Fig. 1). Confirmation of the transgenic nature of the

Fig. 1. **Initiation of hairy root formation in *S. altissima* and *S. albida* explants**

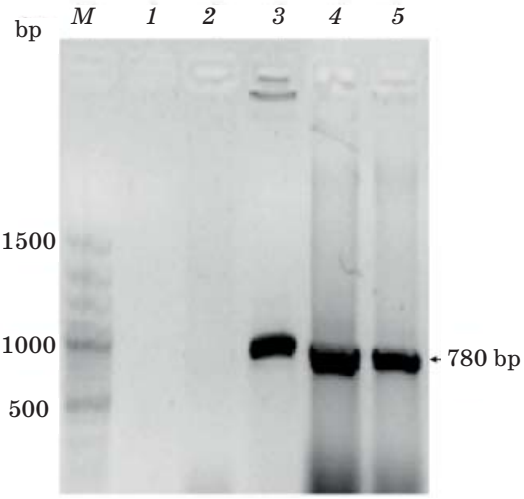

Fig. 2. **Electrophoregram of PCR analysis for the presence of rolB gene:**
M — Marker (1 kb Plus DNA Ladder, Fermentas); *1* — negative control (sample without DNA); *2* — negative control (DNA of a non-transformed plant); *3* — positive control (plasmid DNA (A4)); *4–5* — DNA of the analyzed samples of the “hairy” root culture

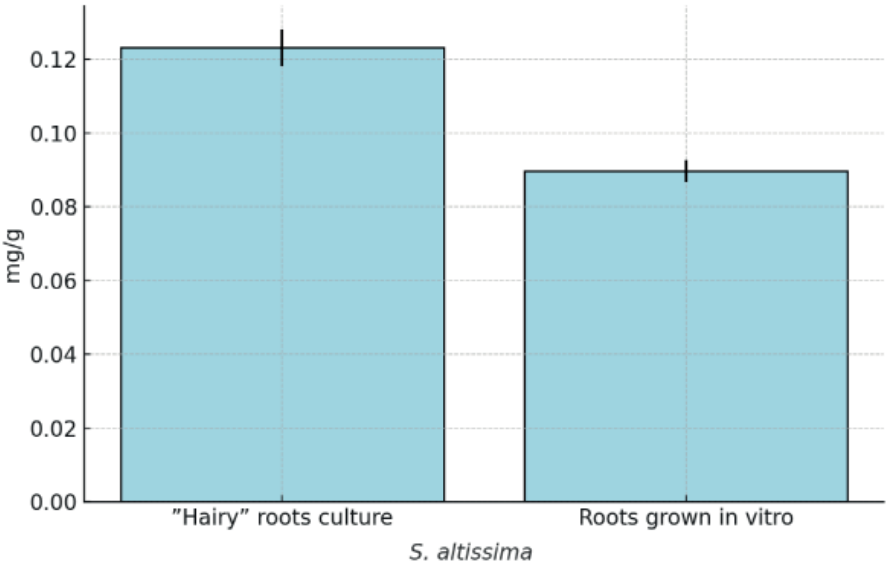

Fig. 3. **Flavonoid content in extracts of transgenic roots and roots of plants grown *in vitro***

obtained root cultures was carried out using the PCR analysis (Fig. 2). For this purpose, a 780 bp fragment of the *Agrobacterium rolB* gene was amplified. The presence of the desired fragment was confirmed for 80% of the analyzed cultures.

In order to analyze the content of flavonoids in the transgenic root and intact root cultures of *S. altissima* plants, the spectrophotometric method was used [3]. This way, the significantly higher flavonoid content was proved for the *Ri*-root culture compared to the roots of plants grown *in vitro* for *S. altissima* plants (Fig. 3).

Conclusions. The obtained data allow us to consider the transgenic root culture of *Scutellaria altissima* L. as a pharmacologically promising one as the high content of flavonoids and beneficial characteristics of cultivation characterized it.

Authors' contribution

Koshchavko K. — planning, data analysis, introduction of plants into *in vitro* culture, genetic transformation of the obtained plants, molecular biological analysis of the obtained cultures, analysis of the flavonoid content in the studied samples, writing article.

Funding source

The author received no financial support for the research, authorship, and publication of this article. At the same time, all the studies were carried out at the Institute of Cell Biology and Genetic Engineering of the National Academy of Sciences of Ukraine and Kyiv Palace Children and Youth.

REFERENCES

1. Georgieva, Y. P. (2021). *Scutellaria altissima L. (Lamiaceae) — Source of biologically significant flavonoids and diterpenes* (PhD dissertation). Medical University of Plovdiv.
2. Shang, X., He, X., He, X., Li, M., Zhang, R., Fan, P., Zhang, Q., Jia, Z. (2010). The genus *Scutellaria*: An ethnopharmacological and phytochemical review. *Journal of Ethnopharmacology*, 128(2), 279–313. https://doi.org/10.1016/j.jep.2010.01.006
3. Stepanova, A. Y., Solov'eva, A. I., Malunova, M. V., Salamaikina, S. A., Panov, Y. M., Lelishentsev, A. A. (2021). Hairy roots *Scutellaria* spp. (Lamiaceae) as promising producers of antiviral flavones. *Molecules*, 26(13), 3927. https://doi.org/10.3390/molecules26133927
4. Murashige, T., Skoog, F. (1962). A revised medium for rapid growth and bioassays with tobacco tissue cultures. *Physiologia Plantarum*, 15(3), 473–497.
5. Pękal, A., Pyrzynska, K. (2014). Evaluation of aluminium complexation reaction for flavonoid content assay. *Food Analytical Methods*, 7, 1776–1782.

UDC 616-006.6:579.61:615.357 **https://doi.org/10.15407/biotech18.02.054**

MODIFICATION OF BREAST CANCER CELLS' SENSITIVITY TO METFORMIN DUE TO CO-CULTIVATION WITH *Bifidobacterium animalis*

T.P. KOZAK, O.O. LYKHOVA, P.A. VIRYCH, V.F. CHEKHUN

R. E. Kavetsky Institute of Experimental Pathology, Oncology, and Radiobiology of the National Academy of Sciences of Ukraine, Kyiv

E-mail: *kozaktamara.work@gmail.com*

Received 2025/03/20
Revised 2025/03/26
Accepted 2025/04/30

Glucose metabolism (GM) disturbances are well-known risk factors for the development of breast cancer (BC). The GM regulator metformin is used as an adjunctive therapy for BC. Another potent modulator of GM in BC cells is the microbiota, particularly bifidobacteria. The combined action of these factors may lead to unpredictable effects on the sensitivity of malignant cells to antitumor agents.

Aim. To investigate the effect of *Bifidobacterium animalis* on the sensitivity of BC cells to the antiproliferative effects of metformin.

Materials and Methods. The impact of *B. animalis* on GM in BC cells was determined by biochemical methods (glucose consumption and lactate production rate, intracellular lactate dehydrogenase activity). Cell viability was evaluated using the trypan blue exclusion test.

Results. Co-cultivation of BC cells with *B. animalis* leads to enhanced glycolysis in malignant cells. These metabolic phenotype changes are accompanied by alterations in the sensitivity of BC cells to metformin. Only in *MCF-7* cells treated with *B. animalis* was a significant enhancement of the antitumor effects of metformin observed compared to cells incubated with either metformin or *B. animalis* alone.

Conclusions. Exposure of *MCF-7* cells to *B. animalis* increases their sensitivity to the antiproliferative effects of metformin, which is a result of GM reprogramming.

Keywords: breast cancer, *Bifidobacterium animalis*, metformin, glucose metabolism.

Breast cancer (BC) is the most common oncological disease and the leading cause of cancer-related mortality among women worldwide. Metabolic disorders are well-established risk factors for breast cancer [1]. Metformin is one of the known regulators of glucose metabolism, which can attenuate metabolic disorders and act as a therapeutic agent against BC. Another powerful modulator of glucose metabolism by BC cells is the microbiota. Among the primary constituents of the human breast microbiota are lactic acid bacteria, particularly bifidobacteria, which can interfere with the lactate cycle in BC cells and influence their sensitivity to agents with antitumor activity [2]an aberrant composition of the microbiome, characterizes breast cancer. In this review we discuss the changes to the metabolism of breast cancer cells, as well as the composition of the breast and gut microbiome in breast cancer. The role of the breast microbiome in breast cancer is unresolved, nevertheless it seems that the gut microbiome does have a role in the pathology of the disease. The gut microbiome secretes bioactive metabolites (reactivated estrogens, short chain fatty acids, amino acid metabolites, or secondary bile acids. Given the potential of bifidobacteria to modulate tumor cell metabolism, it is

Citation: Kozak, T. P., Lykhova, O. O., Virych, P. A., Chekhun, V. F. (2025). Modification of breast cancer cells' sensitivity to metformin *due to* co-cultivation with *B. animalis*. *Biotechnologia Acta*, 18(2), 54–56. https://doi.org/10.15407/biotech18.02.054

of particular relevance to investigate the sensitivity of BC cells to the antitumor effects of metformin under conditions of interaction with the microbiota and its metabolites.

Aim. To investigate the effect of metformin on the viability of intact and *Bifidobacterium* animalis-treated human breast cancer (BC) cells *in vitro*.

Methods. Human breast cancer (BC) cells (luminal T47D, MCF-7; basal MDA-MB-231) were seeded at 1×10^6 cells per 75 cm^2 in DMEM with 10% FBS without antibiotics and incubated for 10 hours in a 5% CO_2 atmosphere. Cells were then treated with *Bifidobacterium animalis subsp. lactis BB-12* (1:400 eukaryotic/bacterial ratio). Untreated cells served as controls. After 72 hours, cells were washed, counted, and analyzed for glucose consumption rate (GCR), lactate production rate (LPR), and lactate dehydrogenase (LDH) activity using biochemical methods and standard formulas [3]. Additionally, 1.5×10^5 untreated and *B. animalis*-treated BC cells were incubated for 24 hours, followed by metformin treatment (50 mM for T47D, 10 mM for MCF-7, and MDA-MB-231). After 48 hours, cell viability was assessed using the trypan blue exclusion assay. Statistical analysis was performed with GraphPad Prism 8.0.1 ($P < 0.05$, Welch's t-test).

Results and Discussion. After 72 hours of incubation of BC cells with *B. animalis*, a decrease in the number of viable T47D and MCF-7 cells by 40–50% ($P < 0.05$) and MDA-MB-231 cells by 25% ($P < 0.05$) was observed compared to untreated cells without bacteria. A shift in the metabolic phenotype of *B. animalis*-treated BC cells towards enhanced glycolysis was also noted, as evidenced by a statistically significant increase in GCR and LPR 2-4 times in T47D and MCF-7 cells and 1.8–2 times in MDA-MB-231 cells compared to untreated cells. The intracellular LDH activity further confirmed these changes in glucose metabolism in B. animalis-treated BC cells. An increase in enzyme activity by 80–90% ($P < 0.05$) in luminal subtype cells and 40% ($P < 0.05$) in basal subtype cells compared to untreated cells was observed. These results suggest that the most significant changes in the metabolic phenotype of BC cells occur in the luminal subtype, likely because the MDA-MB-231 cells preferentially utilize the glycolytic pathway for glucose consumption [4].

The results of the viability analysis of untreated and *B. animalis*-treated BC cells after exposure to metformin show that combined treatment of T47D cells inhibits the antiproliferative effects of *B. animalis* and metformin, which are observed in the monotherapy (Fig. *A*). In MDA-MB-231 cells treated with both agents, no statistically significant difference in cell viability was found compared to cells treated with either metformin or *B. animalis* alone (Fig. *C*). Only in MCF-7 cells treated with *B. animalis*, a statistically significant enhancement of the antiproliferative effect of metformin was observed compared to cells incubated with metformin or *B. animalis* separately (Fig. *B*).

Such an effect of metformin on the viability of *B. animalis*-treated BC cells can be explained by changes in the expression of the insulin receptor in the studied cells. According to the literature, one of the primary mechanisms behind the antitumor effect of metformin is its ability to reduce insulin resistance in malignant cells by increasing the expression of the insulin receptor [5]. Our previous studies [6] have shown that co-cultivation of BC cells with *B. animalis* leads to a decrease in the number of RI+ cells and the receptor expression level in T47D cells. Conversely, it increases both the number of RI+ cells and the level of receptor expression in MCF-7 cells. Furthermore, the increased sensitivity of *B. animalis*-treated MCF-7 cells to the effects of metformin may also be attributed to

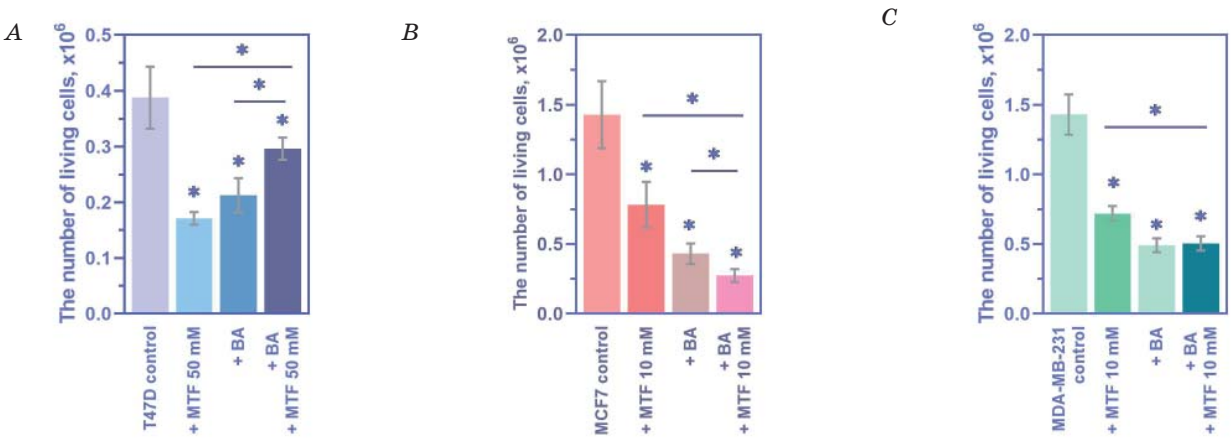

Figure. **Viability of untreated and *B. animalis*-treated human BC cells after incubation with metformin**
$P < 0.05$ to the intact control cells; $P < 0.05$ between the two experimental groups.

the fact that the metabolic phenotype of these cells undergoes the most significant changes as a result of co-cultivation with *B. animalis*.

Conclusions. Pre-treatment of MCF-7 cells with *B. animalis* enhances their sensitivity to the antiproliferative effects of metformin. These changes result from the reprogramming of glucose metabolism in BC cells after co-cultivation with *B. animalis*, which is reflected at the level of receptor expression and metabolite production. The obtained results contribute to our understanding of the role of the microbiota as a component of therapeutic strategies to enhance the efficacy of antitumor therapy.

Authors' contribution

TPK maintained cell culture, conducted experiments with BC cells, *B. animalis*, and metformin, statistical analysis; OOL cell viability assessment and analyzed the results; PAV biochemical analysis; VFC development of research ideas and experimental design.

Funding source

The work was part of the research project "Study of the Impact of Lactobacilli, Bifidobacteria, and Opportunistic Representatives of the Human Microbiota on the Mechanisms of Metabolic Disorders in Tumor Progression" (No. 0121U113840).

REFERENCES

1. Yee, L. D., Mortimer, J. E., Natarajan, R., Dietze, E. C., Seewaldt, V. L. (2020). Metabolic Health, Insulin, and Breast Cancer: Why Oncologists Should Care About Insulin. *Frontiers in Endocrinology*, 11, 58. https://doi.org/10.3389/fendo.2020.00058
2. Mikó, E., Kovács, T., Sebő, É., Tóth, J., Csonka, T., Ujlaki, G., Sipos, A., Szabó, J., Méhes, G., Bai, P. (2019). Microbiome — Microbial Metabolome — Cancer Cell Interactions in Breast Cancer — Familiar, but Unexplored. *Cells*, 8(4), 293. https://doi.org/10.3390/cells8040293
3. Solyanik, G. I., Kolesnik, D. L., Prokhorova, I. V., Yurchenko, O. V., Pyaskovskaya, O. N. (2024). Mitochondrial dysfunction significantly contributes to the sensitivity of tumor cells to anoikis and their metastatic potential. *Heliyon*, 10(12), e32626. https://doi.org/10.1016/j.heliyon.2024.e32626
4. Zare, M. E., Kansestani, A. N., Hemmati, S., Mansouri, K., Vaisi-Raygani, A. (2021). The rate of aerobic glycolysis is a pivotal regulator of tumor progression. *Journal of Diabetes & Metabolic Disorders*, 20(1), 523–531. https://doi.org/10.1007/s40200-021-00774-7
5. Salani, B., Rio, A. D., Marini, C., Sambuceti, G., Cordera, R., Maggi, D. (2014). Metformin, cancer and glucose metabolism. *Endocrine-Related Cancer*, 21(6), R461–R471. https://doi.org/10.1530/ERC-14-0284
6. Kozak, T., Lykhova, O., Bezdieniezhnykh, N., Chekhun, V. (2024). Changes in glucose metabolism in human breast cancer cells after their co-cultivation with Bifidobacterium animalis *in vitro* [in Ukrainian]. *The materials of the 7th Congress of the All-Ukrainian Public Organization "Ukrainian Society of Cell Biology" with international representation*, 38. https://doi.org/10.30970/uscb.2024

UDC 612.33:577.1:615.322 **https://doi.org/10.15407/biotech18.02.057**

EFFECT OF RESVERATROL ON REGULATED CELL DEATH OF ENTEROCYTES UNDER CONDITIONS OF OXIDATIVE STRESS *in vitro*

A.P. LYTVYNENKO, O.T. BLASHKIV, T.Yu. VOZNESENSKA

Bogomoletz Institute of Physiology of the National Academy of Sciences of Ukraine, Kyiv

E-mail: alina_lit@ukr.net

Received 2025/03/12
Revised 2025/03/18
Accepted 2025/04/30

Aim. **The study purposed** to evaluate a concentration-dependent effect of Sirtuin 1 (SIRT1) modulators on cell death of enterocytes in the ileum of the small intestine under conditions of oxidative stress.

Materials and Methods. The experiments were conducted using female Alba mice. *Isolation of enterocytes* was carried out according to Kimura et al. 2015. *Modeling of oxidative stress* (OS) by adding hydrogen peroxide to phosphate-buffered saline: "weak" (50 μM); "medium" (250 μM); "strong" (500 μM). Apoptotic and necrotic death of enterocytes was assessed by morphological characteristics using the in vivo method of the two-color fluorescent nucleic acid dye Hoechst 33342 and propidium iodide. *Substances used*: Resveratrol — SIRT1 activator and Ex527 — specific SIRT1 inhibitor (2 μM, 20 μM, 100 μM).

Results. An increase in the number of live cells ($P < 0.01$) and a decrease in apoptotic ($P < 0.01$) and necrotic ($P < 0.01$) cells was observed with increasing Resveratrol concentration (from 2 to 200 μM) under OS conditions.

Conclusion. The obtained results suggest that Resveratrol reduces cell death of enterocytes, involving activation of SIRT1 under oxidative stress conditions *in vitro*. Further research is needed to confirm the effectiveness of this strategy and to establish protocols for the inclusion of antioxidants in treatment regimens for inflammatory bowel disease.

Keywords: oxidative stress, Sirtuin1, enterocytes, apoptosis, necrosis.

Inflammatory bowel disease (IBD) is a chronic, immune-mediated disorder that affects the gastrointestinal tract [1, 2]. Although the exact etiology of IBD remains unclear, dysfunctional intestinal immunoregulation is believed to be the underlying cause. Among the immunoregulatory factors, reactive oxygen species are produced at abnormally high levels in IBD. The role of oxidative stress (OS) in the pathophysiology of IBD, its diagnostic targets, and the potential use of antioxidant therapy for the prevention and treatment of IBD are under active investigation [3].

Sirtuins (SIRT1 — SIRT7) are nicotinic adenine dinucleotide (+)-dependent histone deacetylases that regulate essential signaling pathways and are involved in numerous biological processes. The role of SIRT1 in OS is under active investigation [4]. SIRT1 can be activated by Resveratrol (Res, 3,4′,5-trihydroxy-trans-stilbene), naturally occurring polyphenolic compound with anti-oxidant, anti-inflammatory and anti-apoptotic effects [5].

Regulated cell death (RCD) plays a vital role in development, tissue homeostasis, inflammation, immunity, and in the development of various pathophysiological conditions. Currently, the study of

Citation: Lytvynenko, A. P., Blashkiv, O. T., Voznesenska, T. Yu. (2025). Effect of resveratrol on regulated cell death of enterocytes under conditions of oxidative stress *in vitro*. *Biotechnologia Acta*, 18(2), 57–59. https://doi.org/10.15407/biotech18.02.057

RCD is promising as one of the possible new therapeutic strategies for prevention of both functional intestinal disorders themselves and the negative consequences of OS.

The study aimed to evaluate a concentration-dependent effect of SIRT1 modulators on cell death of enterocytes in the ileum of the small intestine under conditions of oxidative stress.

Methods. The experiments were conducted using female Alba mice (weighing 18–22 g) and approved by the ethics committee of Bogomoletz Institute of Physiology.

Isolation of enterocytes was performed according to Kimura Y et al. 2015 [1].

O*xidative stress* was simulated using hydrogen peroxide (H_2O_2). By adding calculated amounts of H_2O_2 (88597, Sigma-Aldrich, USA) to phosphate-buffered saline (PBS), pH 7.4, OS was obtained: "weak" (50 µM); "medium" (250 µM); "strong" (500 µM).

Apoptotic and necrotic death of enterocytes was assessed by morphological characteristics using the in vivo method of the two-color fluorescent nucleic acid dye Hoechst 33342 and propidium iodide.

Substances used: Res — SIRT1 activator (2 µM, 20 µM, 100 µM, Carl Roth GmbH Co. KG, Germany) and Ex527 — specific SIRT1 inhibitor (2 µM, 20 µM, 100 µM, Sigma). The results were statistically processed in the Graph Pad Prism version 10.3.0 (507) (GraphPad Software, California USA). Differences were considered statistically significant at $P < 0.05$.

Results and Discussion. A decrease in the number of live cells and an increase in necrotic and apoptotic cells of the ileum were found under the influence of Ex527. No significant changes were found under the influence of Res.

Under conditions of "weak" OS, there were lower live cells to 78.13±1.96% and raised cells with signs of apoptosis to 14.57±2.07 ($n = 6$, $P < 0.05$).

Under conditions of "medium" OS, there is a decrease in live cells to 66.00±1.69% ($n = 6$, $P < 0.05$), an increase in cells with signs of necrosis to 11.88±1.46% ($n = 6$, $P < 0.05$) and apoptosis to 22.13±2.23% ($n = 6$, $P < 0.01$) compared to the control.

Under conditions of "strong" OS, there is a decrease in live cells to 50.75±1.67%, an increase in cells with signs of necrosis to 19.13±1.96%, and apoptosis to 30.13±1.25% ($n = 6$, $P < 0.01$) compared to the control.

It was found that post-incubation with the SIRT1 activator — Res (20 µM) after OS (250 µM) causes an increase in the percentage (of live cells to 75.13±3.31% ($P < 0.05$) and reduces the proportion of cells with signs of apoptosis to 16.13±2.30% ($P < 0.05$) and necrosis to 8.7 ±1.39% ($P < 0.05$, Figure).

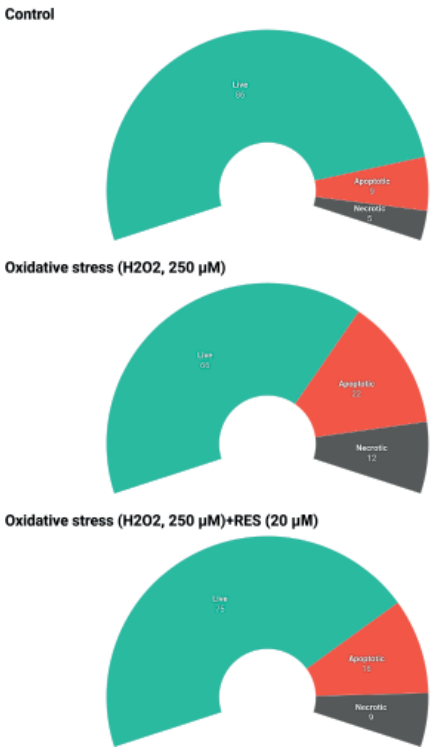

Figure. **Viability of enterocytes of the ileum of the small intestine under experimental conditions:** *1* — control; *2* — oxidative stress; *3* — Resveratrol under oxidative stress

Thus, under conditions of OS, the use of the activator Res causes an increase in the percentage of living cells and a decrease in cells with signs of apoptosis and necrosis.

Conclusions. Resveratrol reduces cell death of enterocytes, involving activation of SIRT1 under oxidative stress conditions *in vitro*. Further research is needed to confirm the effectiveness of this strategy and to establish protocols for the inclusion of antioxidants in treatment regimens for inflammatory bowel disease.

Authors' Contribution

Lytvynenko A.P. — data acquisition, analysis, interpretation; Blashkiv O.T. — data acquisition; Voznesenskaya T.Yu — research design.

Funding source

Budget program "Support for the development of priority areas of scientific research" for 2025–2026.

REFERENCES

1. Kimura, Y., van der Merwe, M., Bering, S. B., Penmatsa, H., Conoley, V. G., Sangild, P. T., Naren, A. P., Buddington, R. K. (2015). Glucose transport by epithelia prepared from harvested enterocytes. *Cytotechnology*, 67(1), 39–49. https://doi.org/10.1007/s10616-013-9656-1.
2. Muzammil, M. A., Fariha, F., Patel, T., Sohail, R., Kumar, M., Khan, E., Khanam, B., Kumar, S., Khatri, M., Varrassi, G., Vanga, P. (2023). Advancements in Inflammatory Bowel Disease: A Narrative Review of Diagnostics, Management, Epidemiology, Prevalence, Patient Outcomes, Quality of Life, and Clinical Presentation. *Cureus*, 15(6), e41120. https://doi.org/10.7759/cureus.41120.
3. Muro, P., Zhang, L., Li, S., Zhao, Z., Jin, T., Mao, F., Mao, Z. (2024). The emerging role of oxidative stress in inflammatory bowel disease. *Front Endocrinol (Lausanne)*, 15, 1390351. https://doi.org/10.3389/fendo.2024.1390351.
4. Wu, Q. J., Zhang, T. N., Chen, H. H., Yu, X. F., Liu, Y. Y., Liu, Y. S., Zheng, G., …, Zhao, Y. H. (2022). The sirtuin family in health and disease. *Signal Transduct Target Ther.*, 7(1), 402. https://doi.org/0.1038/s41392-022-01257-8.
5. Qin, H., Zhang, H., Zhang, X., Zhang, S., Zhu, S., Wang, H. (2021) Resveratrol protects intestinal epithelial cells against radiation-induced damage by promoting autophagy and inhibiting apoptosis through SIRT1 activation. *J. Radiat. Res.,* 62(4), 574–581. https://doi.org/10.1093/jrr/rrab035.

UDC 615.322:616-092 **https://doi.org/10.15407/biotech18.02.060**

EFFECT OF CORNUS FRUIT EXTRACTS ON OXIDATIVE STRESS IN DIABETES

A.A. MOROZ[1], *I.V. BRODYAK*[1], *A.Z. KUCHARSKA*[2], *N.O. SYBIRNA*[1]

[1]Ivan Franko National University of Lviv, Ukraine
[2]Wrocław University of Environmental and Life Sciences, Poland

E-mail: Anna.Moroz@lnu.edu.ua

Received 2025/02/15
Revised 2025/03/07
Accepted 2025/04/30

The biological effects of fruits from different cultivars of the cornelian cherry under diabetes mellitus remain unclear.

Aim. This study was purposed to investigate the effect of fruit extracts from various cultivars of *Cornus mas* L. on primary biomarkers of oxidative stress.

***Materials and Methods*:** oxidative stress metabolites in erythrocytes were assessed by measuring the level of lipid peroxidation and protein oxidation products.

Results. The administration of *C. mas* and *C. mas* × *C. officinalis* hybrids fruit extracts to diabetic rats significantly reduced oxidative stress metabolite levels in erythrocytes.

Conclusions: cornelian cherry fruit extracts are perspective drugs that help inhibit oxidative stress development in erythrocytes under diabetic conditions.

Keywords: cornelian cherry, diabetes mellitus, erythrocytes, oxidative stress, thiobarbituric acid reactive substances, advanced oxidative protein products, oxidatively modified proteins.

Type 1 diabetes mellitus (DM) is a severe metabolic disorder with absolute insulin deficiency that is accompanied by chronic hyperglycemia and the development of oxidative stress. Excessive formation of reactive oxygen species (ROS) and an imbalance in the antioxidants contribute to cellular damage, particularly in erythrocytes [1]. To impede diverse violations caused by oxidation, scientists are exploring natural plant materials with potent antioxidant activity. Cornelian cherry, especially *C. mas* and *C. officinalis* are promising medicinal plants that have strong hypoglycaemic properties [2].

Aim. The effects of cornelian cherry on biomarkers of cell structure oxidation in erythrocytes have not been well studied. Therefore, our study aimed to investigate the effect of fruit extracts of *C. mas* L. (`Uholok´ and `Koralovyi´ cultivars) and *C. mas* × *C. officinalis* hybrids (`Jerzy´ and `Tomasz´ cultivars) on oxidative stress metabolites — thiobarbituric acid reactive substances (TBARS), advanced oxidation protein products (AOPPs) and oxidatively modified proteins of neutral (OMP370) and essential (OMP430) nature in the erythrocytes of rats with DM.

Methods. Type 1 DM was induced in male Wistar rats by intraperitoneal injection of streptozotocin (STZ) at a dose of 55 mg/kg of body weight. The animals were divided into five groups: *first* — control group (healthy rats); *second* — rats with STZ-induced DM; *third*, *fourth* and *fifth* groups — rats with DM that were orally administered fruit extracts from the `Uholok´ cultivar of *C. mas*, fruit extract from the `Koralovyi´ cultivar of *C. mas*, and fruit extract of the hybrids of *C. mas* × *C. officinalis*, respectively, at a dose of 20 mg/kg of body weight for 14 days. The dosage and duration of cornelian cherry extract administration were based on precedent research [2]. The level of TBARS, the contents of AOPPs, and OMPs of neutral and basic nature were measured spectrophotometrically

Citation: Moroz, A. A., Brodyak, I. V., Kucharsk, A. Z., Sybirna, N. O. (2025). Effect of cornus fruit extracts on oxidative stress in diabetes. *Biotechnologia Acta*, 18(2), 60–62. https://doi.org/10.15407/biotech18.02.060

at wavelengths of 532 nm, 340 nm, 370 nm, and 430 nm, respectively [3]. Statistical analysis was performed using a one-way analysis of variance followed by Dunnett's posthoc test ($P < 0.05$ was considered statistically significant).

Results and Discussion. The progressions of oxidative stress in DM lead to ROS interaction with lipids and proteins [1]. Our results showed a significant increase in the TBARS content in erythrocytes of diabetic rats compared to the control group (Figure *A*). Administration of studied fruit extracts to animals with DM reduced the level of this lipid oxidation metabolite (Fig. *A*). The study detected a 30.8% increase in the level of AOPPs in erythrocytes of diabetic rats (Fig. *B*). Additionally, our findings indicate a notable increase in the level of OMPs neutral and basic nature in the erythrocytes of rats with DM (Fig. *C*). The obtained results we associated with excess oxidants and a deficiency of antioxidants [4]. Oral administration of fruit extracts from the `Uholok´ and `Koralovyi´ cultivars and the hybrids `Jerzy´ and `Tomasz´ cultivars to diabetic rats led to a 25.3%, 52.7%, and 29.7% decline in TBARS content, respectively; 24.3%, 16.7% and 34.2% decrease in AOPPs level, accordingly; 35.6%, 27.7% and 35.2% decrease in OMPs of neutral nature content, respectively; and 30.7%, 26.7% and 30.2% decline in OMPs of basic nature level, accordingly (Fig. *A*, *B* and *C*). Such results suggested the potential of the extracts of cornelian cherry to reduce lipid and protein oxidation in blood erythrocytes.

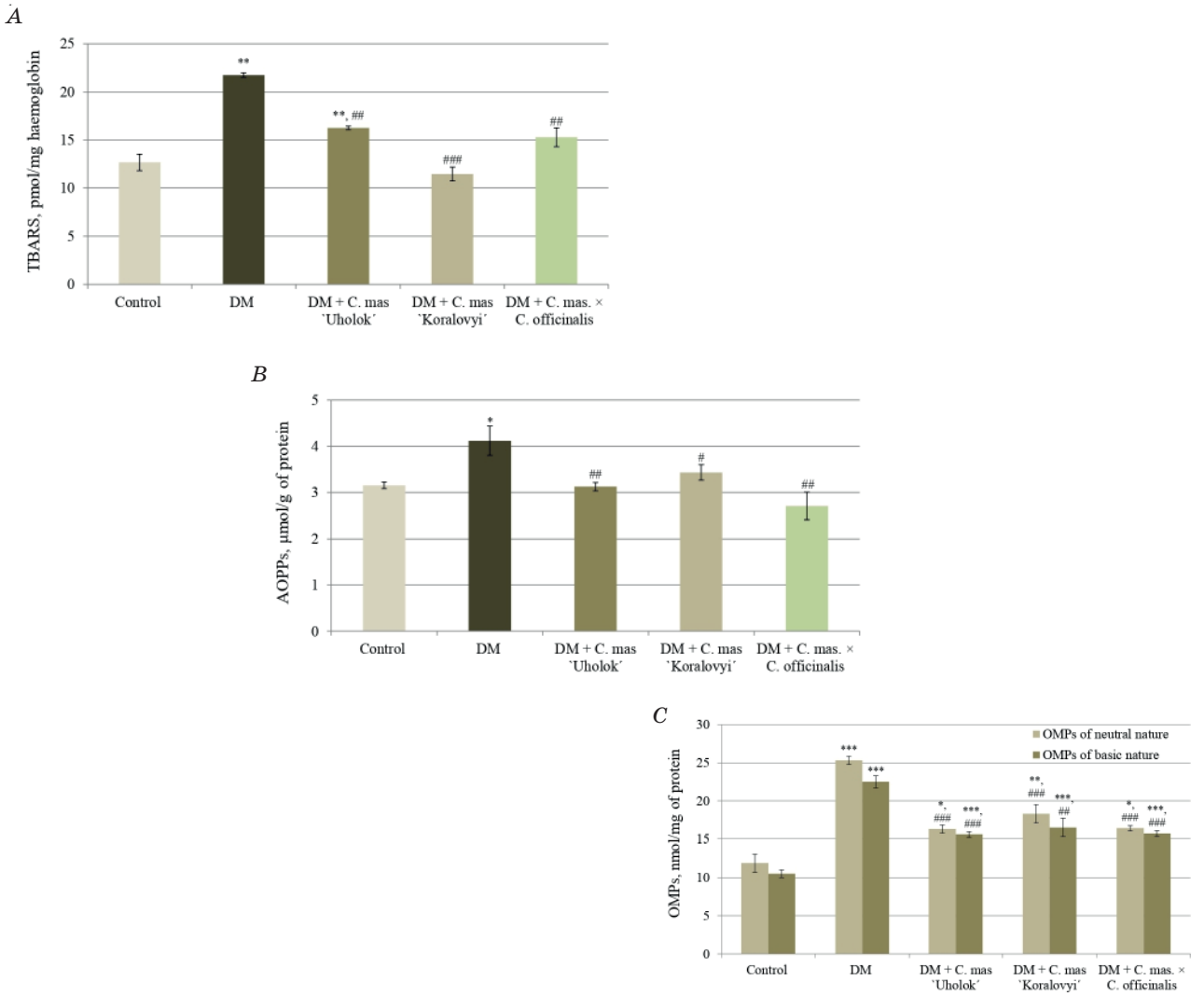

Figure. **Effect of fruit extracts from the `Uholok´ and `Koralovyi´ cultivars of *C. mas* L. and the hybrids of *C. mas* × *C. officinalis* `Jerzy´ and `Tomasz´ cultivars on the level of TBARS (*A*), AOPPs (*B*) and OMPs (*C*) in erythrocytes of rats with DM**

Note: All data are presented as the mean ± SEM ($n = 8$).
* — $P < 0.05$, ** — $P < 0.01$, *** — $P < 0.001$ compared to the control group;
# — $P < 0.05$, ## — $P < 0.01$, ### — $P < 0.001$ compared to the diabetic group

Conclusions. The fruit extracts of cornelian cherry inhibited the oxidation of erythrocytes structural components by ROS and prevented the accumulation of oxidative stress biomarkers in DM. The following positive effect can be attributed to the synergetic influence of bioactive components of extracts, such as iridoids, anthocyanins, tannins, flavonols, and phenolic acids.

Authors' contribution

A.A. Moroz — executing the biochemical part of the work on animal models, data analysis, graphical materials, writing, and presentation; I.V. Brodyak — conceptualization, data analysis, and writing; A.Z. Kucharska — analysis of *Cornus* fruit extracts composition; N.O. Sybirna — conceptualization and supervision.

REFERENCES

1. Orrico, F., Laurance, S., Lopez, A.C., Lefevre, S.D., Thomson, L., Möller, M.N., Ostuni, M.A. (2023). Oxidative stress in healthy and pathological red blood cells. *Biomolecules*, 13, 1262. https://doi.org/10.3390/biom13081262
2. Brodyak, I., Moroz, A., Bernacka, K., Kucharska, A. Z., Sybirna, N. (2025). Alleviation of hyperglycaemia and oxidative stress by fruit extracts of different cultivars of the cornelian cherry (*Cornus mas* L. and *Cornus mas* × *Cornus officinalis*) in rats with diabetes mellitus. *Food & Funct*., 16, 2136–2155. https://doi.org/10.1039/D4FO05426A
3. Strugała, P., Dzydzan, O., Brodyak, I., Kucharska, A.Z., Kuropka, P., Liuta, M., Kaleta-Kuratewicz, K., Przewodowska, A., ..., Sybirna, N. (2019). Antidiabetic and antioxidative potential of the Blue Congo variety of purple potato extract in streptozotocin-Induced diabetic rats. *Molecules*, 24, 3126. https://doi.org/10.3390/molecules24173126
4. Kehm, R., Baldensperger, T., Raupbach, J., Höhn, A. (2021). Protein oxidation — formation mechanisms, detection and relevance as biomarkers in human diseases. *Redox Biol*., 42, 101901. https://doi.org/10.1016/j.redox.2021.101901

UDC 615.37: 578.824.11 **https://doi.org/10.15407/biotech18.02.063**

BIOTECHNOLOGICAL APPROACHES IN CONSTRUCTION OF DRONES FOR MEDICAL PURPOSES

B.O. MOSKALENKO[1] *, N.S. FOMENKO*[1]*, A.G. LIZUNOVA*[2]*, O.M. KLYUCHKO*[1]

[1]National Aviation University, Kyiv, Ukraine;
[2]Luxoft Global Operations GmbH: Zug, CH, USA

E-mails: 1kelenaXX@nau.edu.ua

Received 2025/03/12
Revised 2025/03/18
Accepted 2025/04/30

Aim. Construction of an unmanned controlled complex (drone) with a container for medical care in extreme conditions with the use of biotechnological approaches.

Methods. The methods of analysis and object-oriented programming; use of the Python language; construction of the structure of the container for medical care; development of program supply for object recognition and operations with a container for medical purposes.

Results. The structure of a drone as a carrier of a container for medical care was scrutinized as well as the versions of drones' modules for medical purposes. Simultaneously, the various structures of such drones and containers for medical purposes were studied; the possibilities of biotechnological methods use were examined. A new version of the container for transportation by drone was constructed. Appropriate samples of the software for performing individual tasks of medical care in extreme conditions for various types of drone vehicles started to develop.

Conclusions. The drone with a container for medical care in extreme conditions with the use of biotechnological methods, as well as techniques of object recognition, was developed successfully.

Keywords: similarity, homological series, drones, medical applicatios.

During this project fulfillment, numerous sources of scientific and technical literature [1–4], as well as patent sources, were studied, and the subject area was analyzed carefully. Prototypes and analogs of the developed drone were examined — different versions of the drones for providing various types of medical care in extreme conditions.

The *purpose* of the work done was to develop the structure of a container for medical purposes and to clarify the possibility of its transportation by a drone to a defined person (with object individual features recognition) [5] or to an object specified by the computer program [6].

Research methods. In the processes of these works, the listed methods were used: the methods of analysis and object-oriented programming; use of the Python language; systematization and generalization of information; specification of the functions and parameters of the UAV with a container; construction of the structure of the container for medical care; development of program supply for objects recognition and operations with a container for medical purposes. The subject of this research is an unmanned controlled complex (drone) with a container for medical care in extreme conditions.

Principles of similarity and homology. Homologous series in chemistry, biology — and homologous series of technical elements. Principles of similarity homology very often are put on the base of the novel invented techniques, devices, systems, and their components. The phenomenon of homologous series in organic chemistry is well known. For example, in the case of acyclic

Citation: Moskalenko, B. O., Fomenko, N. S., Lizunova, A. G., Klyuchko, O. M. (2025). Biotechnological approaches in construction of drones for medical purposes. *Biotechnologia Acta*, 18(2), 63–67. https://doi.org/10.15407/biotech18.02.063

hydrocarbons, and according to the definition, a homologous series is an infinite series of organic compounds that have a similar structure and, therefore, similar chemical properties and differ from each other by any number of CH2– groups (homologous difference). Principles of homologous series of chemical compounds help to invent new compounds with predicted characteristics and structures (sometimes with predicted biochemical properties). The Phenomena of homologous series of organisms are well known from the evolution theory. Homologous series of biologically similar organs have also been described, for example, limbs of various terrestrial mammals, or eyes of different biological organisms. But contemporary theoretics in engineering also formulated the principles of a homologous series of technical elements. The last approach permits to invent successfully new systems, devices, and components. Fig. 1 demonstrates the similarity between the insect faceted eye and two types of image detectors in engineering, the principles of which can also be applied in the drones' production; such receptors (biosensors) receive visual information, and the technical "brain" processes it. Perhaps the most convincing implementation of the principles of homology in technology is the development and manufacture of multi-copters according to various construction schemes, which are: a) tri copter, b) quadcopter, c) hexacopter, d) octocopter.

Awareness of such principles helps greatly to invent and develop new analogues in engineering. It also permits to organization of better production of the series of devices or their elements in industry, in conditions of plant factories.

The initial element of such a series is the faceted eye of an insect, an ant (A), according to the principle of which physical models of technical devices for reproducing images of two types have been developed, with hexagonal cells (B) and with square cells (C, D) [7]. It is shown how 2 types of figures are visualized on the screens of such devices: a dot (B, C) and an elongated figure (C).

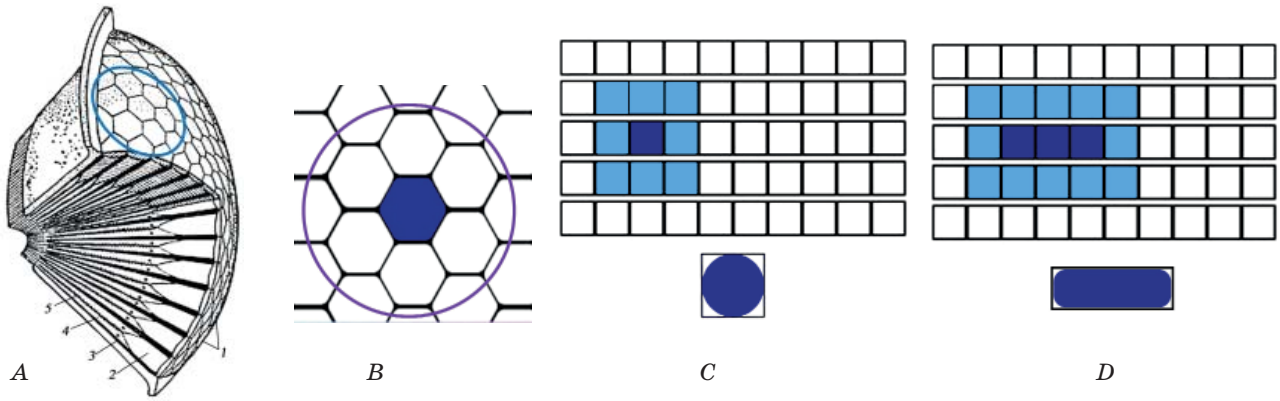

Figure. **Several elements of devices form a homologous series of technical devices; all of them reproduce images**

Construction of a drone carrier of containers for medical care. Development of the drone with such functions, with the possibility of container for medical purposes transportation to a defined person with individual features recognition, was the purpose of the fulfilled project. To achieve this purpose, the following tasks have to be solved:

1. Investigation of the prototypes based on patents' publications and literature reviews with the aim to observe the history of drone series development, their classification, and the areas of drone applications.
2. To observe the development of medical aviation in Ukraine and determine the features of drones' application for medical care.
3. To examine the structure of drones with containers for providing medical care in extreme conditions.
4. To specify the options for UAV modules for providing various types of medical care and/or detecting harmful chemicals in the environment.
5. To develop the structure of a container for medical purposes and to find out the software capabilities of its transportation by a drone to a specific object or person.

The main directions of drone application in civil life. Civilian drones can be used in the areas listed below:

– delivery of goods;

– emergency services (fire safety control, assistance in rescuing people in inaccessible places (mountains, forests, oceans);

– transportation of medicines (quadrocopters deliver blood, transplants, and vaccines to patients);
– aw enforcement agencies (patrol areas, analysis of road traffic incidents, crowd monitoring at mass events, bomb inspection, tracking criminals);
– organization of help in cases of disasters (assessment of damage from accidents at industrial enterprises, assessment of the consequences of railway accidents with dangerous goods, terrorist acts, determining the degree of contamination of large areas with chemical or nuclear waste, providing assistance to victims);
– agricultural activities (crops monitoring), forestry and fisheries (forest protection and control of fishing productions);
– environmental monitoring (monitoring of areas with oil spills, fires, etc.);
– geodesy (mapping);
– monitoring of oil and gas facilities;
– companies of buildings construction (inspection of construction sites, aerial inspection of the finished object, and etc.);
– cinematographic filming;
– journalism (reporting from the scene of hostilities, large-scale events, sporting competitions).

During the project fulfillment, the subject area was analyzed, and the tasks set at the beginning of the work were fully completed. These tasks were as follows.

1. Based on a review of the literature, it was found that the era of unmanned aerial devices and complexes controlled by radio began in the 1930s. The enormous practical potential of UAVs has led to their rapid development, constant modernization, and distribution. Today, according to UVS International (the leading international association of unmanned systems), UAVs are manufactured in 52 countries around the world. Scientists propose various criteria for classifying UAVs, namely: classification by purpose (military and civilian); by type of flight (rigid wing, flexible wing, rotary wing, flapping wing, and aerostatic type); by control principle (unmanned non-controlled, uncrewed automatic, uncrewed remotely piloted aircraft); by risk level (low, medium, high); by weight, speed, and flight range, etc.

2. Analysis of the development of Ukrainian medical aviation in the context of the use of drones in this area showed that UAVs are a progressive and innovative component of modern medical aviation, which every day occupies an increasingly important place in its development. The relevance of the development and modernization of existing UAVs for medical care in extreme conditions was also demonstrated. The improvement and development of uncrewed aerial vehicles for medical care is an essential direction of modern engineering activity.

3. A UAV as a container carrier for providing medical care in extreme conditions should have the following components: a strong but light, balanced, and aerodynamic frame; an engine with sufficiently large propellers; a speed controller to control the on/off of electric motors and the speed of rotation of the blades; a flight controller to collect data from sensors and commands from the user; a power source to provide energy to all multicopter systems.

4. A medical UAV can be equipped with modules for diagnosing a person's condition and providing them with appropriate medical care. The uncrewed aerial vehicle can be used repeatedly, and modular systems can be equipped as needed. Various modules for medical drones can be conditionally divided into two groups: *diagnostic* and *resuscitation*.

The *resuscitation group* of equipment may include a breathing bag for artificial lung ventilation, a mechanically driven aspirator, and a portable automatic external defibrillator.

The *diagnostic group* can be divided into two subgroups: direct diagnostics using appropriate devices and transportation of biomaterials for their further processing. Directly diagnostic subgroup includes a three-channel electrocardiograph; a portable diagnostic monitor with functions for measuring blood pressure, determining oxygen saturation, and measuring temperature; a portable clinical blood analyzer;

The subgroup for transporting biomaterials for their further processing requires the presence of special containers. An analysis of the feasibility of equipping one or more UAVs shows that it is impossible to put all diagnostic and assistance functions into one module of the device.

When providing medical care to a person in extreme conditions, especially in situations of possible chemical contamination due to accidents in industrial regions, it is important to determine the level of chemical pollution in the environment. As a result, the development of detector devices that record chemical pollution of the environment is relevant. For the development of chemosensitive surfaces of detectors, experience in studying the physicochemical nature of ion selectivity and specificity of artificially created and natural membranes is essential.

5. When determining the conditions for transporting biological samples and vaccines, it was found that the container must have certain characteristics: heat resistance, tightness, reliability of fastening test tubes with samples, the possibility of disinfecting the inside of the container, the presence of a bactericidal air filter, aerodynamics of the shape. All these conditions were taken into account during the development of the container, constructed in process of present project fulfillment.

In order to ensure the delivery of the container to a specific object or person in automatic or semi-automatic mode, the appropriate software was found to automate this process. This software is based on a facial recognition technology called a convolutional neural network (CNN).

Results of the project fulfillment. The main parts and components of the constructed drone. The main parts and components of the constructed drone will be represented during the report: the structure of the UAV, the structure and functions of the constructed container, software for its control and receiver recognition, etc.

Prototypes of constructed drones with medical containers were studied. On the basis of the analog, described in one patent, the special device — a medical container was proposed; the structure of the container itself and the software for the drone for performing specific tasks of medical assistance in extreme conditions. So, a container for a medical UAV for transporting medicines in extreme conditions was developed.

To find a programmatically defined object or person, face recognition was used using a web camera [5]. The system acts as a face detector and object detector. Initially, the camera, using the software written by the author [6], determines the appearance of a person or object and captures its image. Next, two possible schemes of operation of the face or object recognition module are implemented: identification or verification. The corresponding software has been developed and will be explained during the report [6]. As a prototype for the device for object recognition was [7], the main theoretical principles were described in [8, 9].

Results of the project fulfillment. 1. The drone with a container for medical care in extreme conditions with the use of biotechnological techniques, as well as techniques of object recognition, was developed successfully.

2. During the project fulfillment, the history of inventions and construction of various unmanned devices and complexes were examined, as well as drones' classification criteria, and areas of their application. The legislative framework of drones' construction and their applications in various civil spheres of activities and functions of drones were studied, too.

3. The structure of a drone as a carrier of a container for medical care was scrutinized as well as the versions of drones' modules for medical purposes. Simultaneously, the various structures of such medical containers were studied.

4. Appropriate samples of the software for performing individual tasks of medical care in extreme conditions for various types of UAVs were started to develop.

5. Recommendations for the use of results: UAVs with medical containers can be recommended for implementation in the spheres of activity of the Ministry of Health of Ukraine, the Ministry of Emergency Situations of Ukraine, and the Ministry of Defense of Ukraine.

Conclusions. The drone with a container for medical care in extreme conditions with the use of biotechnological methods, as well as techniques of object recognition, was developed successfully.

Acknowledgments

The authors express their gratitude to professors Shutko V.M. and Morozova I.V. for their valuable consulting and support in the process of this project's fulfillment and realization.

Authors Contributions

B. Moskalenko — construction of the container for medical purposes for the drone, functions for image recognition, and writing of some fragments of materials; N. Fomenko — development of the systems for the connections and distant control; A. Lizunova — computer simulation, algorithms construction; O. Klyuchko — general supervision, works planning, and writing of the article. All authors contributed to the manuscript's revision and read and approved the submitted version.

The study was funded under the themes according to the State registration 0107U002666 and No. 177-X04 (1.06.2004).

The authors declare no conflict of interest.

REFERENCES

1. Gumenyuk, K.V., Horoshko, V.R. (2020). A look from the past to the future: unmanned flying drones as an element of the evacuation of the wounded in the medical service of the Armed Forces of Ukraine. *Emergency Medicine,* 16(5). (in Ukrainian) URL: http://webcache.googleusercontent.com/search?q=cache:-ov9uMZc9jUJ:emergency.zaslavsky.com.ua/article/download/212220/214318/483250+&cd=5&hl=uk&ct=clnk&gl=ua
2. Prototype of Commission Regulation on Unmanned Aircraft Operations — EASA. URL: https://www.easa.europa.eu/sites/default/files/dfu/Explanatory% 20Note% 20for% 20the% 20UAS% 20Prototype% 20regulation% 20final.pdf (Last accessed: 01.06.2021).
3. Rules of a good drone — Axon. (In Ukrainian). URL: https://axon.partners/uk/uncategorized/the-rules-of-good-drone/ (Last accessed: 01.06.2021).
4. Civil and military drones — European Parliament URL: https://www.europarl.europa.eu/RegData/etudes/BRIE/2019/642230/EPRS_BRI(2019)642230_EN.pdf (Last accessed: 01.06.2021).
5. Facial Recognition — techopedia. URL: https://www.techopedia.com/definition/32071/facial-recognition (Last accessed: 01.06.2021).
6. Drone Programming Course — CVZONE. URL: https://www.computervision.zone/courses/drone-programming/ (01.06 2021).
7. Shutko, V. N., Klyuchko, O. M., Navrotskiy, D. O., Mikolushko, A. M. (2014). Possibility of images recognition in navigation by artificial system. *2014 IEEE 3rd International Conference on Methods and Systems of Navigation and Motion Control, MSNMC*. Proceedings Article, 165–169.
8. Aralova, N. I., Klyuchko, O. M., Mashkin, V. I., Mashkina, I. V. (2017). Software for the reliability investigation of operator professional activity for "Human-Machine" systems. *Electronics and Control Systems*, 51(1), 105–113.
9. Klyuchko, O. M., Klyuchko, Z. F. (2018). Electronic information systems for monitoring of populations and migrations of insects. *Biotechnologia Acta*, 11(5), 5–25. https://doi.org/10.15407/biotech11.05.005

UDC 543.06:577.15:543.553 **https://doi.org/10.15407/biotech18.02.068**

LABORATORY PROTOTYPE OF ELECTROCHEMICAL BIOSENSOR FOR THE QUANTITATIVE ANALYSIS OF ALANINE AMINOTRANSFERASE ACTIVITY

D.O. MRUGA[1], *Y.R. VAKHOVSKY*[1, 2], *S.V. DZYADEVYCH*[1, 2], *O.O. SOLDATKIN*[1, 3]

[1]Institute of Molecular Biology and Genetics of the National Academy of Sciences of Ukraine, Kyiv
[2]Taras Shevchenko National University of Kyiv, Ukraine
[3]National Technical University of Ukraine "Igor Sikorsky Kyiv Polytechnic Institute"

E-mail: darynamruga@gmail.com

Received 2025/03/25
Revised 2025/03/04
Accepted 2025/04/30

Aim. To develop an electrochemical biosensor for the quantitative assessment of alanine aminotransferase (ALT) activity.

Materials and Methods. Three-electrode amperometric scheme of detection with platinum disk working electrode covered with bioselective element based on pyruvate oxidase and photopolymer. Measurements were carried out with an applied potential of 0.6 V.

Results. A laboratory prototype of an amperometric biosensor for ALT detection was developed. The immobilization method was selected, and the procedure was optimized for the type of bioselective material used. The composition of the working buffer was optimized, namely, the kind of buffer, buffer capacity, pH, content of coenzymes of the bioselective material (phosphate ions, magnesium ions, thiamine pyrophosphate), and the analyte (alanine, ketoglutarate, pyridoxal phosphate). The reproducibility of immobilization and reproducibility of responses of the developed biosensor, as well as its analytical characteristics (linear range, detection limit, response time, etc.), were analyzed.

Conclusions. The developed biosensor was characterized by sufficiently good analytical parameters for its further optimization and testing when working with real blood serum samples.

Keywords: alanine aminotransferase, biosensor, enzyme activity.

Alanine aminotransferase (ALT) is a key enzyme of amino acid metabolism that plays a vital role in the diagnosis of liver diseases, including hepatitis, cirrhosis, and fatty degeneration [1]. Determination of ALT activity in serum is a standard biochemical test widely used to monitor liver status. Traditional methods [2–3] for determining the activity of this enzyme are based on spectrophotometric and colorimetric assays, which, although highly accurate, have a number of disadvantages. In particular, they require the use of significant volumes of reagents, complex laboratory equipment, and a long analysis time. In addition, the cost of such studies remains relatively high. In this regard, there is a need to develop alternative detection methods that would be simpler, cheaper, and no less effective.

One of the promising areas in this field is the use of electrochemical biosensors. They have a number of advantages, including high sensitivity and selectivity, the possibility of miniaturization, rapidity of measurements, and accessibility. Due to these characteristics, biosensors can significantly improve the diagnosis of liver diseases, providing a rapid and accurate analysis of ALT activity without the need for complex laboratory equipment.

Citation: Mruga, D. O., Vakhovsky, Y. R., Dzyadevych, S. V., Soldatkin, O. O. (2025). Laboratory prototype of electrochemical biosensor for the quantitative analysis of alanine aminotransferase activity. *Biotechnologia Acta*, 18(2), 68–70. https://doi.org/10.15407/biotech18.02.068

Aim. This work aimed to develop an electrochemical biosensor capable of providing a quantitative assessment of alanine aminotransferase activity in biological fluid samples.

Methods. A three-electrode amperometric of detection was used to create the biosensor, which includes a platinum disk working electrode, as well as a bioselective element on the electrode surface created by photopolymerization of pyruvate oxidase with PVA-SbQ. The principle of operation of the biosensor is based on a two-enzyme system in which ALT catalyzes the reaction between alanine and ketoglutarate, forming pyruvate. The resulting pyruvate is oxidized by pyruvate oxidase to form hydrogen peroxide, which in turn is detected amperometrically using a platinum electrode.

Results and Discussion. During the research, a laboratory prototype of an amperometric biosensor capable of detecting ALT activity was created. The optimal method of immobilization of the bioselective material was selected, which ensures stability and high reproducibility of the obtained results. In addition, the immobilization procedure was optimized, taking into account the specifics of the bioselective material used. The optimal conditions for the sensor's operation were determined, in particular, the composition of the working buffer, which includes the appropriate type of buffer, its buffer capacity, and pH level. To ensure proper operation of the sensor, concentrations of substrates and coenzymes were optimized, including alanine, ketoglutarate, pyridoxal phosphate, phosphate ions, magnesium ions, and thiamine pyrophosphate. The reproducibility of immobilization of the bioselective material was studied, which is an essential parameter for ensuring the stability of the sensor during repeated measurements.

Table. **Analytical characteristics of the biosensor**

Linear range	LOD	Sensitivity	Response time	Baseline noise	Baseline drift
1–500 UL^{-1}	1 UL^{-1}	1 nA min^{-1} per 100 UL^{-1}	2 min	0.4 nA	0.2 nA min^{-1}

The analytical characteristics (Table) of the biosensor were also carefully analyzed. Namely, linear range (Figure), detection limit, and response time were investigated. The results obtained indicate that the sensor has high sensitivity and stability, which makes it promising for further optimization.

Conclusions. The developed amperometric biosensor for determining ALT activity demonstrated good analytical characteristics, which allows us to consider it as a promising tool for further research. The next step in this work is to test the biosensor on real blood serum samples to assess its effectiveness in clinical conditions. The successful implementation of such biosensors in medical practice can significantly simplify and reduce the cost of diagnosing liver diseases, providing a fast and affordable method for analyzing ALT activity in biological fluids.

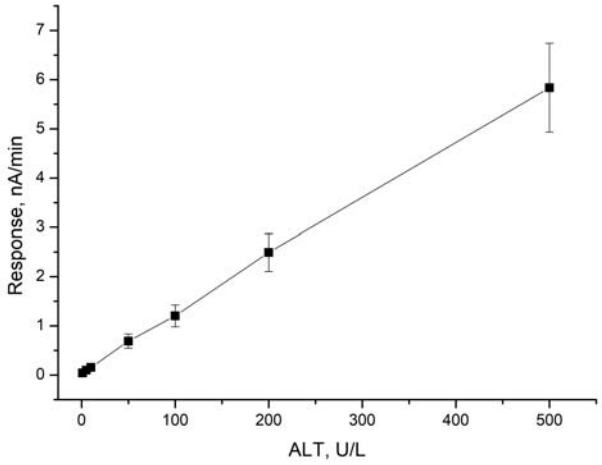

Figure. **Calibration curve of the developed biosensor for the detection of ALT activity**
Working solution content: alanine — 8mM, α-ketoglutarate — 0.5mM, pyridoxal phosphate — 50mkM, $Mg(NO_3)_2$ — 0.5mM, thiamine pyrophosphate — 2mM, KH_2PO_4 — 5mM, working buffer — HEPES 25mM, pH 7.4, applied potential +0.6V, constant mixing, RT

Author's contribution

D.O. Mruga — thesis writing, data curation. Y.R. Vakhovsky — data curation. S.V. Dzyadevych — editing, project administration. O.O. Soldatkin — editing, supervision.

Funding source

The work was carried out within the framework of the work "Development of technology for the creation of biosensor test systems for the analysis of enzyme activity as diagnostic indicators of damage to internal organs" on the use of budget funds "Support for priority scientific research and scientific and technical (experimental) developments for the state" of the budget program 6541230.

REFERENCES

1. Liu, Z., Que, S., Xu, J., Peng, T. (2014). Alanine Aminotransferase—Old Biomarker and New Concept: A Review. *Int. J. Med. Sci.,* 11 (9), 925–935. https://doi.org/10.7150/ijms.8951
2. Valenti, L., Pelusi, S., Bianco, C., Ceriotti, F., Berzuini, A., Iogna Prat, L., Trotti, R., Malvestiti, F.,..., Prati, D. (2021). Definition of healthy ranges for alanine aminotransferase Levels: A 2021 update. *J. Hepatol. Commun*., 5(11), 1824–1832. https://doi.org/10.1002/hep4.1794.
3. Duan, M., Chi, X., Xiao, H., Liu, X., Zhuang, H. (2021). High-normal alanine aminotransferase is an indicator for liver histopathology in HBeAg-negative chronic hepatitis B. *J. Hepatol. Int.,* 15 (2), 318–327. https://doi.org/10.1007/s12072-021-10153-2

UDC 577.1:612.015:615.277 https://doi.org/10.15407/biotech18.02.071

OPTIMIZATION OF PARAOXONASE ORGANOPHOSPHATASE ACTIVITY ASSESSMENT IN MOUSE PLASMA USING PARAOXON-ETHYL

A.R. OKHOVYCH, O.I. DEMIANCHUK, M.M. BAYLIAK

Vasyl Stefanyk Precarpathian National University, Ivano-Frankivsk, Ukraine

E-mail: anna.okhovych@pnu.edu.ua

Received 2025/03/05
Revised 2025/03/21
Accepted 2025/04/30

Aim. To select optimal conditions for determining the organophosphatase activity of paraoxonase in mouse blood plasma using paraoxon-ethyl as a substrate.

Materials and Methods. The method was modified from a protocol developed for rats. Enzyme activity was assessed by measuring the formation of 4-nitrophenol at 405 nm. The optimal pH was determined within the range of 6.0–10.5 using 50 mM buffer solutions. The reaction mixture contained fixed concentrations of $CaCl_2$, NaCl, and paraoxon-ethyl (1 mM). The reaction was initiated by adding 20 µL of blood plasma. For kinetic analysis, Tris-HCl buffer (pH 8.0) and varying concentrations of paraoxon-ethyl (0–2 mM) were used. Absorbance was measured over 90 seconds using a ULAB-102 spectrophotometer at 405 nm. Enzyme activity was calculated using a molar extinction coefficient of 18290 $M^{-1}cm^{-1}$, and protein concentration was determined by the Bradford method. Kinetic parameters (K_m, V_{max}) were calculated using the "KINETICS" software.

Results. The highest paraoxonase activity was observed at pH 8.0–9.0. Thus, pH 8.0 was chosen for further assays. The determined K_m was 229 ± 22 µM, and V_{max} was 0.070 ± 0.009. A paraoxon-ethyl concentration of 1.5 mM (5–10×K_m) ensured substrate saturation. Time-dependence analysis confirmed a linear increase in product formation within the range of 1–50 µL of plasma. A working volume of 15–20 µL was considered optimal.

Conclusions. The assay conditions for paraoxonase activity were optimized: pH 8.0, K_m = 229 µM, V_{max} = 0.070, and a working plasma volume of 15–20 µL.

Keywords: paraoxonase, atherosclerosis, paraoxon-ethyl, kinetics.

Paraoxonase (PON) is a hydrolase enzyme with three isoforms (PON1, PON2, PON3) involved in the detoxification of xenobiotics and protection against oxidative stress. PON1 is the most extensively studied isoform, known to metabolize oxidized lipids, and is considered a protective factor in the development of inflammatory and vascular diseases, particularly atherosclerosis. Paraoxonase exhibits three main types of activity—organophosphatase, arylesterase, and lactonase — depending on the substrate used [1]. These activities are viewed as potentially informative markers for diagnosing metabolic disorders, cardiovascular diseases, and conditions associated with oxidative stress [2]. To improve the accuracy of biochemical analysis, conditions for determining paraoxon-ethyl-dependent (organophosphatase) activity in mouse blood have been optimized. The results may be of scientific value for advancing the understanding of antioxidant defense mechanisms, as well as of practical importance for developing new diagnostic and preventive strategies.

Aim. To select conditions for the determination of organophosphatase activity of paraoxonase using the substrate paraoxon-ethyl in mouse blood plasma.

Citation: Okhovych, A. R., Demianchuk, O. I., Bayliak, M. M. (2025). Optimization of paraoxonase organophosphatase activity assessment in mouse plasma using paraoxon-ethyl. *Biotechnologia Acta*, 18(2), 71–73. https://doi.org/10.15407/biotech18.02.071

Methods. The procedure was adapted from a technique described for rat paraoxonase [3]. The assay was designed to determine the organophosphatase activity of the enzyme using paraoxon-ethyl as a substrate. Enzymatic activity was assessed by the formation of 4-nitrophenol, with absorbance measured at 405 nm.

The optimal pH of the reaction was determined within the range of 6.0–10.5 using appropriate buffer systems at a constant concentration of 50 mM. The reaction mixture contained fixed concentrations of $CaCl_2$, NaCl, and paraoxon-ethyl (1 mM). The reaction was initiated by adding 20 µL of blood plasma.

For kinetic analysis, Tris-HCl buffer (pH 8.0) and varying concentrations of paraoxon-ethyl (0–2 mM) were used. To assess the dependence of reaction rate on enzyme amount, a fixed substrate concentration (1.5 mM) and different volumes of plasma (0–50 µL) were applied. Absorbance was recorded over 90 seconds using a ULAB-102 spectrophotometer at 405 nm. Enzyme activity was expressed in mU/mg of protein and mU/L of plasma, using a molar extinction coefficient of 18290 $M^{-1}cm^{-1}$. The protein concentration was determined by the Bradford method.

Kinetic parameters, including the Michaelis-Menten constant (K_m) and maximum reaction rate (V_{max}), were calculated using the "KINETICS" software based on plots of ΔA/min versus substrate concentration. The program also estimates S0.5 (half-saturation constant) and V_{max}. For accurate enzyme activity determination, substrate concentrations close to saturation (typically 5–10 K_m, corresponding to ~95% of V_{max}) were selected. Statistical analysis was performed using Microsoft Excel and GraphPad Prism 8.0.1. Results were presented as mean ± standard error of the mean (SEM).

Results. There is no consensus in the scientific literature regarding the optimal pH for assessing paraoxonase organophosphatase activity using paraoxon-ethyl as a substrate. Depending on the study, activity has been measured at pH values ranging from 8.0 to 10.5. Therefore, the first step of our study was to determine the pH optimum. The highest PON activity was observed between pH 8.0 and 9.0, with a decline at higher pH levels. For subsequent experiments, pH 8.0 was selected as it is closest to physiological blood pH (Fig. 1).

Kinetic parameters were also established: the Michaelis-Menten constant (K_m) was 229 ± 22 µM, and the maximum reaction rate (V_{max}) was 0.070 ± 0.009. For further measurements, a paraoxon-ethyl concentration of 1.5 mM was used, corresponding to 5–10×K_m, ensuring substrate saturation (Fig. 2).

Time-dependence analysis confirmed a linear increase in reaction product formation using 20 µL of blood plasma. The reaction rate remained linear across a range of 1–50 µL of plasma. Based on these results, a working volume of 15–20 µL was chosen to ensure reliable measurements while minimizing sample consumption (Fig. 3).

Conclusions. This study optimized the paraoxonase activity assay, determining the optimal pH (8.0), kinetic parameters (K_m = 229 µM, V_{max} = 0.070), and plasma volume (15–20 µL) for reliable measurements.

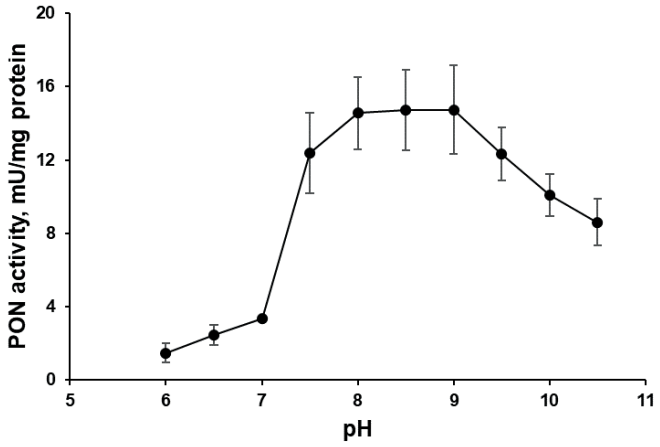

Fig. 1. **Dependence of the specific activity of PON in mouse blood plasma on pH (with the addition of 1 mM paraoxon-ethyl and 20 µl of plasma)**
Values are presented as mean ± standard error of the mean (SEM), n = 3

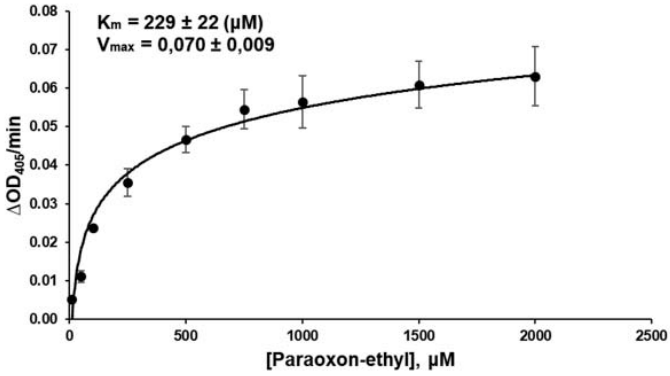

Fig. 2. **Dependence of the reaction rate on the concentration of paraoxon-ethyl in the blood plasma of mice (volume of added blood plasma 20 μL)**
Values are presented as mean ± standard error of the mean (SEM), $n = 3$

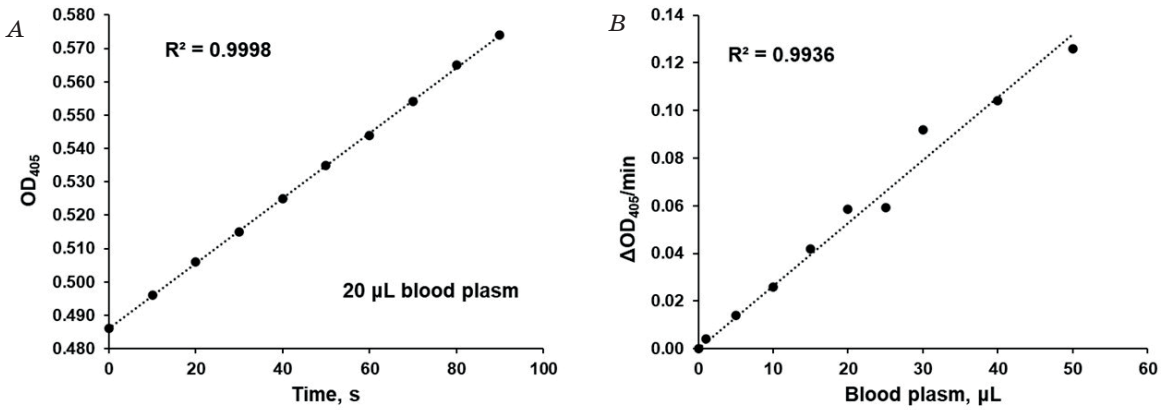

Fig. 3. A **— Dependence of the optical density of the reaction product formed on time (with the addition of 1.5 mM paraoxon-ethyl);** *B* **— Dependence of the reaction rate on the amount of added blood plasma (with 1.5 mM paraoxon-ethyl**

Authors' Contribution

ARO performed spectrophotometric determination of PON activity, processed and statistically analyzed the data, wrote the original draft of the abstract; OID assisted in the experiments; MMB conceptualization and supervision, reviewed and edited the abstract.

Funding source

This work was supported by a grant from the Ministry of Education and Science of Ukraine [grant number 0123U101790].

REFERENCE

1. Mohammed, C. J., Lamichhane, S., Connolly, J. A., Soehnlen, S. M., Khalaf, F. K., Malhotra, D., Haller, S. T., Isailovic, D., Kennedy, D. J. (2022). A PON for All Seasons: Comparing Paraoxonase Enzyme Substrates, Activity and Action including the Role of PON3 in Health and Disease. *Antioxidants*, 11(3), 590. https://doi.org/10.3390/antiox11030590
2. Vatashchuk, M., Hurza, V., Bayliak, M. (2023). Adapting of Spectrophotometric Assay of Paraoxonase Activity with 4-Nitrophenylacetate for Murine Plasma and Liver. *Journal of Vasyl Stefanyk Precarpathian National University*, 9(4), 6–14. https://doi.org/10.15330/jpnu.9.4.6-14.
3. Romani, R., De Medio, G. E., di Tullio, S., Lapalombella, R., Pirisinu, I., Margonato, V., Veicsteinas, A., Marini, M., Rosi, G. (2009). Modulation of paraoxonase 1 and 3 expression after moderate exercise training in the rat. *Journal of lipid research*, 50(10), 2036–2045. https://doi.org/10.1194/jlr.M800493-JLR200

UDC 616-006.6:577.2-085 **https://doi.org/10.15407/biotech18.02.074**

THE ANTICANCER EFFECT OF RAD51-IN-1 IN MDAH-2774 (CVCL_0420) CELLS

Deniz ÖZDEMİR, Can Ali AĞCA

Department of Molecular Biology and Genetics, Bingöl University, 12000, Bingöl, TÜRKİYE

E-mail: ozdemr.dnz@gmail.com

Received 2025/03/06
Revised 2025/03/12
Accepted 2025/04/30

Aim. This study aimed to investigate the effect of pharmacological inhibition of RAD51, via RAD51-IN-1, on the MDAH-2774 cell line

Methods. To achieve these objectives, MDAH-2774 cells were treated with different doses of RAD51-IN-1 to determine the effects on cell viability and the IC50 value of RAD51-IN-1. Intracellular ROS levels of the cells were investigated by DCFDA staining. In the last set of experiments, the effect of RAD51-IN-1 monotherapy application on apoptotic cell death was investigated by acridine orange/ethidium bromide staining.

Results. In the experimental findings obtained, firstly, cells were treated with different doses of RAD51-IN-1 to decrease cell viability and IC50 of RAD51-IN-1 was determined. In addition, it was observed that the amount of intracellular ROS increased after DCFDA staining after RAD51-IN-1 treatment. In the last set of experiments, it was determined that cell death occurred with increasing doses f of RAD51-IN-1.

Conclusion. The RAD51-IN-1 small molecule inhibitor is a promising approach for treating ovarian cancer, but the drug requires further *in vitro* evaluation.

Keywords: Ovarian Cancer, RAD51-IN-1, ROS, Cell Death.

Defects in DNA repair mechanisms are considered one of the fundamental hallmarks of cancer. Cancer cells require DNA repair capacity to repair DNA damage caused by replication stress that occurs during proliferation and exogenous factors such as ionizing radiation and genotoxic antitumor agents. In this context, defects in DNA repair pathways play an important role in tumor formation, progression, and resistance to treatment by leading to genomic instability [1]. For these reasons, the development of inhibitors targeting DNA damage response (DDR) mechanisms at both preclinical and clinical levels has made these pathways attractive targets for therapeutic intervention [2]. Homologous recombination (HR), one of the fundamental components of DDR mechanisms, is a critical pathway for the repair of DNA double-strand breaks (DSBs). This process begins with the recognition of the break site by the MRN complex (MRE11, RAD50, NBS1) and continues with the recruitment and activation of the ATM protein to the site. Activated ATM phosphorylates the Ser139 site of the H2AX protein, resulting in the formation of H2AX; this allows the recruitment of repair proteins such as 53BP1 and RAD50 to the damage site [3]. In addition, other kinases such as ATR and DNA-PK contribute to the DDR response by interacting with the RPA-ATRIP and Ku70/Ku80 complexes, respectively. RAD51 protein, one of the key regulators of homologous recombination, is the homolog of E. coli RecA and recognizes homologous DNA sequences by forming nucleoprotein filaments at the ends of DSBs during the repair process and ensures the repair of the damage through

Citation: Özdemir, D., Ağca, C. A. (2025). The anticancer effect of RAD51-IN-1 in MDAH-2774 (CVCL_0420) cells. *Biotechnologia Acta*, 18(2), 74–78. https://doi.org/10.15407/biotech18.02.074

rearrangement structures called D-loops [4]. RAD51 filament formation is regulated by BRCA2, RAD52 and RAD51 paralogs. In the literature, it is reported that overexpression of RAD51 is observed in various malignancies such as pancreatic adenocarcinoma, ovarian and breast cancer and this contributes to tumor progression and treatment resistance [5–8].

Inhibition of RAD51 prevents the efficient repair of DNA double-strand breaks, leading to the accumulation of DNA damage in cells. This accumulation increases genomic instability and can result in apoptosis, especially in rapidly proliferating cancer cells that are highly dependent on the homologous recombination repair (HRR) pathway. In contrast, since normal cells can resort to alternative DNA repair mechanisms, RAD51 inhibitors have the potential to cause selective cytotoxicity and minimal damage to healthy tissues [9, 10]. With these properties, RAD51 stands out as a promising molecular target in targeted cancer therapies.RAD51-IN-1, a newly developed homologous recombination RAD51 inhibitor in its class, was shown to exhibit anticancer activity in cell growth in a panel of Triple-negative breast cancer (TNBC) cell lines [11].

In conclusion, DDR and especially the HR pathway have a critical place in cancer biology and treatment approaches. Functional analysis and targeting of proteins in this pathway will enable the development of more effective and personalised oncological treatment strategies in the future.

Aim. This study aims to provide a new avenue for personalized cancer therapy and to elucidate the anticancer effects of the small molecule inhibitor RAD51-IN-1 on ovarian cancer cells (MDAH-2774) for the first time.

Methods. The ovarian cancer (MDAH-2774) cell line was cultured in Dulbecco's Modified Eagle Media (DMEM) medium in a humidified environment containing 5% CO_2 at 37 °C. Cells were collected from flasks with the help of trypsin-EDTA. NutriCulture Cell Viability Determination Kit-8 (CVDK-8) is applied using a highly water-soluble tetrazolium salt. NutriCulture CVDK8 allows sensitive colorimetric assays for determining the number of live cells in cell proliferation and cytotoxicity assays. 2000–5000 cells were seeded per well in 100 ul of medium in a 96-well plate. Cells were incubated in a humidified CO_2 incubator at 37 °C for 24 hours. Various concentrations of substances to be tested were applied to the cells. The cells were incubated for an appropriate time (24, 48h). 10 µl CVDK-8 was added to each well of the plate. The plate was incubated in the incubator for 1–4 hours and the absorbance was measured at 450 nm using a microplate reader (SpectraMax Plus 384 Microplate Reader) [12].

Fluorometric analysis was performed with DCFDA dye as a different method to determine reactive oxygen species. Briefly, 25 µM DCFDA solution was added to the medium of the cells after the treatments and kept in a 37 °C CO_2 incubator for 45 min. At the end of the incubation period, the medium was removed from the wells, and 1X washing solution was added to each well. Then, the absorbance was read at Ex 485 nm/Em 535 nm with a fluorescence spectrophotometer [13].

Cells were plated at a quantity of 10×10^5 in 6-well plates and maintained in DMEM medium with 10% fetal bovine serum (FBS, Sigma, USA; cat. no. F7524) at 37 °C in a 5% CO_2 incubator (ESCO, USA). After overnight treatment, cells were removed with trypsin-EDTA after 48 h, followed by centrifugation, and as a final step, 25 µl of cell suspension (0.5×10^6 to 2.0×10^6 cells/ml) was incubated with 1 µl of AO/EB solution. 10 µl of cell suspension was placed on a microscopic slide, covered with a glass coverslip, and cells were examined under a fluorescence microscope using a fluorescent filter and a 20X objective[14].

Results and Discussion. In this study, firstly, the effect of RAD51-IN-1 on cell viability in the ovarian cancer cell line MDAH-2774 was determined by CVDK-8 assay. The MDAH-2774 cell line was treated for 24 and 48 hours using doses of RAD51-IN-1 (0-100 µM). Under experimental conditions, RAD51-IN-1 inhibited cell viability in the ovarian cancer cell line MDAH-2774 in a dose- and time-dependent manner.

However, a more significant decrease in cell viability was observed in the 48-hour treatment compared to the 24-hour treatment. While the IC50 value of MDAH-2774 was determined as 64.20 µM after 24-hour treatment with RAD51-IN-1, it was defined as 17.51 µM after 48-hour treatment. Therefore, the treatment period of the following experiments was continued with the most effective treatment period of 48 hours. In the study of Ruiz et al., which has similar results to our research, RAD51 was inhibited with siRNA in HeLa cells [15]. As a result of the viability obtained using nm doses of siRAD51, cell viability was reduced in a dose-dependent manner.

In this experiment, we evaluated the effect of RAD51-IN-1 on ROS levels in MDAH-2774 cells. First, MDAH-2774 cells were treated with RAD51-IN-1 (0–0.5–10–20 µM) for 48 hours. After

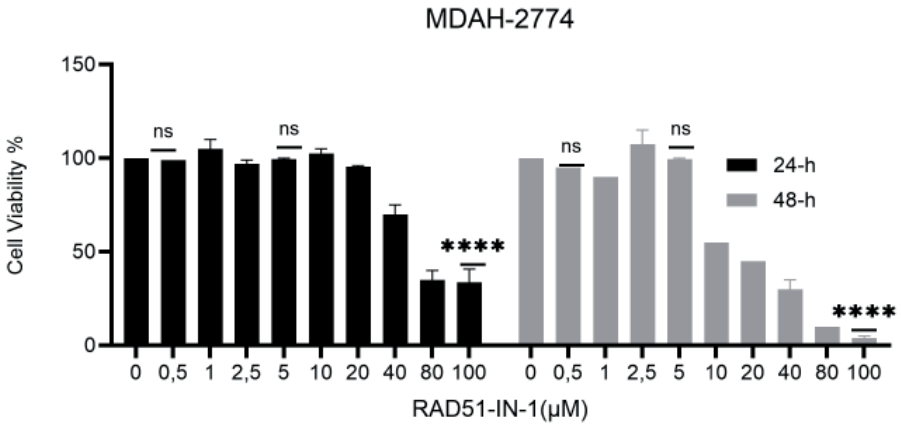

Fig. 1. **The effects of RAD51-IN-1 on cell viability in the MDAH 2774 cell line for 24 and 48 hours of incubation with RAD51-IN-1 at doses of 0, 0.5, 1, 2.5, 5, 10, 20, 40, 80, and 100 μM**
The viability of untreated cells was defined as 100. (****$P < 0.0001$)

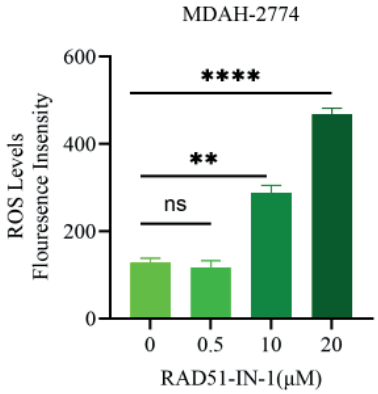

Fig. 2. **ROS levels induced by RAD51-IN-1 treatment. Cellular oxidative stress induced in cells after 48 h of RAD5-IN-1 treatment was measured using a fluorescence spectrophotometer and correlated with the levels of ROS produced. Data represent the mean ± SD of three independent experiments**
(**$P < 0.01$; ****$P < 0.0001$)

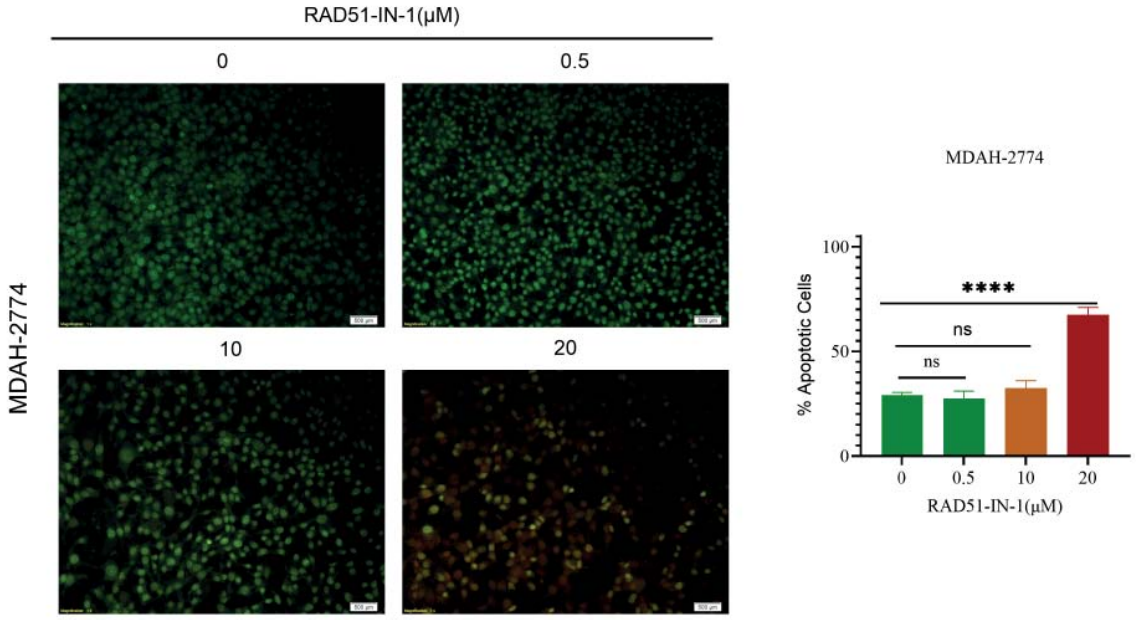

Fig. 3. **Effect of RAD51-IN-1 treatment on apoptosis in MDAH-2774 cells using acridine orange staining and ethidium bromide staining**
Green cells indicate live cells, orange cells indicate early apoptosis, and red cells indicate late apoptosis.
(****$P < 0.0001$)

treatment, cells stained with DCFDA were measured in a fluorescence spectrophotometer. It was observed that RAD51-IN-1 increased the ROS levels of MDAH-2774 cells in a dose-dependent manner and was statistically significant.

To investigate whether RAD51-IN-1 induces apoptotic cell death, an AO/Etbr staining assay was performed. Ovarian cancer cell line MDAH-2774 was treated with RAD51-IN-1 (0-0.5-10-20 μM) for 48 hours. After treatment, cells were stained with AO/Etbr and the images were examined under a microscope. In the obtained microscope images, no significant effect was observed at the dose of 0.5 μM, while a significant effect was observed at the dose of 10-20 μM. As shown statistically, RAD51-IN-1 was shown in MDAH-2774 cells in a dose-dependent manner. In the study by Gu and his team, breast cancer cell lines were treated with RAD-51 (Cpd-1, Cpd-2, Cpd-3, Cpd-4, and Cpd-5). In the apoptotic cell death results obtained, it was statistically determined that it increased cell death, especially in MDA-MB-468 cells [16].

Conclusion. These findings may help develop new treatments for ovarian cancer that exploit the genomic instability of cancer cells.

Authors' contribution

DÖ and CAA provided critical feedback and helped shape the research, analysis and manuscript. DÖ and CAA read and approved the final manuscript.

Funding source

The present research was conducted without any external financial support.

REFERENCES

1. Tew, B. Y. (2023). ATM-Inhibitor AZD1390 Is a Radiosensitizer for Breast Cancer CNS Metastasis.," *Clin. cancer Res. an Off. J. Am. Assoc. Cancer Res.,* 29 (21), 4492–4503. https://doi.org/10.1158/1078-0432.CCR-23-0290
2. Huang, R. X., Zhou, P. K. (2020). "DNA damage response signaling pathways and targets for radiotherapy sensitization in cancer," *Signal Transduct. Target. Ther.,* 5(1) https://doi.org/10.1038/s41392-020-0150-x
3. Alizzi, Z., Saravi, S., Khalique, S. McDonald, T., Karteris, E., Hall, M. (2023). Identification of RAD51 foci in cancer-associated circulating cells of patients with high-grade serous ovarian cancer: association with treatment outcomes. *Int. J. Gynecol. cancer Off. J. Int. Gynecol. Cancer Soc.,* 33(9), 1427–1433. https://doi.org/10.1136/ijgc-2023-004483
4. Holthausen, J., Wyman, T. C., Kanaar, R. (2010). Regulation of DNA strand exchange in homologous recombination. *DNA Repair (Amst).,* 9(12), 1264–1272. https://doi.org/10.1016/j.dnarep.2010.09.014
5. Feng, Y. Wang, D., Xiong, D. L., Zhen, G., Tan, J. (2021). Predictive value of RAD51 on the survival and drug responsiveness of ovarian cancer. *Cancer Cell Int.,* 21(1), 249. https://doi.org/10.1016/j.dnarep.2010.09.014
6. Nagathihalli, N. S., Nagaraju, G. (2011). RAD51 as a potential biomarker and therapeutic target for pancreatic cancer. *Biochim. Biophys. Acta — Rev. Cancer*. ,1816(2), 209–218. https://doi.org/10.1016/j.bbcan.2011.07.004
7. Song, J. (2021). Overexpression of HMGA1 confers radioresistance by transactivating RAD51 in cholangiocarcinoma. *Cell Death Discov.,* 7(1), 322. https://doi.org/10.1038/s41420-021-00721-8
8. Xu,Y., Chen, K., Cai, Y., Cheng, C., Zhang,Z., Xu, G. (2019). Overexpression of Rad51 predicts poor prognosis and silencing of Rad51 increases chemo-sensitivity to doxorubicin in neuroblastoma. *Am. J. Transl. Res.,* 11(9), 5788.
9. Clin, A. (2020). RAD51 Inhibitor Reverses Etoposide-Induced Genomic Toxicity and Instability in Esophageal Adenocarcinoma Cells. *Arch. Clin. Toxicol.,* 2(1), 3–9. https://doi.org/10.46439/toxicology.2.006
10. Alagpulinsa, D., Ayyadevara, A. S., Shmookler Reis, R. J. (2014). A small molecule inhibitor of RAD51 reduces homologous recombination and sensitizes multiple myeloma cells to doxorubicin. *Front. Oncol.,* 4, 1–11, https://doi.org/10.3389/fonc.2014.00289
11. Ward, A. (2017). Quinazolinone derivatives as inhibitors of homologous recombinase RAD51. *Bioorg. Med. Chem. Lett.,* 27(14), 3096–3100. https://doi.org/10.1016/j.bmcl.2017.05.039
12. Doğan, A. A. Doğan, N. C. (2022). Investigation of the effects of sodium phenylpyruvate on pulmonary adenocarcinoma (A549) and mammary adenocarcinoma (MDA-MB-231) on cell lines. *Cauc. J. Sci.,* 9(1), 20–34. https://doi.org/10.48138/cjo.979147

13. Wu, D., Yotnda, P. (2011). Production and detection of reactive oxygen species (ROS) in cancers. *JoVE (Journal Vis. Exp.,* 57, e3357. https://doi.org/ 10.3791/3357
14. Özdemir, D., Saruhan, S., Agca, C. A. (2023). KAN0438757: a novel pfkfb3 inhibitor that induces programmed cell death and suppresses cell migration in non-small cell lung carcinoma cells. *Biotechnol. Acta*, 16(5), 34–44. https://doi.org/10.15407/biotech16.05.034
15. Ruíz, G., Valencia-González, H. A., León-Galicia, I., García-Villa, E., García-Carrancá, A., Gariglio, P. (2018). Inhibition of RAD51 by siRNA and resveratrol sensitizes cancer stem cells derived from HeLa cell cultures to apoptosis. *Stem cells international*, 1, 2493869. https://doi.org/10.1155/2018/2493869
16. Gu, P., Xue, L., Zhao, C., Li, W., Jiang, Z., Liu, A., … Tang, R. (2022). Targeting the homologous recombination pathway in cancer with a novel class of RAD51 inhibitors. *Frontiers in Oncology*, 12, 885186. https://doi.org/10.3389/fonc.2022.885186

UDC 577.112+616.15+616-092.9+663.85 **https://doi.org/10.15407/biotech18.02.079**

BLOOD METALLOPROTEINS IN RATS UNDER CONDITIONS OF ENERGY DRINK CONSUMPTION

KH.Y. PARTSEI, M.B. ARTYSH, H.M. ERSTENIUK, H.V. TOKARYK, T.P. MAKSYMCHUK

Ivano-Frankivsk National Medical University, Ukraine

E-mail: hrustuna012y@gmail.com

Received 2025/03/17
Revised 2025/03/22
Accepted 2025/04/30

The study *aimed* to evaluate the effect of energy drinks on the level of Cu, Fe, ceruloplasmin activity and transferrin saturation in the blood serum of rats.

Materials and Methods. The study was conducted on white male Wistar rats divided into two groups: control and experimental. The experimental group received the energy drink Burn for 30 days. Blood samples were taken under anesthesia by decapitation on the 1st day after the drink was discontinued. The content of Cu and Fe was determined by atomic absorption spectrophotometry. Ceruloplasmin activity and transferrin saturation were studied by the method of Babenko G.O.

Results. Against the background of energy drink consumption in the experimental group, a decrease in the level of Cu by 43% and Fe by 67% was observed compared to the control. Transferrin saturation decreased by 42% and ceruloplasmin activity by 40%. The data obtained indicate that the consumption of an energy drink causes complex changes in the metabolism of Cu and Fe, which is reflected in a decrease in the level of these trace elements in the blood and the activity of metalloenzymes, in particular ceruloplasmin and transferrin, which can lead to the development of oxidative stress and impaired functioning of both individual organs and the body as a whole.

Conclusions. The results obtained indicate the development of dysmicroelementosis in the context of energy drink consumption, which can have adverse effects on the functioning of red blood cells, body systems, and tissues, an increase in the level of endogenous intoxication, and impaired tissue respiration.

Keywords: energy drink, rats, blood, Cu, Fe, ceruloplasmin, transferrin saturation.

Recent decades have seen a significant increase in the popularity of energy drinks, which are actively consumed by people of all ages to improve performance and concentration and reduce fatigue. The main active ingredients of such beverages are caffeine, taurine, B vitamins, and other stimulants that affect metabolic processes in the body. However, the effect of energy drinks on mineral metabolism, in particular on the level of vital trace elements and metalloenzymes, remains insufficiently studied.

Copper and Iron are among the key trace elements involved in critical biochemical processes. Iron is necessary for the synthesis of hemoglobin, myoglobin, and a number of enzymes in the respiratory chain that ensure cellular respiration and oxygen transportation [2]. At the same time, Copper plays the role of a cofactor of many enzymes, including ceruloplasmin, superoxide dismutase, and cytochrome oxidase, which are involved in redox reactions and antioxidant protection of cells.

The balance of these trace elements in the blood is maintained by specialized transport proteins. Ceruloplasmin is the main protein that transports Cu and is involved in the regulation of the oxidation of Fe to its trivalent form (Fe^{3+}), which is necessary for binding to transferrin, the main transport protein of Fe. Disruption of this balance can lead to changes in the absorption, transport, and deposition of trace elements, which, in turn, can have negative consequences for metabolic processes.

Citation: Partsei, Kh. Y., Artysh, M. B., Ersteniuk, H. M., Tokaryk, H. V., Maksymchuk, T. P. (2025). Blood metalloproteins in rats under conditions of energy drink consumption. *Biotechnologia Acta*, 18(2), 79–81. https://doi.org/10.15407/biotech18.02.079

This study aimed to evaluate the effect of energy drinks on the level of Cu, Fe, ceruloplasmin activity and transferrin saturation in the blood serum of rats.

Materials and Methods. The experimental study was conducted on white male Wistar rats weighing 150–220 g, which were kept in the vivarium of IFNMU. All manipulations complied with modern ethical and legal requirements for animal experiments. In particular, the study was in accordance with the norms of the European Convention for the Humane Treatment of Laboratory Animals (Strasbourg, 1986), the Order for the Improvement of Experimental Work with Animals, and the General Principles of Animal Experiments adopted at the First National Congress on Bioethics (Kyiv, 2001). In addition, all procedures complied with the provisions of the Law of Ukraine "On Protection of Animals from Cruelty" (2010).

Animals were kept in groups of five in standard laboratory conditions with controlled light, temperature, a balanced diet, and unlimited access to water. The rats were divided into two groups: the control group - healthy animals receiving a standard diet and water; and the experimental group - animals that consumed the energy drink for 30 days, after which blood was taken on the first day after the experiment was terminated. The Burn energy drink was administered orally through drinkers to rats daily for 30 days. The animals were housed in separate cages while receiving the drink. The dosage was calculated taking into account body weight (per 1 kg) and species characteristics of the rats.

Blood was taken under anesthesia (intramuscular injection of sodium thiopental, 60 mg/kg) by decapitation on the 1st day after the cessation of the drink. The level of ceruloplasmin and transferrin saturation in the blood serum was estimated according to the method of Babenko G.O. [1]. The principle of the method is based on determining the reserve capacity of blood serum for ron binding. To do this, a solution containing a precisely specified amount of Iron is added to the serum. When transferrin is completely saturated with Iron, excess iron ions precipitate an equivalent amount of this excess iron on serum protein, which will cause a certain degree of serum turbidity. The intensity of the turbidity, determined using a photoelectrocolorimeter, gives an idea of the degree of transferrin saturation with iron in the test serum. The principle of the method for determining ceruloplasmin activity is based on the oxidation of p-phenylenediamine with the participation of CP. The enzymatic reaction was stopped by the addition of sodium chloride. The test samples are colorimetrically analyzed using a photoelectrocolorimeter against a control sample under a 530 mm green light filter. The determination of the content of Cu and Fe in the blood of animals was carried out by atomic absorption spectrophotometry using a SHIMADZU AA-7000 spectrophotometer [6]. STATISTICA 7 software was used for statistical processing of the results using Student's t-test.

Results and Discussion. The trace elements Cu and Fe perform essential biological functions; in particular, they are involved in the processes of metabolism and antioxidant defense. Copper plays a significant role in ensuring oxidative reactions and is also part of key enzymes that regulate the antioxidant balance [4]. Our results indicate a gradual decrease in the content of copper in the blood of experimental animals under the influence of the energy drink by 43% compared to the control (Fig. 1). Ferrous, which is a necessary element for oxygen transport and the functioning of a number of enzyme systems, has also changed. The content of Fe in the blood decreased in experimental animals by 67% compared to control values. Such dynamics may indicate an imbalance in the iron transport system, which is likely due to changes in the structure of proteins responsible for its regulation.

One of the key regulators of iron metabolism is transferrin, which ensures the binding and transfer of Fe in the body. Under the influence of the energy drink, its saturation in the experimental group of animals decreased by 42% compared to the control animals (Fig. 2). Such a change may contribute to an increase in the proportion of total iron, which is a catalyst for the formation of reactive oxygen species and increases oxidative stress [3]. A decrease

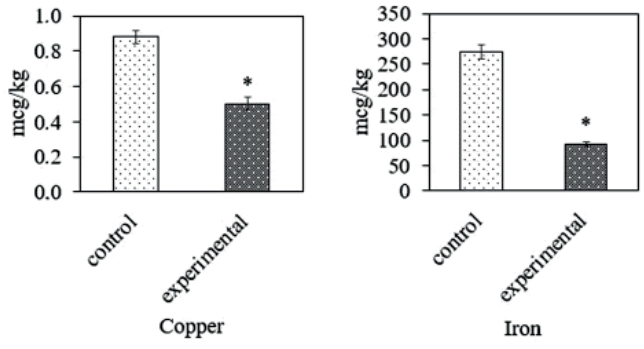

Fig. 1. **Effect of energy drink on the content of Cu and Fe in the blood serum of rats**
* — $p < 0.001$ — reliability compared to the control group

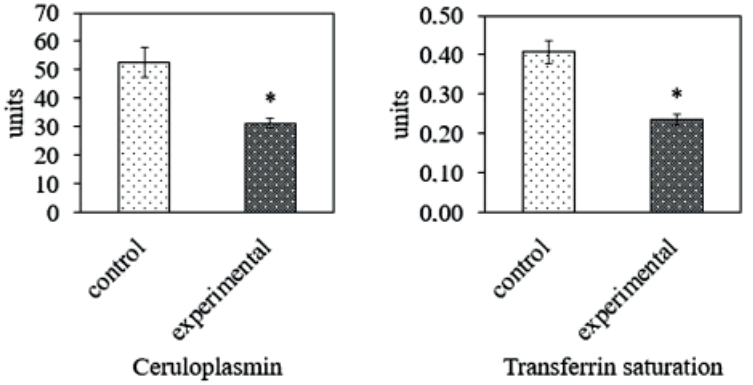

Fig. 2. **Effect of energy drink on ceruloplasmin activity and transferrin saturation in the blood serum of rats**
* — $p < 0.001$ — reliability compared to the control group

in ceruloplasmin activity, which is also involved in the regulation of iron metabolism and antioxidant defense, confirms the negative impact of energy drinks on the balance of trace elements. Already on the 1st day after the end of the drink administration, this indicator decreased by 40% compared to the control. It is known that ceruloplasmin deficiency can lead to the accumulation of free-form Fe ions, which puts an additional burden on the antioxidant system and increases the risk of oxidative cell damage.

The data obtained indicate that the consumption of an energy drink causes complex changes in the metabolism of Cu and Fe, which is reflected in a decrease in the level of these trace elements in the blood and the activity of metalloenzymes, in particular ceruloplasmin and transferrin, which can lead to the development of oxidative stress[5] and impaired functioning of both individual organs and the body as a whole.

Conclusion. The results obtained indicate the development of dysmicroelementosis in the context of energy drink consumption, which can have adverse effects on the functioning of red blood cells, body systems, and tissues, an increase in the level of endogenous intoxication, and impaired tissue respiration. The findings emphasize the potential risks of energy drink consumption and the need for further research to assess their impact on homeostasis and metabolic processes in the body.

Authors` contribution

Partsei Kh. Y. — experimental study, collection of material, analysis of the data obtained, preparation of theses for publication; Artysh M.B. — participated in the collection of material; Ersteniuk H. M. advising on the formation of the purpose and objectives of the study; Tokaryk H.V. — participated in the editing of the abstracts; Maksymchuk T.P. — participated in the formulation of conclusions.

Funding source

The work is a fragment of interdepartmental research work "Scientific substantiation and improvement of diagnosis and treatment of endocrinopathies based on the study of priority etiopathogenetic factors and comorbidities" (2019–2024, State registration number 0120U0105103) without special funding.

REFERENCES

1. Guranych, S. P., Voronych-Semchenko, N. M., Guranych, T. V. (2017). Prooxidant-antioxidant status of dental pulp and oral mucosa of rats with experimental iodine deficiency and insulin resistance. *Ukr. J. Medic., Boil. Ta Sport*., 2(4), 16–20. (In Ukrainian).
2. Gkouvatsos, K., Papanikolaou G, Pantopoulos K. (2012). Regulation of iron transport and the role of transferrin. *Biochim. Biophys. Acta*., 1820(3), 188–202. https://doi.org//10.1016/j.bbagen.2011.10.013.
3. Khan, F., Ahmad, N., Ahmed, S. (2021). Role of ceruloplasmin in oxidative stress and energy drink-induced toxicity. *Oxid Med. Cell Longev*., 6634792. https://doi.org//10.1155/20/663479
4. Lewandowski, Ł., Kepinska, M., Milnerowicz, H. (2018). Inhibition of copper-zinc superoxide dismutase activity by selected environmental xenobiotics. *Environmental Toxicology and Pharmacology. Elsevier BV*., 58, 105–13. URL: http://dx.doi.org/10.1016/j.etap.2017.12.022.
5. Maury, P. K., Kumar, P., Chandra, P. (2015). Biomarkers of oxidative stress in erythrocytes as a function of human age. *World Journal of Methodology. Baishideng Publishing Group Inc.,* 5(4), 216. URL: http://dx.doi.org/10.5662/wjm.v5.i4.216.
6. Shkurashivska, S., Ersteniuk, H. (2019). The effect of adrenaline on the mineral and trace element status in rats. *Open Life Sciences. Walter de Gruyter GmbH*., 14, 158–64. URL: http://dx.doi.org/10.1515/biol-2019-0018.

UDC 601.02: 577.29 **https://doi.org/10.15407/biotech18.02.082**

EVALUATING THE EFFECTS OF DISINTEGRIN ON TUMOUR GROWTH

O. M. PLATONOV, Y. D. VINNYCHUK

Palladin Institute of Biochemistry of the National Academy of Sciences of Ukraine, Kyiv

E-mail: *chaosplaton@gmail.com*

Received 2025/03/06
Revised 2025/03/16
Accepted 2025/04/30

Cancer is the second leading cause of death in the world after cardiovascular disease, and many types of cancer have no symptoms in the early stages, making it difficult to diagnose. At the same time, some tumors do not respond well to therapy, with its severe side effects. Tumor cells themselves can spread through the bloodstream or lymphatic system, making treatment difficult, so the search for compounds with antiproliferative and antimetastatic effects is ongoing. In our study, we tested disintegrin from *Echis multisquamatus* venom as an antitumor drug in an *in vivo* animal model to determine the degree of inhibition of Walker-256 carcinosarcoma tumor growth.

Aim. The work purposed to investigate the effect of disintegrin on the growth dynamics of Walker-256 carcinosarcoma in rats.

Materials and Methods. Crude venom of *Echis multisquamatus* was fractionated using ion-exchange chromatography followed by size-exclusion chromatography on Superdex 75 using the FPLC system (ÄKTA, GE Healthcare, USA). Analysis of the molecular weight of protein components was performed using SDS-PAGE. *The concentration of protein was measured using a spectrophotometer Optizen POP (Korea) at 280 nm.* Walker-256 carcinosarcoma cells for transplantation into laboratory animals were obtained from the National Bank of Cell Lines and Tumour Strains of the R.E. Kavetsky Institute of Experimental Pathology, Oncology and Radiobiology of the National Academy of Sciences of Ukraine.

Results. The two-step chromatography protocol allowed us to obtain the polypeptide from the venom of Echis multisquamatus that possessed the anti-aggregatory action. SDS-PAGE analysis confirmed the homogeneity of the obtained polypeptide with a molecular weight of 14,889 kDa. The tumor cells of Walker-256 carcinosarcoma were transplanted subcutaneously into the inguinal area of the right lower limb of 10 rats in the amount of 1.5×106 cells in 300 µl of saline (0.9% NaCl). The inhibition of tumor growth, which is one of the criteria for the effectiveness of the test substance, was observed during the period of intensive tumor growth and amounted to 18.7% on day 9 after inoculation and 36.2% on day 11.

Conclusions. The studies showed that the use of disintegrin from *Echis multisquamatus* venom led to inhibition of the growth of Walker's carcinosarcoma W-256 on the 9th to 11th day after tumor inoculation in rats. The observed inhibitory effect was moderate and less than the expected effect of antitumor agents. From the point of view of the mechanism of action of disintegrins, a reduction in the quality of cell attachment should be expected, which is not crucial in the conditions of tumor grafting.

Keywords: disintegrin, integrin receptors, cancer cells lines, cancer animal models, metastasis

The state of intercellular communication, in many cases, determines the development, tissue organization, and functioning of multicellular organisms. Therefore, one of the priorities of modern biology and medicine is to study the cellular and molecular mechanisms of intercellular interactions.

Citation: Platonov, O. M., Vinnychuk, Y. D. (2025). Evaluating the effects of disintegrin on tumour growth. *Biotechnologia Acta*, 18(2), 82–85. https://doi.org/10.15407/biotech18.02.082

Adhesion molecules play a key role in cell proliferation and differentiation, stabilization of intercellular contacts, as well as processes underlying intercellular signaling, being an essential intermediate between extracellular structures and the cell cytoskeleton [1, 2]. The binding of these molecules to their respective ligands initiates a number of intracellular biochemical reactions that can lead to changes in the cytoskeleton state and affect other processes [3].

The research of adhesion mechanisms in oncology is essential. Adhesion molecules are the key to cancer cells interacting with the endothelium of distant organs and non-cellular matrix elements, as a necessary property of malignant cells is a change in their morphology and locomotion [4].

The main categories of adhesion receptors include integrins, which are necessary for the dynamic regulation of adhesion and migration processes [5]. The expression of integrins on the surface of malignant cells is highly prognostic, as they are involved in almost every stage of progression, from primary tumor development to metastasis [6].

Integrins are transmembrane glycoproteins consisting of a and b-subunits that can bind to each other non-covalently in different ways to form more than 20 types of integrins. Various combinations of subunits determine the specificity of binding of the receptor's non-cellular domain to a particular ligand (most often, these are different non-cellular matrix proteins: collagens, laminin, fibronectin, etc.) [7].

Thus, the study of the complex interrelationships between adhesive and metastatic signaling networks is urgent to find new treatment approaches [3]. And, in particular, integrins are attractive targets for the development of cancer therapeutics [6, 8]. Therefore, the study of the potential of blocking integrin receptors on tumour cells, which helps to inhibit integrin-mediated interaction at different stages of the disease, may help to find new practical approaches to the treatment of malignancies. The use of experimental animal models as an object of study has excellent advantages in assessing the effectiveness of treatment, which also allows the reproducing of tumour growth in more pathophysiological conditions, ensures genomic heterogeneity of human cancer, and creates a complex tumour microenvironment [9].

The work aimed to investigate the effect of disintegrin on the growth dynamics of Walker-256 carcinosarcoma in rats.

Methods. The study of the effect of disintegrin on tumor growth *in vivo* was performed on Wistar rats aged 2.5 months and weighing 180–200 g (vivarium of the Palladin Institute of Biochemistry of the National Academy of Sciences of Ukraine). The rats were kept in standard vivarium conditions with natural light and a standard diet.

Walker-256 carcinosarcoma was used as a model of tumor growth. Taking into account the morphological characteristics and the course of the tumor process, this tumor can be considered an experimental model of breast cancer, which allows the reproduction of the processes that occur sequentially at all stages of growth over a short period [10]. Walker-256 carcinosarcoma cells were obtained from the National Bank of Cell Lines and Tumour Strains of the R.E. Kavetsky Institute of Experimental Pathology, Oncology and Radiobiology of the National Academy of Sciences of Ukraine.

To obtain isolated tumor cells, tumors were removed from animals, tissue fragments without blood vessels and necrosis were cut out, reduced to a particle size of less than 0.2 mm^3 with scissors, and incubated for 5 min at 37 °C in 0.2% trypsin solution in RPMI-1640 medium (Sigma, USA) with constant use of magnetic stirrer. The liquid was collected, filtered through 3 layers of nylon, and washed with 10% fetal calf serum. The cells were incubated with trypsin 3 times. The isolated cells were washed 3 times by centrifugation at 425 g in RPMI-1640 medium. The percentage of cell viability was counted in a Goryaev chamber by trypan blue staining. Tumor cells were transferred subcutaneously into the inguinal area of the right lower limb of 10 rats in the amount of 1.5×10^6 cells in 300 µl of physiologically buffered saline (0.9% NaCl).

The rats were divided into two groups: a control group, which received saline together with tumor cells, and an experimental group, which received cells in a 750 µg/ml disintegrin solution. On every second day, equal volumes of saline and disintegrin solution were injected into the tail vein of the control and experimental groups, respectively.

To evaluate the tumor growth, the tumor diameter was measured in two directions for each animal using a caliper every 2 days during the experiment. The tumor volume was calculated, as well as the percentage of tumor growth inhibition and the index of effectiveness of the test substance according to the formulas [11]:

$$\text{Volume (V)} = \text{length} \times (\text{width})2/2$$

$$\text{Percentage of tumour growth inhibition} = [(\text{Vcontrol} - \text{Vtest})/\text{Vcontrol}]\times100\%.$$

$$\text{Efficiency index (EI)} = \text{Vcontrol}/\text{Vtest}$$

All animal studies were carried out in accordance with the standards established by the Law of Ukraine No. 3447-IV 'On the Protection of Animals from Cruelty' and the standards established by the European Convention for the Protection of Vertebrate Animals Used for Experimental and Scientific Purposes of 20.09.1985.

Results and Discussion. The effect of disintegrin on the growth of Walker W-256 carcinosarcoma was measured by determining the change in tumor volume in rats of the control and experimental groups on days 9, 11, and 14 after tumor implantation. At each time point of the experiment, the tumor diameter was measured in two directions, and the tumor volume, tumor growth inhibition, and the factor effectiveness index were calculated.

When comparing the results obtained, there was a tendency to reduce the tumor volume in the experimental group (especially on day 11 of tumor growth). Statistically significant differences in the mean values of tumor volumes in rats of both groups were not found, as there were substantial individual fluctuations in tumor size in animals (Table 1). However, the inhibition of tumor growth, which is one of the criteria for the effectiveness of the test substance, was recorded during the period of intensive tumor growth and amounted to 18.7% on day 9 after inoculation and 36.2% on day 11. The calculation of the efficacy index, as an indicator of the sensitivity of the tumor to the effects of the test substances, was 1.23 (day 9) and 1.56 (day 11).

Table 1. **Effect of disintegrin on the dynamics of tumor growth in rats**

Control group (n = 5)				**Experimental group (n = 5)**		
Day after tumour replantation	Length, cm	Width, cm	Volume, cm^3	Length, cm	Width, cm	Volume, cm^3
9 day	4.94±0.7	3.62±0.5	46.04±16.6	4.46±0.6	3.68±0.3	37.42±11.7
11 day	5.66±0.5	4.76±0.6	78.02±21.0 [21.3: 63.5]	4.78±0.7	4.18±0.5	49.92±19.2 [25.3: 56.2]

Conclusions. In an *in vivo* model system, it was shown that disintegrin in a dose of 100 μg/ml leads to inhibition of growth of Walker's carcinosarcoma W-256 on days 9–11 after tumor inoculation in rats.

Authors' contribution

Vinnychuk — research, conceptualization, data collection, visualization, writing original draft, review, proofreading the manuscript; Platonov — research, editing.

Funding source

The research was financed by project No. 0124U000251, "Research and search for ways to regulate molecular mechanisms of intravascular and extravascular thrombosis" (2024–2028).

Acknowledgment

The authors gratefully acknowledge Dr. Chernyshenko V. for his endless support of this research and Dr. Karatsuba T. for the help with the cancer modeling.

REFERENCES

1. Ushakova, G. O., Nedzetskyi, V. S., Kyrychenko, V. S. (2018). Molecular mechanisms of intercellular communication. (G. O. Ushakova, Ed.). Kyiv.
2. Khalili, A. A., Ahmad, M. R. (2015). A review of cell adhesion studies for biomedical and biological applications. *International Journal of Molecular Sciences,* 16(8), 18149–18184. https://doi.org/10.3390/ijms160818149
3. Yayan, J., Franke, K.-J., Berger, M., Windisch, W., Rasche, K. (2024). Adhesion, metastasis, and inhibition of cancer cells: A comprehensive review. *Molecular Biology Reports,* 51(1), 165. https://doi.org/10.1007/s11033-023-09089-2
4. Rozumenko, V. D., Glavatskyi, O. Ya., Vasilyeva, I. G., Chopyk, N. G., Lysenko, S. M. (2004). Main phenotypic manifestations and principles of genotype formation of malignant brain tumors. *Ukrainian Journal of Neurosurgery,* 3, 4–13. http://nbuv.gov.ua/UJRN/Unkhj_2004_3_3 (In Ukrainian).

5. Glusman, D. F., Abramenko, I. V., Sklyarenko, L. M., Pysniachievska, H. V. (1993). Immunocytochemical diagnosis of malignant exudates. *Naukova Dumka.* 147. (In Ukrainian).
6. Liu, F., Wu, Q., Dong, Z., Liu, K. (2023). Integrins in cancer: Emerging mechanisms and therapeutic opportunities. *Pharmacology & Therapeutics*, 247, 108458. https://doi.org/10.1016/j.pharmthera.2023.108458
7. Cooper, J., Giancotti, F. (2019). Integrin signaling in cancer: Mechanotransduction, stemness, epithelial plasticity, and therapeutic resistance. *Cancer Cell*, 35(3), 347–367. https://doi.org/10.1016/j.ccell.2019.01.007
8. Hamidi, H., Ivaska, J. (2018). Every step of the way: Integrins in cancer progression and metastasis. *Nature Reviews Cancer,* 18(9), 533–548. https://doi.org/10.1038/s41568-018-0038-z
9. Mendes, N., Carvalho, P., Martins, F., Mendonça, S., Malheiro, A., Ribeiro, A., Carvalho, J., Velho, S. (2020). Animal models to study cancer and its microenvironment. *Advances in Experimental Medicine and Biology,* 1219, 389–401. https://doi.org/10.1007/978-3-030-32656-2_16
10. Aparecida do Amaral, L., Santos, M., Oliveira de Souza, G. (2019). Walker-256 tumor: Experimental model, implantation sites and number of cells for ascitic and solid tumor development. *Brazilian Archives of Biology and Technology*, 62(12), e19180284.
11. McKenzie, R., Oran, A., Dinarello, C., Sauder, D. (1996). Interleukin-1 receptor antagonist inhibits subcutaneous B16 melanoma growth *in vivo*. *Anticancer Research,* 16*(*1), 437–441.

UDC 577.21:578.1 https://doi.org/10.15407/biotech18.02.086

EVALUATION OF NUCLEIC ACID EXTRACTION METHODS FOR PATHOGEN DETECTION USING PCR

D.K. PROKHORENKO[1, 2], *I. I. GRYNYUK*[1]

[1]Igor Sikorsky Kyiv Polytechnic Institute, Kyiv, Ukraine
[2]"XEMA" LLC, 23 Akademika Yefremova St., Kyiv, Ukraine

E-mail: pdmytro378@gmail.com

Received 2025/03/06
Revised 2025/03/16
Accepted 2025/04/30

This work focuses on evaluating nucleic acid extraction methods and optimizing lysis buffer components to enhance nucleic acid yield and minimize the impact of potential inhibitors on target gene amplification to improve the detection of causative pathogens and facilitate their integration into diagnostic practice.

Aim. To compare nucleic acid extraction methods from patient biological samples and to optimize lysis buffer composition to enhance nucleic acid yield.

Methods. Spectrophotometric and fluorometric methods were used to assess the efficiency and quality of nucleic acid extraction. The concentration of the obtained nucleic acids was measured using a Qubit 4 fluorometer. The quality of the extracted nucleic acids was analyzed by electrophoretic separation in agarose gel, which allowed for the assessment of their integrity and the presence of degradation. To evaluate the inhibition of target genes by extraction agents, real-time PCR was applied.

Results. Solid-phase extraction using silica-coated magnetic particles demonstrated superior performance compared to liquid-liquid extraction. Optimal lysis conditions were achieved using 2.7 M guanidinium thiocyanate with 30% isopropanol, which enhanced DNA recovery and inhibitor removal. The addition of glycogen-linear polyacrylamide improved DNA precipitation in the liquid-liquid method. Overall, the solid-phase approach showed better amplification efficiency and nucleic acid yield.

Conclusions. It was established that solid-phase extraction methods based on silica-coated magnetic carriers are optimal for isolating nucleic acids from patients' biological samples for pathogen differentiation.

Keywords: nucleic acid extraction, pathogen identification, polymerase chain reaction, diagnostics.

Given the increasing importance of pathogen diagnostics, particularly under conditions of active warfare, there is a need to refine and implement rapid and selective methods for pathogen identification applicable at the early stages of infection. Compared to traditional bacteriological methods, which require 24 to 72 hours, real-time polymerase chain reaction (PCR) enables significantly faster results — within a few hours, which is critically important for patients in severe condition [1, 2]. PCR is a highly sensitive method capable of rapidly detecting pathogens, however, its effectiveness depends on the quality of the prepared nucleic acid sample. Despite the widespread use of solid-phase and liquid-liquid extraction of nucleic acids in clinical practice, both methods require adaptation and optimization according to the biological properties of the specific pathogen and the source of biological material.

Citation: Prokhorenko, D. K., Grynyuk, I. I. (2025). Evaluation of nucleic acid extraction methods for pathogen detection using PCR. *Biotechnologia Acta*, 18(2), 86–88. https://doi.org/10.15407/biotech18.02.086

Aim. To compare nucleic acid extraction methods from patient biological samples and to optimize lysis buffer composition to enhance nucleic acid yield.

Methods. The concentration of the obtained nucleic acids was measured using a Qubit 4 fluorometer (Thermo Fisher Scientific, USA) [3]. The quality of the extracted nucleic acids was analyzed by electrophoretic separation in agarose gel [4]. To evaluate the inhibition of target genes by extraction agents, real-time PCR was applied. Nucleic acid amplification was performed using the Bio-Rad CFX96 Touch^{TM} Real-Time PCR Detection System in a two-phase thermal cycling mode. The amplification protocol included an initial denaturation at 94 °C for 3 minutes, followed by 9 cycles consisting of denaturation at 94 °C for 20 seconds, annealing at 58 °C for 30 seconds, and elongation at 72 °C for 30 seconds. This was followed by 38 additional cycles with shortened durations: 94 °C for 15 seconds, 58 °C for 15 seconds, and 72 °C for 15 seconds, with fluorescence measurement conducted during the elongation step. The total number of cycles was 47. Fluorescence analysis was performed during the elongation phase of the second block-phase.

Results and Discussion. The study compared two nucleic acid extraction methods of solid-phase extraction using silica-based sorbents on magnetic particles and liquid-liquid extraction — to assess their efficiency and potential for automation.

A human plasma sample spiked with a known quantity of target DNA (10^4 copies) was used for extraction. Real-time PCR was performed with a reference standard equivalent to 10^4 copies of the target fragment, providing a benchmark Ct value of 22.4 under the defined threshold conditions. An analysis of how the extraction method affects target gene amplification (see Table) showed that solid-phase extraction using silica-coated magnetic particles resulted in higher nucleic acid copies count and less inhibition of probe (Ct = 22.8 ± 0.2), improved purity (A260/280 = 1.91), less time consumption and was more suitable for PCR automation.

Comparison of solid-phase and liquid-liquid nucleic acid extraction methods (n = 5)

Extraction method	A260/280	Ct (qPCR)	Time (min)	DNA Degradation Level
Solid-phase extraction	1.91	22.8±0.2	40	Low
Liquid-liquid extraction	1.73	23.0±0.4	60	Moderate

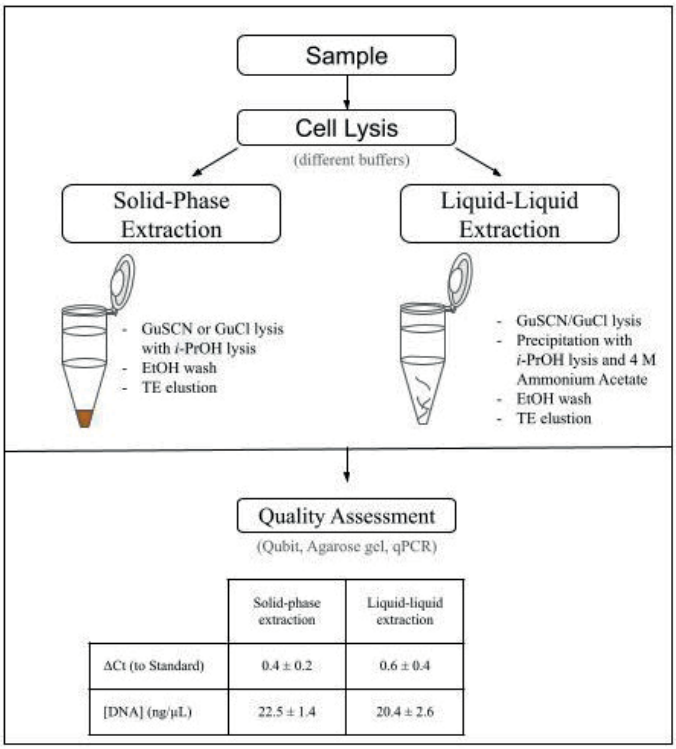

Schematic representation of the research results

To ensure efficient disruption of the cell membrane and release of nucleic acids, different types of lysis buffers containing chaotropic agents – solutions of guanidinium thiocyanate (1.5 M–6 M) and guanidinium chloride (1.5 M–5 M) in isopropanol (0–40%) were tested. Real-time PCR analysis showed that the absence of an organic phase significantly reduced the amount of recoverable target DNA template.

The use of urea and alkali metal thiocyanates had no notable effect on DNA yield, while alkaline conditions negatively affected RNA stability. The most effective lysis buffers contained 2.7 M guanidinium thiocyanate in 30% isopropanol, which facilitated both the removal of PCR inhibitors and the precipitation of nucleic acids. In the case of liquid-liquid extraction, the addition of glycogen-linear polyacrylamide (4 mg/mL) proved to be an efficient co-precipitant for improving DNA recovery.

The figure presents the main steps of solid-phase and liquid-liquid DNA extraction methods, including cell lysis using guanidinium-based buffers, washing steps, elution, and subsequent quality assessment using qPCR and spectrophotometry.

Comparative evaluation of solid-phase and liquid-liquid nucleic acid extraction methods based on ΔCt values (relative to standard) and DNA concentration (ng/μL) confirmed the advantage of the solid-phase method in both the quantity of recovered nucleic acids and their amplification efficiency.

Conclusions. It was established that solid-phase extraction using silica-coated magnetic particles is optimal for isolating nucleic acids from patient biological samples for downstream pathogen identification. The optimal extraction conditions include the use of lysis buffers containing 2.7 M guanidinium thiocyanate and 30% isopropanol, which increase DNA yield and reduce PCR inhibition.

Authors' contribution

D.K. Prokhorenko conducted biochemical studies, processed and analyzed the obtained results, wrote the abstract, I. I. Grynyuk analyzed the data and edited the text.

Funding source

The work was supported by the LLC "XEMA", Ukraine.

REFERENCES

1. Singer, M., Deutschman, C.S., Seymour, C.W., Shankar-Hari, M., Annane, D., Bauer, M., Bellomo, R., Bernard.,..., Angus, D.C. (2016). The Third International Consensus Definitions for Sepsis and Septic Shock (Sepsis-3). *JAMA*, 23, 315(8), 801–810. https://doi.org/10.1001/jama.2016.0287
2. World Health Organization. Sepsis [Electronic resource] / World Health Organization. URL: https://www.who.int/news-room/fact-sheets/detail/sepsis. (Accessed. April, 2025).
3. Lucena-Aguilar, G., Sánchez-López, A.M., Barberán-Aceituno, C., Carrillo-Ávila, J.A., López-Guerrero, J.A., Aguilar-Quesada, R. (2016). DNA Source Selection for Downstream Applications Based on DNA Quality Indicators Analysis. *Biopreserv Biobank*, 14(4), 264–270. https://doi.org/10.1089/bio.2015.0064
4. Stellwagen, N. C. (2009). Electrophoresis of DNA in agarose gels, polyacrylamide gels and in free solution. *Electrophoresis*, 30(S1). https://doi.org/10.1002/elps.200900052.

UDC 616.155.392-089.843:611.018.46+616-097

https://doi.org/10.15407/biotech18.02.089

LIMITATIONS OF HUMAN LEUKOCYTE ANTIGEN MOLECULAR TYPING METHODS FOR PATIENTS WITH ACUTE MYELOID LEUKEMIA RELAPSE AFTER HEMATOPOIETIC STEM CELL TRANSPLANTATION

L.O. SISHCHUK, I.I. TUBALTSEVA, N.A. TSOKOLENKO, A.O. MAKSYMCHUK, A.V. KUKHOL, V.V. ANDRUSENKO, A.O. MAZANOVA, Y.A. HROHUL

National Specialized Children's Hospital "OKHMATDYT"
of the Ministry of Health of Ukraine, Kyiv

E-mail: sishchuklesia1313@gmail.com

Received 2025/03/18
Revised 2025/03/24
Accepted 2025/04/30

Aim. The work purposed to compare molecular typing methods with different resolutions in clinical cases without loss of heterozygosity (LOH) in HLA genes.

Methods. HLA typing was performed using molecular techniques based on sequence-specific primers (SSP) or high-resolution sequencing (NGS and Sanger sequencing).

Results. the presence of an extra allelic variant in testing DNA samples was determined only with the low-resolution SSP method. At the same time, any type of sequencing did not allow for distinguishing donors' alleles from patients.

Conclusion. Despite the high sensitivity of NGS and Sanger sequencing, the use of these methods is associated with difficulties in accurately determining the absence of HLA-LOH.

Keywords: HLA-LOH, HLA typing, hematopoietic stem cell transplantation, sequencing.

Human leukocyte antigen (HLA) typing plays a key role in hematopoietic stem cell transplantation (HSCT) by ensuring the selection of the most genetically compatible donor and, as a result, reducing the risk of graft-versus-host disease. Molecular genetic methods, including Next-Generation Sequencing (NGS) and Sanger sequencing-based typing (SBT), improved the accuracy of HLA gene determination and decoding [Geo, 2024]. However, their application for patients who have been diagnosed with relapse of acute myeloid leukemia (AML) after HSCT shows significant limitations. Loss of heterozygosity (LOH) at HLA loci and the presence of mixed chimerism can complicate accurate genotyping and affect the interpretation of results [Lee, 2024]. Additionally, standard methodologies may fail to distinguish between donor-derived and residual malignant cells, leading to diagnostic challenges [Arnold, 2022; Lozac'hmeur, 2024]. Understanding these constraints is essential for the optimization of post-transplant monitoring and improving treatment strategies.

Our study aimed to compare molecular HLA typing methods with different resolutions in clinical cases without loss of heterozygosity of HLA genes in patients with hematological disease relapse after HSCT.

Methods. DNA was extracted from peripheral blood using the "Genomic DNA from Blood Extraction Kit" (Macherey-Nalel, Germany). The concentration and purity of samples were assessed

Citation: Sishchuk, L. O., Tubaltseva, I. I., Tsokolenko, N. A., Maksymchuk, A. O., Kukhol, A. V., Andrusenko, V. V., Mazanova, A. O., Hrohul, Y. A. (2025). Limitations of human leukocyte antigen molecular typing methods for patients with acute myeloid leukemia relapse after hematopoietic stem cell transplantation. *Biotechnologia Acta*, 18(2), 89–91. https://doi.org/10.15407/biotech18.02.089

using NanoDrop (Thermo Fisher Scientific, USA). Sequence-specific primers method (SSP) was performed using Micro SSP Generic typing kits for Class I (One Lambda, USA) according to the manufacturer's protocol. SBT SeCore Kit (One Lambda, USA) was used for the SBT method. PCR amplification was followed by sequencing using a 3500xL Dx Genetic analyzer (Thermo Fisher Scientific, USA). Sequence alignment and allele identification were performed using Fusion 4.6.1 and Fusion 6.0 software (One Lambda, USA). NGS was performed using AllType FASTplex 11 Loci Kit (One Lambda, USA). Data analysis was performed using TSV 3.1 software (One Lambda, USA).

Results and Discussion. We used DNA staples of patients who were diagnosed with relapsed AML after allo-HCST. To demonstrate the influence of HLA-A locus-related alleles belonging to the same split group on typing results performed by different methods, from the archive of the Tissue Typing Department of NSCH "OKHMATDYT" were selected DNA samples, in which allelic variants of the HLA-A genes have been previously determined by NGS method.

Two patients with AML received bone marrow allo-HSCT. On day +106 and day +396, the patients were diagnosed with central disease relapse. Post-transplant monitoring showed a partial chimerism without any confirmed HLA-LOH. SSP confirmed parallelism but was not observed using NGS or SBT.

Due to the limitations of genotyping methodologies, the presence of true LOH cannot be entirely neither confirmed nor denied. This is especially important to consider for alleles with minimal nucleotide sequence differences. The experimental part of our study demonstrated that extra alleles present in a patient's peripheral blood cells, which may belong to both the patient and the bone marrow donor, and at the same time differ by 15 or fewer nucleotides, may not be detected using high-resolution molecular genotyping methods.

Two experimental DNA samples simulated a clinical situation where a patient can receive allo-HSCT from a haploidentical donor with a mismatch at the HLA-A locus containing allelic variants belonging to the same split group. The first mixed sample consisted of *HLA-A*33:01* and *HLA-A*68:01* + *HLA-A*29:01* and *HLA-A*68:01* with a 1:4 ratio, while the second experimental sample included *HLA-A*25:01* and *HLA-A**26:01 + *HLA-A*26:01, HLA-A**66:01 with 1:1 ratio. SBT results analysis demonstrated the presence of three nucleotides at some positions that matched the HLA-Fusion 6.1 software database references. Still, the sequencing result remained indeterminate even after the step-by-step substitution of nucleotides at each doubtful position manually by the operator (Figure).

Figure. **Sanger sequencing results of a mixed sample, fusion data analysis. Red color refers to T nucleotide, green color refers to A nucleotide, blue color refers to C nucleotide and black color refers to G nucleotide**

Testing of these samples by NGS also did not reveal the presence of an extra allelic variant, which may be due to a number of reasons, such as the belonging of selected alleles to the same split group and the ratio of the samples, which reflects a low percentage of partial chimerism.

Conclusion. Thus, despite the high sensitivity of NGS and Sanger sequencing, the use of these methods is associated with difficulties in accurately determining the absence of HLA-LOH.

Authors' contribution

LOS carried out SBT, data analysis, and writing original draft; IIT carried out library preparations for NGS, NAT, and AOM and performed NGS and data analysis; AVK performed SSP method; VVA performed DNA extraction, AOM conceptualization, data curation, writing original draft YAH conceptualization, supervision.

Funding source

National Specialized Children's Hospital "OKHMATDYT" of the Ministry of Health of Ukraine.

Acknowledgment

The authors gratefully acknowledge Dr. Natalia Olkhovych for support.

REFERENCES

1. Arnold, P. Y. (2022). HLA Loss and Detection in the Setting of Relapse from HLA-Mismatched Hematopoietic Cell Transplant. *Hum. Immunol.*, 83, 712–720. https://doi.org/10.1016/j.humimm.2022.08.004.
2. Geo, J. A., Ameen, R., Shemmari, S. A., Thomas, J. (2024). Advancements in HLA Typing Techniques and Their Impact on Transplantation Medicine. *Med. Princ. Pract.*, 33, 215–231. https://doi.org/10.1159/000538176.
3. Lee, M. Y., You, E. (2024). The Importance of Confirming False Homozygosity in Pretransplant HLA Typing Results of Patients with Hematologic Malignancies. *Int. J. Med. Sci.*, 21, 2430–2436. https://doi.org/10.7150/ijms.99883.
4. Lozac'hmeur, A., Danek, T., Yang, Q., Rosasco, M. G., Welch, J. S., Go, W. Y., Eric, W., Ng, E. W., ..., Hecht, J. R. (2024). Detecting HLA Loss of Heterozygosity within a Standard Diagnostic Sequencing Workflow for Prognostic and Therapeutic Opportunities. *NPJ Precision Oncol.*, 8, 174. https://doi.org/10.1038/s41571-024-00814-6.

UDC 616.314.17-008.1:613.25-053.6 **https://doi.org/10.15407/biotech18.02.092**

THE EFFECT OF PROBIOTIC TREATMENT ON OBESITY-RELATED CHANGES IN THE PERIODONTIUM OF OBESE RATS

M. SKRYPNYK[1], *K. NEPORADA*[1], *M. SPIVAK*[2]

[1]Poltava State Medical University, Poltava
[2]Institute of Microbiology and Virology, National Academy of Sciences of Ukraine, Kyiv

E-mail: maximskrypnik97@gmail.com

Received 2025/03/07
Revised 2025/03/14
Accepted 2025/04/30

Obesity is a significant global health concern associated with various systemic diseases, including periodontitis. Probiotics have shown promising outcomes as an adjunctive therapy in both clinical and microbiological parameters; however, their impact on obesity-induced periodontal alterations remains unclear.

This study aimed to evaluate the biochemical changes in soft periodontal tissues of obese rats and assess the potential protective effects of probiotic supplementation.

Methods. A total of 46 rats were divided into three groups: (1) control, (2) obesity, and (3) obesity with probiotic treatment. Obesity was induced via neonatal monosodium glutamate administration, and probiotic supplementation was provided for three months. Biochemical analyses of periodontal tissues included oxidative stress markers, enzymatic activity, and inflammatory mediators.

The results showed that obesity significantly decreased markers of oxidative stress and reduced the activity of antioxidant enzymes. Probiotic treatment effectively normalized BMI, reduced oxidative damage, and restored enzymatic balance in periodontal tissues. Additionally, probiotic supplementation modulated nitric oxide synthase activity, suggesting a potential regulatory effect on inflammatory and vascular responses.

Conclusion. This study highlights the detrimental effects of obesity on periodontal health and suggests that probiotics may serve as a protective intervention against obesity-induced oxidative and inflammatory damage.

Keywords: obesity, periodontitis, probiotic, oxidative stress.

Obesity is a growing global health concern that has been linked to various systemic diseases, including periodontitis [1]. Periodontal tissues are particularly susceptible to oxidative stress and enzymatic imbalances associated with obesity, which may exacerbate tissue degradation and inflammatory responses. Probiotics are live microorganisms that provide health benefits to the host by influencing the composition and activity of the microbiota [2]. The mechanisms by which probiotics aid in the prevention and treatment of periodontal disease include inhibiting the growth and virulence of pathogenic species through competition for resources and the production of antimicrobial compounds, modulating the immune response to reduce inflammation and promote healing, and restoring microbial balance within the oral microbiome [3, 4]. Studies in probiotics as an adjunctive therapy showed a promising outcome in both clinical and microbiological parameters [5]. However, the impact of probiotics on obesity-induced periodontal tissue alterations remains unclear.

Aim. This study aims to evaluate the biochemical changes in soft periodontal tissues of obese rats and assess the potential protective effects of probiotic supplementation.

Citation: Skrypnyk, M., Neporada, K., Spivak, M. (2025). The effect of probiotic treatment on obesity-related changes in the periodontium of obese rats. *Biotechnologia Acta*, 18(2), 92–95. https://doi.org/10.15407/biotech18.02.092

Methods. Experiments were conducted on 46 rats of both genders, divided into three groups: Group I (Control): Intact newborn rats received a subcutaneous injection of 8 μL/g saline ($n = 18$). Group II (MSG-Induced Obesity): Rats received subcutaneous injections of monosodium glutamate (MSG) at a dose of 4 mg/g on days 2, 4, 6, 8, and 10 of life ($n = 16$) [6]. Group III (Obesity + Probiotic Treatment): Rats with MSG-induced obesity received the dry bacterial concentrate of probiotic microorganisms at a dose of 14 mg/g for 3 months, following a regimen of 2 weeks of administration followed by a 2-week break ($n = 12$). The distribution of animals into groups and the corresponding interventions are illustrated in Fig. A.

As a probiotic, the dry bacterial concentrate of probiotic microorganisms was used, developed under project TU 21.1.-2960512097-005:2015, which has undergone State Sanitary and Epidemiological. The concentrate is a powder of a dried suspension containing live probiotic Registration microorganisms of the genera *Lactobacillus, Bifidobacterium,* and *Bacillus* in a physiological sodium chloride solution. The microbial strains are deposited in the Microorganism Depository of the D.K. Zabolotny Institute of Microbiology and Virology of the National Academy of Sciences of Ukraine. The concentrate includes monocultures of: *Lactobacillus casei* IMB B-7280, *Lactobacillus acidophilus* IMB B-7279, *Lactobacillus delbrueckii* subsp. *bulgaricus* IMB B-7281, *Bifidobacterium animalis* VKL and/or *B. animalis* VKB, *Bacillus subtilis* IMB B-7393 and/or *B. subtilis* IMB B-7392. The concentration of viable microorganisms is no less than 4×10^{11} CFU/g.

After four months, body weight changes and body mass index (BMI) were analyzed in all groups. Soft periodontal tissues were excised, minced, treated with collagenase, homogenized, and centrifuged. The following parameters were assessed in the periodontal tissue homogenate: total proteolytic activity, antitrypsin activity, free fucose content, nitrite anion levels, total NO-synthase (NOS) activity, TBA-reactive substances, oxidatively modified proteins (OMP), and catalase activity.

Statistical analysis was performed using the non-parametric Mann–Whitney U test to compare two independent groups. Results are expressed as M ± SD, with significance set at $P < 0.05$.

Results and Discussion. We observed the development of obesity in 4-month-old MSG-treated rats, confirmed by a significant increase in BMI compared to the control group ($P < 0.05$). In the probiotic-treated group, BMI was normalized ($P < 0.01$) compared to untreated obese rats (Fig. *B*). MSG-induced obesity contributed to the activation of free radical oxidation in soft periodontal tissues, as evidenced by a significant increase in TBA-reactive substances, nearly 1.92-fold in both male and female rats ($P < 0.05$, Fig. *D*), and a 1.67-fold increase in oxidatively modified proteins (OMP) compared to controls (Fig. *C*). Under these conditions, catalase activity significantly decreased by 1.52-fold in the periodontal tissues of female rats compared to control animals ($P < 0.05$, Fig. *E*). In probiotic-treated rats, OMP and TBA levels were significantly lower than in untreated obese rats (Fig. *C* and *D*), while catalase activity in periodontal tissue was significantly higher (Fig. *E*).

In homogenates of periodontal tissues of obese rats, an imbalance between proteinases and their inhibitors' activity was observed (Fig. F and G), and treatment with probiotics restored it. The free fucose concentration was not affected significantly by probiotic treatment (Fig. *H*). NOS activity in periodontal tissues was significantly affected by obesity. Treatment with probiotics significantly decreased it. Our study demonstrated that MSG-induced obesity in rats led to significant metabolic and biochemical alterations in soft periodontal tissues, characterized by increased oxidative stress, enzymatic imbalance, and inflammatory changes. The observed increase in BMI in the MSG-treated group confirms the successful induction of obesity, which was significantly normalized following probiotic treatment. These findings suggest a potential modulatory effect of probiotics on obesity-related metabolic dysregulation.

Oxidative stress plays a crucial role in obesity-related pathologies, including periodontal tissue damage. The significant elevation of TBA-reactive substances and OMP in obese rats suggests increased lipid peroxidation and protein oxidation, indicative of heightened free radical activity, which aligns with previous findings [7]. The observed decline in catalase activity further supports an impaired antioxidant defense mechanism in periodontal tissues. Probiotic treatment effectively reduced oxidative damage by lowering OMP and TBA levels while restoring catalase activity, suggesting its protective role in mitigating obesity-induced oxidative stress. The antioxidant effect of probiotic supplementation in the treatment of periodontitis was confirmed by clinical studies [8].

Furthermore, we identified an imbalance in proteinase and inhibitor activity in the periodontal tissues of obese rats, which was restored with probiotic supplementation. This imbalance may contribute to tissue degradation and inflammation, further exacerbating periodontal damage [9]. Interestingly, free fucose levels remained largely unaffected by probiotic treatment, indicating that the intervention may not significantly alter carbohydrate metabolism in periodontal tissues.

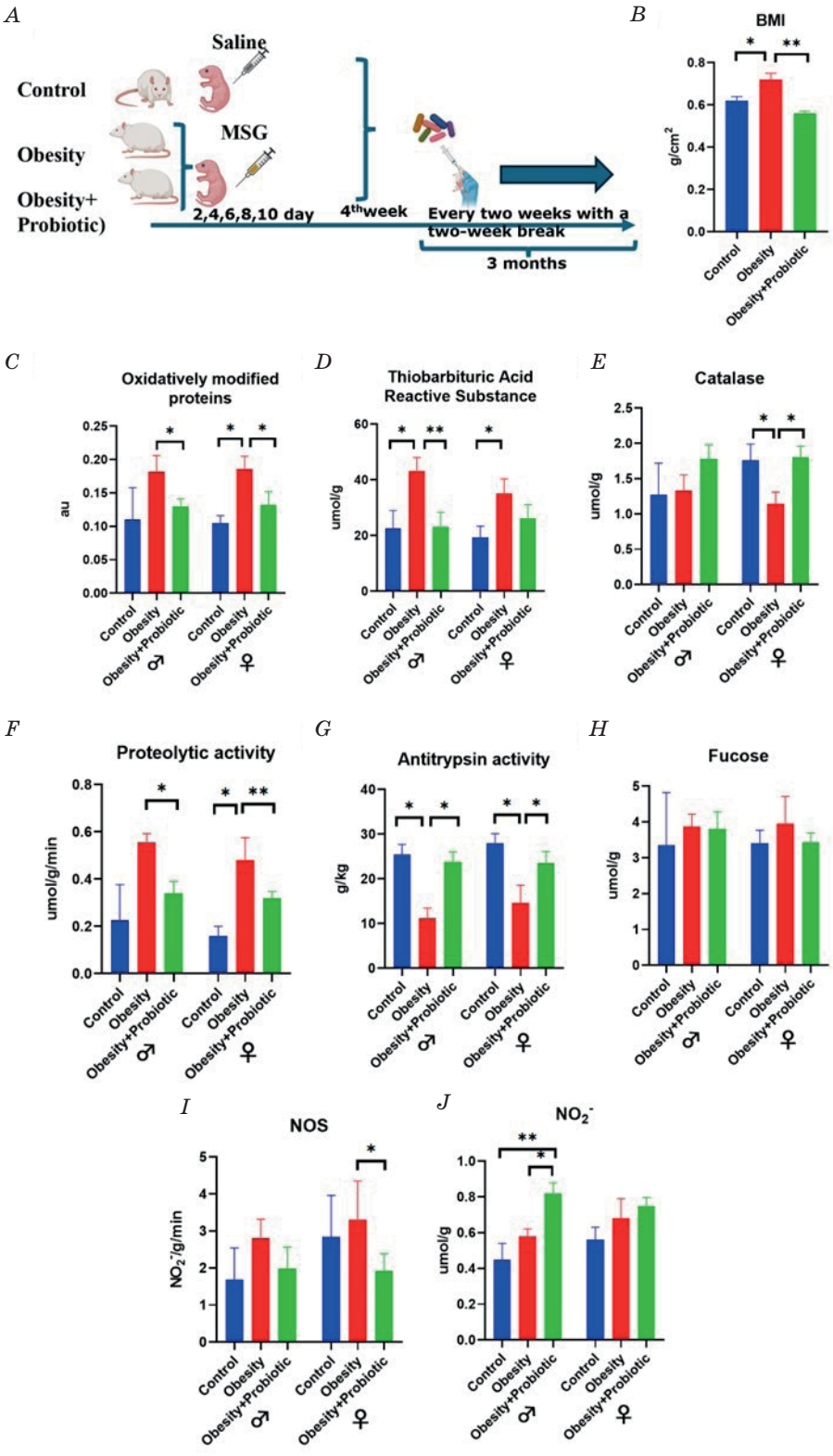

Figure. **Changes in biochemical parameters in the soft periodontal tissues of obese rats treated with probiotics:**

A — Flowchart illustrating the sequence of events in the experiment; *B* — Changes in body mass index (BMI) of rats throughout the experiment timeline; *C* — Concentration of oxidatively modified proteins in soft periodontal tissues; *D* — Levels of thiobarbituric acid reactive substances; *E* — Catalase activity; *F* — Proteolytic activity; *G* — Antitrypsin activity; *H* — Fucose concentration; *I* — NO-synthase activity; *J* — Nitrite anion levels

Conclusions. Overall, our findings underscore the detrimental effects of obesity on periodontal health and highlight the therapeutic potential of probiotics in mitigating obesity-induced oxidative and inflammatory damage. Further studies are needed to elucidate the precise molecular mechanisms underlying these protective effects and to evaluate the long-term benefits of probiotic interventions in the management of periodontitis in obese individuals.

Authors' contribution

MSk and KN conducted the experiment, measured biochemical parameters, and performed data analysis and presentation. MSp provided the necessary resources for this study. All authors contributed to the thesis writing and revision.

REFERENCES

1. Skrypnyk, M., Petrushanko, T., Neporada, K., Petrushanko, V., Skrypnyk, I. (2023). Changes in the Periodontium against the Background of Systemic Vascular Reactions in Young Individuals with Obesity. *Dent. Med. Probl.,* 61, 0–0, https://doi.org/10.17219/dmp/157294.
2. Baddouri, L., Hannig, M. (202). 4Probiotics as an Adjunctive Therapy in Periodontitis Treatment—Reality or Illusion—a Clinical Perspective. *NPJ Biofilms Microbiomes*, 10, 148, https://doi.org/10.1038/s41522-024-00614-5.
3. Plaza-Diaz, J., Ruiz-Ojeda, F. J., Gil-Campos, M., Gil, A. (2019). Mechanisms of Action of Probiotics. *Advances in Nutrition.* 10, S49–S66, https://doi.org/10.1093/advances/nmy063.
4. Guo, N., Lv, L. (2023). Mechanistic Insights into the Role of Probiotics in Modulating Immune Cells in Ulcerative Colitis. *Immun. Inflamm. Dis*., 11, https://doi.org/10.1002/iid3.1045.
5. Baddouri, L., Hannig, M. (2024). Probiotics as an Adjunctive Therapy in Periodontitis Treatment—Reality or Illusion—a Clinical Perspective. *NPJ Biofilms Microbiomes.,* 10, 148, https://doi.org/10.1038/s41522-024-00614-5.
6. Miśkowiak, B., Partyka, M. (1993). Effects of Neonatal Treatment with MSG (Monosodium Glutamate) on Hypothalamo-Pituitary-Thyroid Axis in Adult Male Rats. *Histol Histopathol*., 8, 731–734.
7. Beregova, T. V., Neporada, K. S., Skrypnyk, M., Falalyeyeva, T. M., Zholobak, N. M., Shcherbakov, O.B.; Spivak, M.Y.; Bubnov, R.V. (2017). Efficacy of Nanoceria for Periodontal Tissues Alteration in Glutamate-Induced Obese Rats-Multidisciplinary Considerations for Personalized Dentistry and Prevention. *EPMA Journal*, 8, https://doi.org/10.1007/s13167-017-0085-7.
8. Karaca, B., Yilmaz, M., Gursoy, U. K. (2022). Targeting Nrf2 with Probiotics and Postbiotics in the Treatment of Periodontitis. *Biomolecules*, 12, 729, https://doi.org/10.3390/biom12050729.
9. Skrypnyk M. (2019). Effectiveness of Nanocrystalline Cerium Dioxide for Secondary Prevention of Inflammatory Periodontal Diseases in Young Individuals with Obesity. *Letters in Applied NanoBioScience*, 8, 754–761, https://doi.org/10.33263/LIANBS84.754761.
10. Dursun, E., Akalin, F. A., Genc, T., Cinar, N., Erel, O., Yildiz, B.O. (2016). Oxidative Stress and Periodontal Disease in Obesity. *Medicine*, 95, e3136, https://doi.org/10.1097/MD.0000000000003136.

UDC 543.42:577.1:615.47 **https://doi.org/10.15407/biotech18.02.096**

SYNTHESIS OF MONODISPERSE GOLD NANOSPHERES FOR THEIR USE IN DNA HYBRIDIZATION BIOSENSORS

M.S. SOBOLEVSKYI[1], *I.S. KUCHERENKO*[1], *A.M. LOPATYNSKYI*[2], *S.V. DZYADEVYCH*[1], *O.O. SOLDATKIN*[1]

[1]Institute of Molecular Biology and Genetics of the National Academy of Sciences of Ukraine, Kyiv
[2]V.Ye. Lashkaryov Institute of Semiconductor Physics of the National Academy of Sciences of Ukraine, Kyiv

E-mail: m.s.sobolevsky@imbg.org.ua

Received 2025/03/07
Revised 2025/03/15
Accepted 2025/04/30

Aim. In this work, we describe a reliable and straightforward method of synthesis of monodisperse spherical gold nanoparticles (AuNPs) for DNA labeling in hybridization biosensors based on surface plasmon resonance (SPR) spectrometry.

Materials and Methods. Several samples of colloid AuNPs were prepared by citrate reduction of gold (III) chloride and studied with dynamic light scattering to determine their distribution by diameter. The samples with the least variance of AuNP diameters (8–33 nm) were designated for labeling of DNA probes used to amplify the signal of the SPR-based hybridization DNA biosensor.

Results. The experiments showed the possibility of the synthesis of precision AuNPs from gold (III) chloride through control of the duration of their boiling. An optimal variation of the method of synthesis of such AuNPs was proposed. AuNPs synthesized by the described method were instrumental in achieving a substantial specific increase in biosensor signal.

Conclusions. The proposed method can be used to produce precision citrate-capped AuNPs suitable for use in a wide range of biosensors.

Keywords: hybridization DNA biosensors, surface plasmon resonance, gold nanoparticles, Turkevich synthesis, AuCl3.

Gold nanoparticles (AuNPs) of many sizes, shapes, and surface modifications are currently used in biotechnology [1]. The significant structural and functional diversity of AuNPs contributes to the booming field of their application, but at the same time makes it hard for a researcher without a substantial background in materials science, wave physics, and biochemistry to predict their physical and biological properties. Such properties are hard to verify experimentally due to the particular sensitivity of AuNPs to the conditions of their synthesis; in other words, the production of two identical batches of AuNPs using currently established protocols is an arduous task. Scarcity of our knowledge about the health effects of AuNPs is but one consequence of such uncertainty [2]. Therefore, establishing novel, precise methods of synthesis of AuNPs, as well as clarification of existing ones, is a priority task in any AuNP-related research.

The AuNPs studied here are intended for use as a colloidal part of a DNA hybridization biosensor system based on surface plasmon resonance (SPR) spectrometry [3]. Given that such an application demands that AuNPs are low in diameter, monodisperse, resistant to aggregation, and fit for modification of their surface with thiolated DNA probes, we settled on their synthesis by citrate reduction [4,5]. In this technique, boiling is the most crucial step of the synthesis during which Au ions are incorporated into growing nanoparticles. However, few citrate reduction protocols specify their duration, which can lead to discrepancies between the results of different researchers who use

Citation: Sobolevskyi, M. S., Kucherenko, I. S., Lopatynskyi, A. M., Dzyadevych, S. V., Soldatkin, O. O. (2025). Synthesis of monodisperse gold nanospheres for their use in DNA hybridization biosensors. *Biotechnologia Acta*, 18(2), 96–99. https://doi.org/10.15407/biotech18.02.096

the same guidelines. Therefore, it was decided to dedicate this research to the determination of the influence of the boiling of AuNPs during their synthesis on their size.

Additionally, previous research indicated the presence of sub-4 nm fractions in the AuNPs synthesized by citrate reduction of $HAuCl_4$ [5]. Current evidence points toward potential genotoxicity of such nanoparticles, suggesting maximum caution during work with them [2]. Due to this, it was decided to explore the possibility of the synthesis of precision AuNPs by citrate reduction of AuCl3 instead of $HAuCl_4$.

Aim. The primary aim of this work was to thoroughly describe a method of precision synthesis of AuNPs for biosensor modification. The additional objective of our research consisted of demonstrating the possibility of the use of $AuCl_3$ as the precursor of gold nanoparticles synthesized by citrate reduction (instead of the usual $HAuCl_4$).

Methods. The general method of synthesis of AuNPs is similar to the one in our previous research [3], with the volume of precursor solution halved (down to 11 mL), $HAuCl_4$ substituted for $AuCl_3$, and without reflux. Keeping in mind the desired simplicity and safety of the procedure, the synthesis must take place under a fume hood to minimize the risk of inhalation of nanoparticles. Here, the boiling of AuNP precursor solutions was achieved with the MSH-300 magnetic stirrer manufactured by Biosan. All synthesized AuNP samples were analyzed with a photon correlation spectroscopy system of the Malvern Zetasizer Nano series to obtain their size distribution. Here, these size distributions are presented graphically with mean values and standard deviations.

Lastly, the synthesized AuNPs were modified with probe DNA oligonucleotides and applied for signal enhancement of the SPR biosensor according to the earlier established methods [3].

Results and discussion. At the beginning of our research, the synthesis of several batches of AuNPs was conducted. A few seconds after 1 mL of 38.8 mM $Na_3C_6H_5O_7$ is injected into 10 mL of boiling 1 mM $AuCl_3$, the color of the solution changes to black. This indicates the start of AuNP growth, which goes on for 80–130 seconds (for different samples) before the colloid gradually assumes a bright red color. In different samples, boiling was manually stopped after one of three events:

- The solution starts changing color from black to red.
- Solution entirely changes color from black to red;
- Solution fully changes color from black to red and keeps being boiled for 30 seconds.

Several samples of AuNPs were prepared using the described method of synthesis with different durations of boiling. It was noted that boiling of solutions after they assume a bright red color leads to the formation of a visible black precipitate on the inner surface of the synthetic vessel (Fig. 1).

The most probable cause for this phenomenon consists of the aggregation of AuNPs on the glass surface due to the dissociation of protective citrate ions from AuNP surfaces under high temperature. Since AuNP aggregation is irreversible, the presence of such aggregates in the colloid would effectively contaminate the sample, rendering it unusable for biosensor modification.

Nextly, the size distribution of prepared samples was investigated. The results of these measurements are present in Fig. 2.

As it is visible from the graph, prolonged boiling of AuNP colloid leads to substantial increase in mean diameter of AuNPs, potentially resulting in appearance of particles that are far from nanosized (>100 nm in diameter). Of all studied AuNPs, the ones in which boiling was stopped the earliest were determined to be the least polydisperse. They were subsequently selected for modification with thiolated oligonucleotides to test the effectiveness of synthesized AuNPs in enhancement of SPR signal. The sensor responses of SPR-based DNA biosensor to injection of complementary and noncomplementary oligonucleotides labeled with monodisperse AuNPs are demonstrated below (Fig. 3).

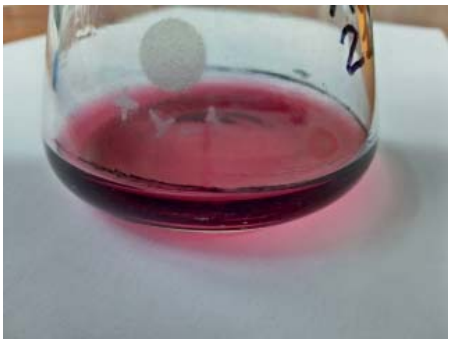

Fig. 1. **Black precipitate becomes visible above the meniscus in excessively boiled AuNPs**

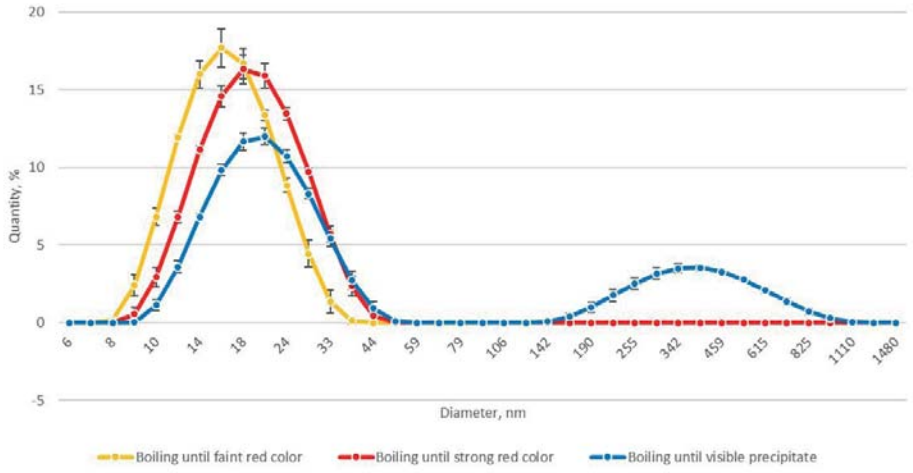

Fig. 2. **Size distribution of AuNP samples synthesized with different duration of boiling.** X axis scale is logarithmic

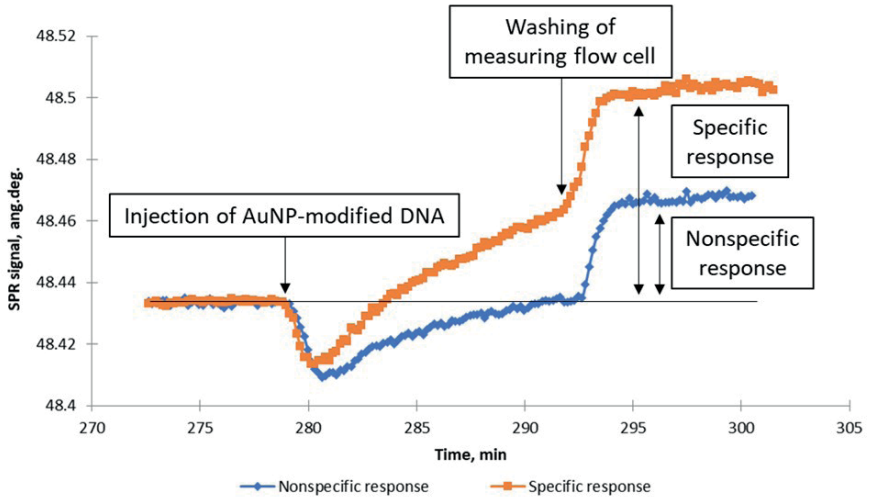

Fig. 3. **Nonspecific and specific responses of the hybridization SPR biosensor to injection of 450 pM DNA labeled with AuNPs**

It can be seen that the level of nonspecific and specific response to AuNP-modified 450 pM DNA is in line with the previously published results, which indicates successful reproduction of AuNPs with particular properties. The limit of detection (LOD) of DNA by SPR biosensor without AuNPs is 50 nM [3], while the newly synthesized AuNPs allow for the lowering of the LOD by several orders of magnitude (to 450 pM).

Conclusions. In this work, a novel perspective method for the synthesis of gold nanoparticles was proposed. It has been shown that the lowest polydispersity of such AuNPs can be achieved through early discontinuation of heating during their synthesis.

The AuNPs synthesized by citrate reduction of AuCl3 were successfully utilized as a colloidal part of a DNA hybridization biosensor system based on SPR spectrometry. As the exact replication of the results of synthesis is dependent on the perception of color of the colloid, it may be suggested that the experimental setup be supplemented with a real-time spectrophotometer.

Authors' contribution

SMS was engaged in the main research work and creation of the original text of theses; KIS was engaged in consultations on biomolecular electronics; LAM was engaged in consultations on AuNP

physics and dynamic light scattering; DSV — helping in planning experiments; SOO — editing theses, supervision.

The work was carried out at the expense of a grant of the National Academy of Sciences of Ukraine to research laboratories/groups of young scientists of the National Academy of Sciences of Ukraine for conducting research in priority areas of development of science and technology in 2024–2025.

REFERENCES

1. Karnwal, A., Kumar Sachan, R.S., Devgon, I. (2024). Gold Nanoparticles in Nanobiotechnology: From Synthesis to Biosensing Applications. *ACS Omega*, 9(28), 29966–29982. Published 2024 Jul 5. https://doi.org/10.1021/acsomega.3c10352
2. Alkilany, A. M., Murphy, C. J. (2010). Toxicity and cellular uptake of gold nanoparticles: what we have learned so far? *J. Nanopart. Res.*, 12(7), 2313–2333. https://doi.org/10.1007/s11051-010-9911-8
3. Sobolevskyi, M., Soldatkin, O., Lopatynskyi, A., Chegel, V., Samoylov, A., Matsishin, M., Dzyadevych, S., Soldatkin, A. (2023). Application of modified gold nanoparticles to improve characteristics of DNA hybridization biosensor based on surface plasmon resonance spectrometry. *Applied Nanoscience,* 12, 7521–7529. https://doi.org/10.1007/s13204-023-02930-2
4. Kimling, J., Maier, M., Okenve, B., Kotaidis, V., Ballot, H., Plech, A. (2006). Turkevich method for gold nanoparticle synthesis revisited. *J. Phys. Chem. B.*, 110(32), 15700–15707. https://doi.org/10.1021/jp061667w
5. Dong, J., Carpinone, P. L., Pyrgiotakis, G., Demokritou, P., Moudgil, B. M. (2020). Synthesis of Precision Gold Nanoparticles Using Turkevich Method. *Kona,* 37, 224–232. https://doi.org/10.14356/kona.2020011

UDC 577: 616.03: 546.1 https://doi.org/10.15407/biotech18.02.100

EFFECT OF SELENIUM CITRATE ON THE GLUTATHIONE STATUS AND THYROID HORMONES IN RATS WITH EXPERIMENTALLY INDUCED HYPOTHYROIDISM

O.O. SUSHKO[1], *R.JA. ISKRA*[2]

[1]Krupynskyi Lviv Medical Academy
[2]Ivan Franko National University of Lviv

E-mail: sushko.ola@gmail.com

Received 2025/03/20
Revised 2025/04/11
Accepted 2025/04/30

Aim. The research aimed to determine the effects of selenium citrate on the characteristics of the antioxidant system and hormone levels in the blood of rats with experimentally induced hypothyroidism.

Materials and Methods. The hypothyroid state was induced using Mercazolil in a dose of 5 mg/kg. The levels of triiodothyronine, thyroxine, and thyroid-stimulating hormone determine a hypothyroid state. Animals under the research consumed selenium citrate at doses of 100 and 200 µg/kg of body weight.

Results. It was found that the levels of thyroid hormones significantly decreased during hypothyroidism and had a tendency to normalize under the influence of selenium citrate. Thyroid-stimulating hormone significantly increased during hypothyroidism, though selenium compounds did not affect its level. Changes in the activity of the glutathione status enzymes were monitored; in particular, glutathione reductase significantly increased, and glutathione peroxidase decreased in animals with hypothyroidism compared to controls. Selenium citrate in amounts of 100 and 200 µg/kg of body weight reduced glutathione reductase activity considerably and increased glutathione peroxidase activity compared to animals with hypothyroidism.

Conclusions. The obtained results indicate a normalization of hormone levels and glutathione link indicators under the influence of selenium citrate in the blood of rats with experimentally induced hypothyroidism. These results form the basis for the development of methods and means for the prevention and treatment of hypothyroidism.

Keywords: selenium citrate, glutathione status, hypothyroidism.

Selenium (Se) is a vital element that prevents oxidative stress. However, its concentration is critical: while Se is an indispensable nutrient, excessive amounts can be harmful. The thyroid gland contains the highest concentration of Se in selenoproteins and is involved in hormone metabolism. A dysfunctional gland can be a sign of hormone deficiency, which can lead to a pathological condition called hypothyroidism [1]. Se supplements can reduce levels of antibodies such as thyroid peroxidase antibody, which often leads to hypothyroidism.

Aim. The study aimed to assess the effects of selenium citrate on antioxidant system parameters and hormone levels in rats with experimentally induced hypothyroidism, and to explore potential corrective strategies for metabolic disorders associated with thyroid dysfunction.

Methods. The study involved 32 male white laboratory rats (290–300 g), fed a standard laboratory diet ("Vita"). Rats were divided into 4 groups: I — control group; II — rats with experimental

Citation: Koshchavko, K. S. (2025). "Hairy" root culture of *Scutellaria altissima* L. for high-level flavonoid production. *Biotechnologia Acta*, 18(2), 100–102. https://doi.org/10.15407/biotech18.02.100

hypothyroidism (EHT); III – rats with EHT treated with selenium citrate (100 μg/kg body weight) in drinking water for one month; IV – rats with EHT treated with selenium citrate (200 μg/kg body weight) in drinking water for one month. Selenium citrate was obtained via aquananotechnology (Nanomaterials and Nanotechnologies, Ukraine). EHT was induced in the rats from groups II, III, and IV by adding 5 mg/kg of Mercazolil ("Zdorovya") daily for 21 days. Hypothyroid state was evaluated by measuring serum triiodothyronine (T3), thyroxine (T4), and thyroid-stimulating hormone (TSH). Glutathione status was determined by the activity of glutathione peroxidase (GPx) and glutathione reductase (GR). Statistical analysis was performed using ANOVA in Microsoft EXCEL.

Results and Discussion. Thyroid hormones exhibit antioxidant properties [2]. In hypothyroidism, key changes include decreased T3 and T4 and elevated TSH, reflecting reduced free radical formation. In group II (EHT), T3 and T4 levels decreased significantly (by 1.5 and 1.3 times, respectively), while TSH increased 10-fold compared to control, indicating a compensatory response from the hypothalamic-pituitary system. TSH levels tended to increase under the influence of selenium citrate compared to the indicators in animals of group II. The effect of Se on TSH levels is controversial. There is published data on the insignificant impact of Se on TSH levels, and there is also data on a decrease in TSH levels [3, 4]. Notably, T3 and T4 levels increased in Se-treated groups, approaching control values (Table). Thyroid hormones regulate the synthesis and degradation of proteins, vitamins, and antioxidant enzymes, and play an essential role in the production of free radicals. Thyroid hormones regulate protein, vitamin, and antioxidant enzyme metabolism and modulate cellular oxidative stress by stimulating various enzyme systems [5, 6].

GR, crucial for synthesizing reduced glutathione, showed a 2.4-fold increase in group II, indicating enhanced synthesis in hypothyroidism. Selenium citrate administration reduced GR activity significantly: by 3 times at 100 μg/kg and 5.9 times at 200 μg/kg compared to the indicators of group II.

GPx, a selenium-dependent enzyme that protects thyroid cells from oxidative damage, was significantly suppressed (by 4.9 times) in hypothyroid rats compared to controls. GPx activity decreased in the blood of animals of groups III and IV by 1.9 and 1.5 under the influence of selenium compared to group I. However, the enzyme was significantly increased by 2.5 and 3.2 times compared to the indicators of group II.

Table. **Effect of selenium citrate on hypothyroidism indicators**

Parameter	Control (n=8)	EHT (n=8)	EHT + Se 100 μg/kg (n=8)	EHT + Se 200 μg/kg (n=8)
TSH (mIU/L)	0.01±0.01	0.13±0.10*	0.14±0.11*	0.16±0.09*
T3 (nmol/L)	1.29±0.49	0.84±0.29*	1.61±0.25	0.89±0.16*
T4 (nmol/L)	18.89±1.86	15.04±1.25*	15.02±0.70*	15.37±0.30*
GR (μmol/ min×mg of protein)	9.69±1.07	23.25±3.21*	7.67±1.17*#	3.94±1.40*#
GPx (μmol/ min×mg of protein)	24.81±0.85	5.11±0.59*	13.01±2.67*#	16.24±5.16*#

Values are means ± SD. EHT: Experimental hypothyroidism; TSH: Thyroid-stimulating hormone; T3: Triiodothyronine; T4: Thyroxine; GPx: Glutathione peroxidase; GR: Glutathione reductase;
*$P < 0.01$ compared to control; #$P < 0.01$ compared to EHT.

Conclusions. Selenium citrate administration helped normalize hormone levels and glutathione system parameters in rats with experimental hypothyroidism. These findings suggest selenium citrate may be valuable for developing strategies to prevent and treat hypothyroidism.

Author contribution

O.O. Sushko carried out: determination of biochemical indicators, calculation of average values and standard errors, statistical analysis of data. R.Ya. Iskra carried out: interpretation and description of data, search and study of literature by topic.

Funding source

The present research was conducted without any external financial support.

REFERENCES

1. Taylor, P. N., Albrecht, D., Scholz, A., Gutierrez-Buey, G., Lazarus, J., Dayan, C. M., Okosieme, O. E. (2018). Global epidemiology of hyperthyroidism and hypothyroidism. *Nat. Rev. Endocrinol.,* 14, 301–316. https://doi.org/10.1038/nrendo.2018.18
2. Oziol, L., Faure, P., Bertrand, N., Chomard, P.(2003). Inhibition of *in vitro* macrophage-induced low density lipoprotein oxidation by thyroid compounds. *J. Endocrinol*., 177, 137–146. https://doi.org/10.1677/joe.0.1770137
3. Omrani, H. R., Rahimi, M., Nikseresht, K. (2015). The effect of selenium supplementation on acute phase reactants and thyroid function tests in hemodialysis patients. *Nephrourol. Mon*., 7, e24781. https://doi.org/10.5812/numonthly.24781
4. Winther, K. H., Bonnema, S. J., Cold, F., Debrabant, B., Nybo, M., Cold, S., Hegedus, L. (2015). Does selenium supplementation affect thyroid function? Results from a randomized, controlled, double-blinded trial in a Danish population. *Eur. J. Endocrinol*, 172, 657–667. https://doi.org/10.1530/EJE-15-0069
5. Campos, C., Casado, A. (2022). Oxidative stress, thyroid dysfunction and down syndrome. *Indian J. Med. Res.,* 142(2), 113–119.
6. De Vito, P., Balducci, V., Leone, S., Percario, Z., Mangino, G., Davis, P. J., Davis, F. B., …, Incerpi, S. (2021). Nongenomic effects of thyroid hormones on the immune system cells: New targets, old players. *Steroids*, 77(10), 988–995. https://doi.org/10.1016/j.steroids.2012.02.018

UDC 616.314.17:612.08:577.115:599.323.4 https://doi.org/10.15407/biotech18.02.103

PERIODONTOPROTECTIVE EFFECT OF NIMESULIDE AND NaHS UNDER SIRS CONDITIONS

O.T. TKACHENKO, V.V. PLETNOV, A.O. MYKYTENKO

Poltava State Medical University, Poltava, Ukraine

E-mail: yixelo.tkachenko@gmail.com

Received 2025/03/24
Revised 2025/03/03
Accepted 2025/04/30

Hydrogen sulfide donors can protect the gastric mucosa from nimesulide damage, but their combined effect is unknown.

Aim. The work purposed to determine the concentration of peroxynitrites ($ONOO^-$), nitrites (NO_2^-), and malondialdehyde (MDA) in the periodontal soft tissues of rats under the conditions of administration of nimesulide and NaHS during systemic inflammatory response syndrome (SIRS) modeling.

Materials and Methods. Thirty sexually mature male Wistar rats were divided into groups: I — control, II — intraperitoneal injection with 0.4 μg/kg of bacterial lipopolysaccharide *S.typhi* (SIRS group), III — 18 mg/kg/day nimesulide gavage during SIRS, IV group — 5 mg/kg/day NaHS injection during SIRS, V group — NaHS and nimesulide administration during SIRS. We studied concentrations of $ONOO^-$ and NO_2^- and MDA.

Results and Discussion. During SIRS, ONOO- concentration in soft periodontal tissues increased by 1.12 times, NO_2^- by 7.02 times, and MDA by 4.51 times compared to the control ($P < 0.05$). Nimesulide lowers ONOO- content by 1.04 times, NO_2^- by 1.22 times, and MDA by 1.5 times compared to the SIRS group ($P < 0.05$). NaHS lowers NO_2^- by 11.79 times and MDA by 1.46 times compared to the SIRS group ($P < 0.05$). The combination of NaHS and nimesulide increases $ONOO^-$ content by 1.4 times, lowers NO_2^- content by 6.7 times, and MDA by 1.36 times compared to the SIRS group ($P < 0.05$).

Conclusions. The combination of nimesulide and NaHS lowers the intensity of lipid peroxidation in soft periodontal tissues during SIRS modeling.

Keywords: nitrites, peroxynitrite, lipid peroxidation, lipopolysaccharide, hydrogen sulfide, nimesulide.

It is known that under conditions of systemic inflammatory response syndrome (SIRS), periodontal tissues are damaged by the mechanism of oxidative stress. The reaction between the superoxide anion radical and nitric oxide forms peroxynitrite. The biochemistry of peroxynitrite is multifaceted, including one- or two-electron oxidation and nitration reactions. Experimental studies confirm that peroxynitrite is an essential mediator in physiological and pathological processes [1]. Nimesulide is an effective anti-inflammatory drug for the treatment of periodontitis, but it has an ulcerogenic effect [2]. Hydrogen sulfide donors can protect the gastric mucosa from the adverse impacts of nimesulide. Still, such a combined effect on periodontal tissues has not previously been studied, and the role of peroxynitrite under these conditions is unknown.

Aim. The work was purposed to establish the concentration of peroxynitrite, nitrites, and malondialdehyde in the periodontal soft tissues of rats under the conditions of administration of nimesulide and NaHS against the background of modeling of systemic inflammatory response syndrome.

Citation: Tkachenko, O. T., Pletnov, V. V., Mykytenko, A. O. (2025). Periodontoprotective effect of nimesulide and NaHS under SIRS conditions. *Biotechnologia Acta*, 18(2), 103–105. https://doi.org/10.15407/biotech18.02.103

Materials and Methods. The experiments were performed on 30 sexually mature male Wistar rats weighing 190–210 g. Group I — control, Group II — rats that were injected intraperitoneally with 0.4 μg/kg of bacterial lipopolysaccharide (LPS) *S.typhi*, simulating SIRS, with a frequency of 3 times in the first 7 days, then once a week, for 30 days, Group III — animals that were injected intragastrically with 18 mg/kg nimesulide once a day in the last 7 days of SIR's simulation, Group IV — rats that were injected intraperitoneally with 5 mg/kg NaHS once a day in the previous 7 days of SIRS simulation, Group V — animals that were injected intragastrically with 18 mg/kg nimesulide and intraperitoneally with 5 mg/kg NaHS once a day in the last 7 days of SIRS simulation. The object of the study was the soft periodontal tissues of rats, where the concentration of peroxynitrite and nitrites [3] and malondialdehyde (MDA) [4] was determined. The data were statistically processed using a nonparametric method – the Mann-Whitney test.

Results and Discussion. Administration of *S. typhi's* LPS led to an increase of peroxynitrite concentration by 1.12 times compared to the control ($P < 0.05$). Nimesulide administration during SIRS reduced the concentration of peroxynitrite in the periodontal soft tissues of rats by 1.04 times compared to the SIRS group ($P < 0.05$). Under the conditions of administration of the hydrogen sulfide donor NaHS and nimesulide, the concentration of peroxynitrites increased by 1.56 times compared to the control group and by 1.4 times compared to the SIRS group ($P < 0.05$). Under the conditions of administration of *S. typhi's* LPS, the concentration of nitrites in the soft periodontal tissues of rats increased by 7.02 times compared to the control ($P < 0.05$). The administration of nimesulide during SIRS reduced the concentration of nitrites by 1.22 times compared to the control group and by 8.54 times compared to the SIRS group ($P < 0.05$). Under the conditions of administration of the hydrogen sulfide donor NaHS, the concentration of nitrites decreased by 1.68 times compared to the control group and by 11.79 times compared to the SIRS group ($P < 0.05$). Under the conditions of administration of the hydrogen sulfide donor NaHS and nimesulide, the concentration of nitrites increased by 1.05 times compared to the control. It decreased by 6.7 times compared to the SIRS group ($P < 0.05$). Under the conditions of *S. typhi's* LPS administration, the concentration of MDA increased by 4.51 times compared to the control ($P < 0.05$). The administration of nimesulide during SIRS reduced the concentration of MDA by 1.5 times compared to the SIRS group and was 3.01 times higher compared to the control group ($P < 0.05$). Under the conditions of administration of the hydrogen sulfide donor NaHS, the concentration of MDA decreased by 1.46 times compared to the SIRS group. It was 3.09 times higher compared to the control group ($P < 0.05$). Under the conditions of administration of the hydrogen sulfide donor NaHS and nimesulide, the concentration of MDA decreased by 1.36 times compared to the SIRS group. It was 3.32 times higher compared to the control group ($P < 0.05$).

One of the essential properties of H_2S is its bell-shaped (or biphasic/bimodal) pharmacological mode of action. At low concentrations, H_2S exhibits physiological, regulatory, or modulating effects and acts as a cytoprotective, antioxidant, and anti-inflammatory agent. At high concentrations, H_2S can have harmful effects, including pro-oxidant effects and cytostatic or cytotoxic reactions. To exert its cytoprotective effects, H_2S engages a multitude of molecular pathways and mechanisms. Molecular targets and signaling pathways of H_2S include K-ATP channels, Akt, AMPK, PTEN, NF-κB, Nrf2, proline-rich kinase 2, as well as the adenylate cyclase and guanylate cyclase systems, etc. [5]. Numerous studies have shown that H_2S activates Nrf2, which provides antioxidant effects, playing a significant role in the development of respiratory diseases such as COPD, asthma, acute lung injury, etc. According to Wang Y. et al., intraperitoneal administration of NaHS alleviates emphysema and airway inflammation by restoring redox balance and inhibiting ferroptosis by regulating the Nrf2-PPAR-ferritinophagy signaling pathway [6].

Nitration does not always have a negative impact, as previously believed. Nitration reactions can modify other compounds, altering their bioactivity and perhaps even forming new signaling molecules. Unsaturated fatty acids (FA) in lipids, including oleic and linoleic acids, are modified to form nitrolipids (NO_2-FA), which make them electrophilic. Through this mechanism, NO_2-FA potently antagonizes NF-κB and activates Nrf2 signaling, two significant effects that explain their broad anti-inflammatory and antioxidant activities [7]. The role of peroxynitrite and its metabolites in the development of various pathological conditions still requires more detailed study.

Conclusions: the combined effect of nimesulide and the hydrogen sulfide donor NaHS on the soft tissues of periodontal tissues of rats under conditions of modeling systemic inflammatory response syndrome reduces the intensity of lipid peroxidation, the content of nitrites, and increases the content of peroxynitrites.

Authors' contribution

Tkachenko O. T. — data acquisition, data analysis, writing the original draft; Pletnov V. V. — data acquisition, data analysis, writing the original draft; Mykytenko A. O. — project administration, project supervision, data analysis, writing original draft, review of the original draft.

All authors approved the final version of the article.

REFERENCES

1. Prolo, C., Piacenza, L., Radi, R. (2024). Peroxynitrite: a multifaceted oxidizing and nitrating metabolite. *Current Opinion in Chemical Biology*, 80, 102459. https://doi.org/10.1016/j.cbpa.2024.102459.
2. Salvi, G., Lang, N. (2005). The Effects of Non-Steroidal Anti-Inflammatory Drugs (Selective and Non-Selective) on the Treatment of Periodontal Diseases. *Current Pharmaceutical Design*, 11(14), 1757–1769. https://doi.org/10.2174/1381612053764878.
3. Akimov, O. Y., Kostenko, V. O. (2016). Functioning of nitric oxide cycle in gastric mucosa of rats under excessive combined intake of sodium nitrate and fluoride. *Ukrainian biochemical journal*, 88(6), 70–75. https://doi.org/10.15407/ubj88.06.070.
4. Gérard-Monnier, D., Erdelmeier, I., Régnard, K., Moze-Henry, N., Yadan, J. C., Chaudière, J. (1998). Reactions of 1-methyl-2-phenylindole with malondialdehyde and 4-hydroxyalkenals. Analytical applications to a colorimetric assay of lipid peroxidation. *Chemical research in toxicology*, 11(10), 1176–1183. https://doi.org/10.1021/tx9701790.
5. Dilek, N., Papapetropoulos, A., Toliver-Kinsky, T., Szabo, C. (2020). Hydrogen sulfide: An endogenous regulator of the immune system. *Pharmacological Research*, 161, 105119. https://doi.org/10.1016/j.phrs.2020.105119.
6. Wang, Y., Liao, S., Pan, Z., Jiang, S., Fan, J., Yu, S., Xue, L., Yang, J., ..., Chen, Y. (2022). Hydrogen sulfide alleviates particulate matter-induced emphysema and airway inflammation by suppressing ferroptosis. *Free Radical Biology and Medicine*, 186, 1–16. https://doi.org/10.1016/j.freeradbiomed.2022.04.014.
7. Lundberg, J. O., Weitzberg, E. (2022). Nitric oxide signaling in health and disease. *Cell*, 185(16), 2853–2878. https://doi.org/10.1016/j.cell.2022.06.010.

UDC 577.23:[616.36-089.873+615.212.035.3] https://doi.org/10.15407/biotech18.02.106

ADENYL NUCLEOTIDES CONTENT IN LIVER MITOCHONDRIA OF RATS WITH ACETAMINOPHEN INTOXICATION AFTER PARTIAL HEPATECTOMY

M.S. URSATYI, H.P. KOPYLCHUK, I.M. NYKOLAICHUK

Yuriy Fedkovych Chernivtsi National University, Chernivtsi

E-mail: ursatyi.mariia@chnu.edu.ua

Received 2025/03/12
Revised 2025/04/11
Accepted 2025/04/30

The work aimed to assess the content of adenyl nucleotides (ATP, ADP, AMP) and Atkinson's adenylate energy charge in the mitochondrial fraction of rat liver with acetaminophen-induced toxic injury following partial hepatectomy.

Materials and Methods. The experiments were carried out on white non-linear rats divided into two groups: I — control rats subjected to resection of 2/3 of the liver tissue, and II — rats that underwent partial hepatectomy following acetaminophen-induced toxic injury. Animals were removed from the experiment at 0 (preoperative period), 24, 48, 72, and 168 hours after partial hepatectomy.

Results. In the mitochondrial fraction of the liver in rats with acetaminophen-induced toxic injury after partial hepatectomy, a decrease in ATP content was observed during the three days of the experiment, accompanied by simultaneous increases in ADP and AMP levels during 72 and 168 hours, respectively, against the background of a decline in the adenylate energy charge with minimal values at 72 h of the regenerative period.

Conclusions. Liver regeneration in rats after partial hepatectomy under conditions of acetaminophen-induced toxic injury is accompanied by a quantitative redistribution of adenyl nucleotides in mitochondria: a maximal increase in AMP content occurs alongside a simultaneous decrease in ATP levels at the terminal stage of organ recovery. Such changes cause the most substantial reduction in Atkinson's adenylate energy charge, which can be regarded as a critical stage in the dysfunction of the energy supply system under these experimental conditions.

Keywords: liver, partial hepatectomy, acetaminophen, adenyl nucleotides.

In ensuring the organism's homeostasis during the progressive development of various pathological conditions of the liver (toxic or traumatic injuries, infectious or metabolic diseases), endowed with a broad functional and metabolic profile, a decisive position belongs to the organ's capacity for compensatory regeneration. The implementation of the regenerative cascade of events, in addition to the typical mechanisms driven by hepatocyte proliferation, may occur through alternative pathways involving hepatic progenitor cells, which are especially important in cases of chronic or significant acute injuries. Reparative regeneration is considered crucial for the restoration of hepatostat and the functional activity of the liver following the hepatotoxic effects of acetaminophen. However, the suppression of regenerative potential noted when threshold doses of hepatotoxins are exceeded leads to the development of liver failure, which in some instances requires transplantation [1, 2]. The liver's unique ability to regenerate creates the possibility of

Citation: Ursatyi, M. S., Kopylchuk, H. P., Nykolaichuk, I. M. (2025). Adenyl nucleotides content in liver mitochondria of rats with acetaminophen intoxication after partial hepatectomy. *Biotechnologia Acta*, 18(2), 106–108. https://doi.org/10.15407/biotech18.02.106

performing partial hepatectomy in cases of tumor formations, parasitic or non-parasitic cysts, abscesses, as well as toxic injuries, including those caused by medicinal xenobiotics [3]. As is known, metabolic reorganization that promotes the regression of liver cell damage is inextricably linked to meeting the increased demands for macronutrient substrates for the endergonic reactions involved in the hepatoregeneration process [4]. The key components of the energy supply system are adenyl nucleotides, whose role lies not only in coupling the processes of energy generation and utilization but also in regulating metabolic (as cofactors and allosteric regulators) and signaling pathways [5, 6]. The work aimed to assess the content of adenyl nucleotides (ATP, ADP, AMP) and Atkinson's adenylate energy charge in the mitochondrial fraction of rat liver with acetaminophen-induced toxic injury following partial hepatectomy.

Methods. Experiments were conducted on white non-linear rats of reproductive age (140–150 days) weighing 130–150 g. The modeling of acute toxic injury induced by acetaminophen was carried out through its intragastric administration using a gastric probe at a dose of 1.25 g/kg for two days in a 2% starch suspension [7]. A partial hepatectomy was performed according to the Mitchell and Willenbring method [8]. The study model involved dividing animals into two groups: control rats that underwent partial resection of 2/3 of liver tissue (C/PH) and rats that underwent partial hepatectomy after acetaminophen-induced injury (TI/PH). Animals were removed from the experiment at 0 (preoperative period), 24, 48, 72, and 168 hours after partial hepatectomy. Quantification of ATP, ADP, and AMP content in the liver mitochondrial fraction was accomplished by thin-layer chromatography using ALUGRAM Xtra SIL G/UV254 plates (Macherey-Nagel, Germany) [9]. The adenylate energy charge (AEC) was calculated according to the formula by Atkinson: AEC = (ATP + 0.5ADP) / (ATP + ADP + AMP). Statistical analysis was carried out using two-way analysis of variance (Two-way ANOVA) with Tukey's post hoc test in GraphPad Prism version 8.0.1. The results are presented as mean ±SEM; statistical significance was established at $P < 0.05$.

Results and Discussion. Studies have shown that in the mitochondrial fraction of the liver from control rats after partial hepatectomy (C/PH), ATP content decreased during the 48-hour regeneration period (24 h — by 29%; 48 h — by 24%, $P < 0,05$) compared to preoperative values at 0 h (intact control) (Fig. *A*). Instead, ADP and AMP levels in the liver mitochondria of animals in this group exceeded the 0 h values throughout the 48 hours (ADP: 24 h — by 40%, $P < 0,01$; 48 h — by 54%, $P < 0,001$; AMP: 24 h — by 48%, $P < 0,05$; 48 h — by 53%, $P < 0,01$) (Fig. *B* and *C*). Therefore, the multidirectional changes in ATP, ADP, and AMP content established in our study lead to a decrease in AEC only at the initial stages of liver regeneration in animals of the C/PH group (from 0.69±0.01 to 0.51±0.02). Analysis of scientific publications indicates no dysfunction of respiratory and phosphorylation activity in mitochondria following liver tissue resection [10, 11]. Accordingly, the obtained results can be considered adaptive changes associated with enhanced ATP release from mitochondria to meet the energy demands of the processes of structural component synthesis of liver cells. This is clearly reflected in the catalytic activity of DNA replication enzymes that utilize energy from ATP hydrolysis and of protein synthesis enzymes, particularly at the stage of aminoacyl-tRNA formation following partial hepatectomy. In addition, it is known that with an increase in the energy needs of cells (metabolic challenge), there is a compensatory increase in the concentration of ADP [12]. One of the reasons for the increased ADP content in mitochondria may be the intensification of ATP transfer from the mitochondrial matrix to the intermembrane space and, consequently, into the cytosol, which occurs when ADP is simultaneously transported in the opposite direction, mediated by the ADP/ATP antiporter.

Regarding the animals of the TI/PH group, a decrease in ATP content in liver mitochondria occurred during the 72 h of the regeneration process compared to the preoperative values in rats of the toxic injury group at 0 h (24 h — by 34%, $P < 0,05$; 48 h — by 31%, $P < 0,05$; 72 h — by 44%, $P < 0,01$) (Fig. *A*). Such changes were observed against the background of an increase in ADP levels during the 72 hours of liver parenchyma recovery, with a maximum at 48 h (by 60%, $P < 0,001$) and an elevation in AMP levels throughout the entire experimental period (168 h), with maximum values at 72 h (by 54%, $P < 0,001$) (Fig. *B* and *C*). The deepening of disturbances in the adenyl nucleotide system, compared to rats of the C/PH group, is confirmed by the most pronounced decrease in AEC at 72 h of liver regeneration (from 0.61±0.02 to 0.36±0.02). As is known, the toxic metabolite of acetaminophen, N-acetyl-p-benzoquinoneimine, forms adducts with the α-subunit of ATP synthase, with a decrease in its activity [13]. Therefore, the registered changes likely indicate suppression of the resynthesis processes of the main macroregion compound against the background of the

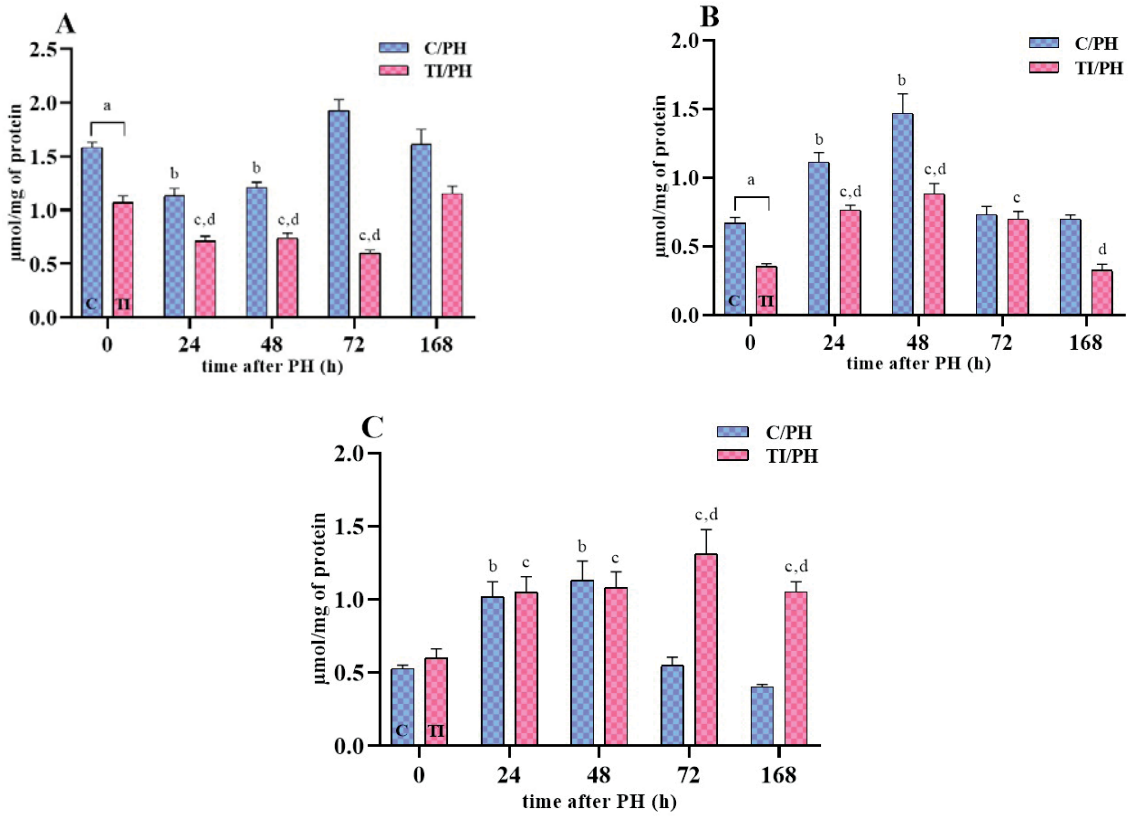

Figure. **ATP (*A*), ADP (*B*), and AMP (*C*) content in the mitochondrial fraction of the liver of rats with acetaminophen-induced toxic injury after partial hepatectomy:**
a, b, c, d — values indicated by these letter indices differ statistically significantly; *a* — statistically significant difference between the TI group and the control group (C) at 0 h; *b* — statistically significant difference of the C/PH groups at each time point compared to the C group at 0 h; *c* — statistically significant difference of the TI/PH groups at each time point compared to the TI group at 0 h; *d* — statistically significant difference between the TI/PH and C/PH groups at the corresponding time point (e.g., 24 h vs 24 h, etc.)

dominance of ATP and ADP dephosphorylation under conditions of increased energy demands caused by partial hepatectomy following acetaminophen-induced injury.

Conclusions. Thus, liver regeneration in rats after partial hepatectomy under conditions of acetaminophen-induced toxic injury is accompanied by a quantitative redistribution of adenyl nucleotides in mitochondria: a maximal increase in AMP content occurs alongside a simultaneous decrease in ATP levels at the terminal stage (72 h) of organ recovery. Such changes cause the most substantial reduction in Atkinson's adenylate energy charge, which can be regarded as a critical stage in the dysfunction of the energy supply system under these experimental conditions. The results obtained may be helpful in creating an algorithm of corrective schemes for restoring liver energy resources in the postoperative period against the background of drug-induced toxic injuries, which is essential under functional load during regeneration.

Authors' contribution

MSU — experimental work, data analysis, and interpretation, manuscript writing; HPK — experiment planning, result generalization, critical editing of the manuscript; IMN — experiment planning, result analysis, manuscript writing.

Funding source

The work was conducted within the framework of the departmental theme "Biochemical mechanisms of integral regulation of nutrient-metabolic status of living organisms and complex biotechnological approaches to their correction" (2021–2025, State registration number 0120U105710).

REFERENCES

1. Kiseleva, Y. V., Antonyan, S. Z., Zharikova, T. S., Tupikin, K. A., Kalinin, D. V., Zharikov, Y. O. (2021). Molecular pathways of liver regeneration: A comprehensive review. *World journal of hepatology*, 13 (3), 270–290. https://doi.org/10.4254/wjh.v13.i3.270
2. Bhushan, B., Apte, U. (2019). Liver Regeneration after Acetaminophen Hepatotoxicity: Mechanisms and Therapeutic Opportunities. *Am. J. Pathol.*, 189 (4), 719–729. https://doi.org/10.1016/j.ajpath.2018.12.006
3. Sun, R., Zhao, H., Huang, S., Zhang, R., Lu, Z., Li, S., Wang, G., Aa, J., Xie, Y. (2021). Prediction of Liver Weight Recovery by an Integrated Metabolomics and Machine Learning Approach After 2/3 Partial Hepatectomy. *Front. Pharmacol.*, (12), 760474. https://doi.org/10.3389/fphar.2021.760474
4. Huang, J, Rudnick, D. A. (2014). Elucidating the metabolic regulation of liver regeneration. *Am. J. Pathol.*, 184 (2). 309–321. https://doi.org/10.1016/j.ajpath.2013.04.034
5. De la Fuente, I. M., Cortés, J. M., Valero, E., Desroches, M., Rodrigues, S., Malaina, I., Martínez, L. (2014). On the dynamics of the adenylate energy system: homeorhesis vs homeostasis. *PloS One*, 9(10), e108676. https://doi.org/10.1371/journal.pone.0108676
6. Camici, M., Allegrini, S., Tozzi, M. G.(2018). Interplay between adenylate metabolizing enzymes and AMP-activated protein kinase. *FEBS J.*, 285 (18), 3337–3352. https://doi.org/10.1111/febs.14508
7. Kopylchuk, H. P., Nykolaichuk, I. M., Ursatyi, M. S. (2024). Age-dependence of biochemical manifestations of hepatotoxicinjury in rat exposed to xenobiotics of various genesis. *Biological systems*, 16(1), 3–13. https://doi.org/10.31861/biosystems2024.01.003
8. Kopylchuk, H., Voloshchuk, O. (2024). Adenine nucleotide content and activity of AMP catabolism enzymes in the kidney of rats fed on diets with different protein and sucrose content. *Studia Biologica*, 18(3), 57–68. https://doi.org/10.30970/sbi.1803.783
9. Mitchell, C., Willenbring, H. (2008). A reproducible and well-tolerated method for 2/3 partial hepatectomy in mice. *Nature protocols*, 3(7), 1167–1170. https://doi.org/10.1038/nprot.2008.80
10. Crumm, S., Cofan, M., Juskeviciute, E., Hoek, J. B.(2008). Adenine nucleotide changes in the remnant liver: An early signal for regeneration after partial hepatectomy. *Hepatology*, 48(3), 898–908. https://doi.org/10.1002/hep.22421
11. Kataoka, M., Tanaka, A., Ikai, I., Yamaoka, Y., Ozawa, K., Chance, B. (1993). Kinetic analysis of ATP-synthetase and ATPase in regenerating rabbit liver. *Eur. Surg. Res.*, 25(2), 91–97. https://doi.org/10.1159/000129262
12. Wilson, D. F. (2017). Oxidative phosphorylation: regulation and role in cellular and tissue metabolism. *J. Physiol.*, 595 (23), 7023–7038. https://doi.org/10.1113/JP273839
13. Ramachandran, A., Jaeschke, H. (2019). Acetaminophen hepatotoxicity: A mitochondrial perspective. *Adv. Pharmacol.*, 85. 195–219. https://doi.org/10.1016/bs.apha.2019.01.007

UDC 615.262.1:615.454.1].07:616.147.17-007.64-085
https://doi.org/10.15407/biotech18.02.110

EFFICACY OF COMBINED RECTAL CREAM "DILATIL" (DILTIAZEM/LIDOCAINE/METHYL-URACIL) IN PRE-CLINICAL STUDY ON A MODEL OF ACUTE COMPLICATED ANAL FISSURE

G.V. ZAYCHENKO, M.P. TYMOFIEIEV

Pharmacology department of the Bogomolets National Medical University, Kyiv

E-mail: maksym.tymofieiev90@gmail.com

Received 2025/03/04
Revised 2025/03/21
Accepted 2025/04/30

Aim. To assess efficacy of a new rectal cream "Dilatil" (diltiazem/lidocaine/methyluracil) (D) in pre-clinical study on a model of acute complicated anal fissure (ACAF).

Materials and Methods. Animal model of anal fissure, macroscopic assessment, enzyme-linked immunosorbent assay, statistical Student's and Wilcoxon's tests.

Results. At the end of the study, in the D group, the severity of the pathological process was statistically lower than in the Control pathology (CP) and N groups. Levels of IL-6, IL-10, and TNF- in the homogenate of anodermal tissue (HAT) in the D group were significantly lower compared to CP. The level of IL-6 was significantly lower in the D group compared to the N group.

Conclusions. Better efficacy of D vs N was observed in a pre-clinical study, which was also confirmed by the level of IL-10 in HAT tissue at the end of the experiment.

Keywords: rectal cream, anal fissure, Dilatil, Nifecain, macroscopic assessment, enzyme-linked immunosorbent assay, IL-10, IL-6, HIF-1α, TNF-α, calcium channel blockers, diltiazem.

Anal fissure (AF) affects a significant percentage (2%) of the adult population. Among proctological diseases, hemorrhoids and anal fissures rank first and third in frequency, respectively1. According to 2022 clinical guidelines for the treatment of anal fissures by the American Society of Colon and Rectal Surgeons, conservative treatment of acute anal fissures is safe and, as a rule, should be the first-line treatment (strong recommendation based on moderate-quality evidence, grade 1B) 2. However, conservative treatment is effective in approximately half of patients with anal fissures 3. Compared to topical nitrates, the use of calcium channel blockers for chronic anal fissures has similar effectiveness but a better safety profile (lower frequency and severity of side effects), and they can be used as first-line treatments (strong recommendation based on moderate-quality evidence, grade 1B)2. According to the current understanding of pathogenesis, pain is caused by spasms of the internal anal sphincter, which leads to impaired blood circulation in the area of the anal fissure (AF), hypoxia, and inflammation, which contribute to tissue damage on one hand and delay healing, thus causing pain again, leading to a "vicious cycle." 4,5,6 As of now, there are no soft medicinal forms in Ukraine that can comprehensively affect the key links in the pathogenesis of anal fissures — sphincter spasm, inflammation, tissue damage, and quickly relieve pain, the most unpleasant symptom containing calcium channel blockers. Therefore, the development of a new rectal cream capable of achieving this is both relevant and promising.

Citation: Zaychenko, G. V., Tymofieiev, M. P. (2025). Efficacy of combined rectal cream "dilatil" (diltiazem/lidocaine/methyl-uracil) in pre-clinical study on a model of acute complicated anal fissure. *Biotechnologia Acta*, 18(2), 110–113. https://doi.org/10.15407/biotech18.02.110

The work was aimed at assessing the efficacy of rectal cream D in a pre-clinical study on a model of ACAF.

Methods. The total macroscopic pathology process severity was assessed on a scale from 0 to 10 points based on the sum of the 5 following parameters: severity of edema, hyperemia, local bleeding, purulent-necrotic processes, and anatomical defect (each parameter was assessed on a scale from 0 to 2 points). The protein concentration of IL-10, IL-6, HIF-1α, and TNF-α in HAT was analyzed in the homogenate of anodermal tissue using the enzyme-linked immunosorbent assay (ELISA) method. The study was conducted on 26 non-linear male white rats, weighing 200–240 g, using a model of ACAF. The animals were divided into four experimental groups: Intact Control (IC) ($n = 6$). Control Pathology (CP) ($n = 8$). Treatment with D ($n = 6$) — rats treated with D were administered into the anal canal using an insulin syringe with a blunt needle (0.3 ml, once daily throughout the treatment period). Treatment with N ($n = 6$) — rats treated with N administered into the anal canal using an insulin syringe with a blunt needle (0.3 ml, once daily throughout the treatment period). Pathology modeling lasted 4 days. The further treatment phase lasted 12 days. The results were analyzed using parametric (Student's t-test) and non-parametric (Wilcoxon test) methods. A significance level of $P < 0.05$ was considered statistically significant.

Results and Discussion. At the end of the study in the D group, the severity of the pathological process was statistically lower than in the Control pathology (CP) and N groups (Fig. 1).

Levels of IL-6 (Fig. 2, $P = 0.03$), IL-10 (Fig. 3, $P = 0.01$), and TNF-α (Fig. 4, $P = 0.02$) in the homogenate of endodermal tissue (HAT) in the D group were significantly lower compared to CP.

The level of IL-6 ($P = 0.001$) was significantly lower in the D group compared to N (Fig. 2). A trend toward a lower level of hypoxia factor HIF-1α (Fig. 5, $P = 0.065$) was observed in the D group compared to CP.

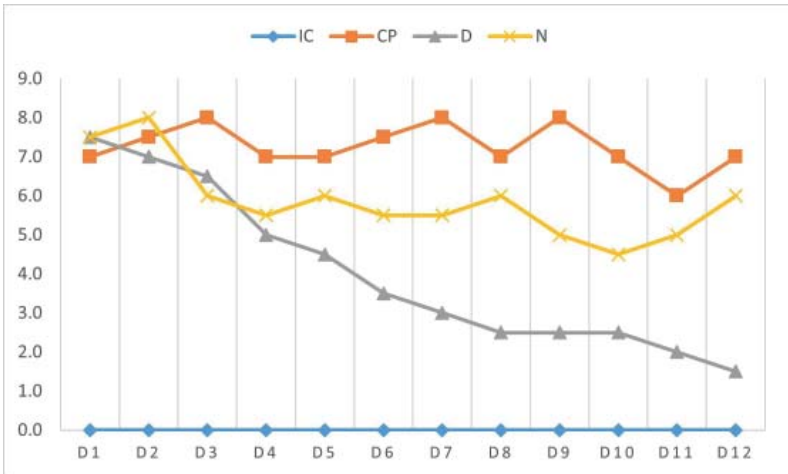

Fig. 1. **Macroscopic assessment of pathology process severity**

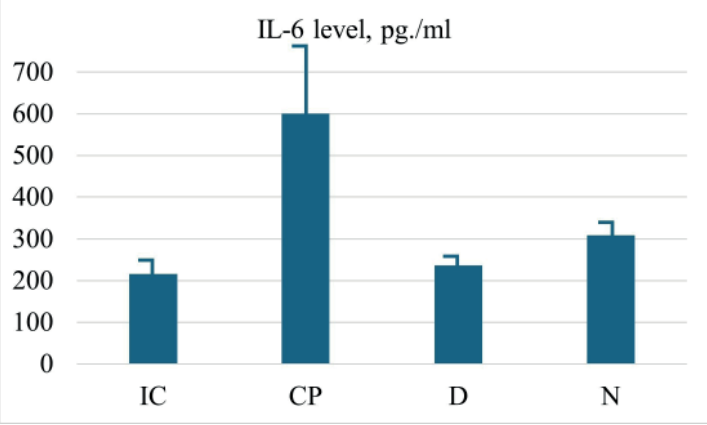

Fig. 2. **IL-6 levels in HAT after 12 days of treatment (pg/ml)**
* — difference between groups is statistically significant ($P < 0.05$)

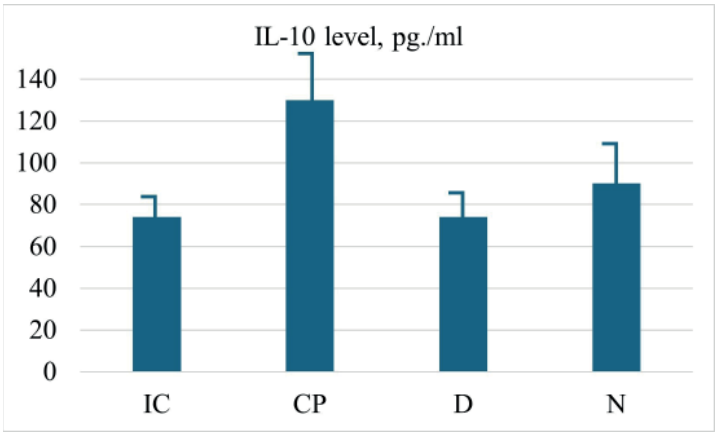

Fig. 3. **IL-10 levels in HAT after 12 days of treatment (pg/ml)**
* — difference between groups is statistically significant (P <0.05)

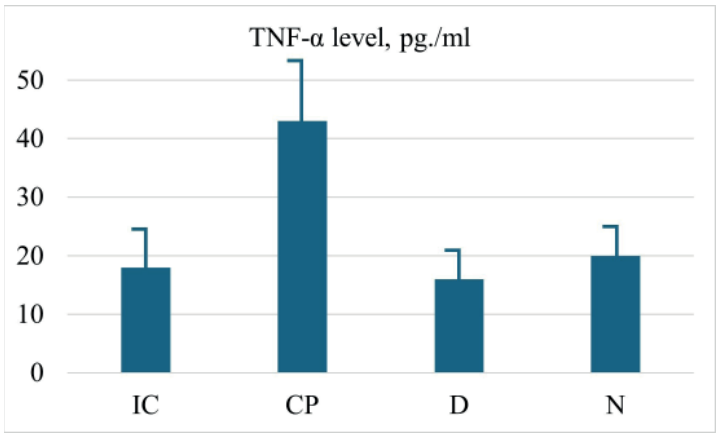

Fig. 4. **TNF-α levels in HAT after 12 days of treatment (pg/ml)**
* — difference between groups is statistically significant (P <0.05)

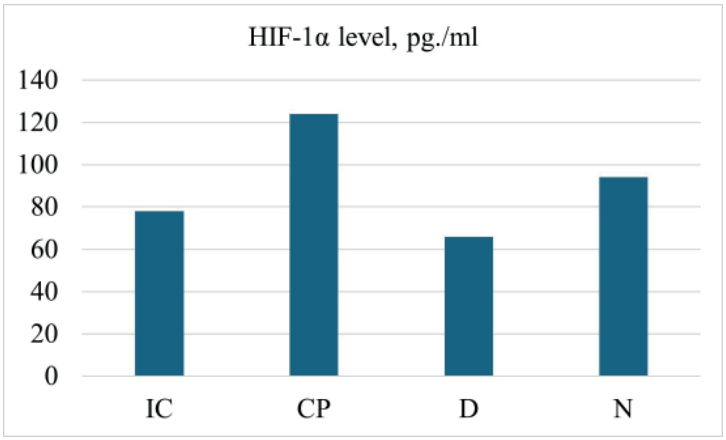

Fig. 5. **HIF-1α levels in HAT after 12 days of treatment (pg/ml)**

Study results indicate a higher therapeutic efficacy of the investigational medical product Dilatil than the comparison Nifecain, which is probably related to Dilatil's complex composition. The components of Dilatil affect the main pathogenetic mechanisms of AF. Methyl-uracil provides an anti-inflammatory effect, stimulates reparation; diltiazem (calcium channel blocker, benzothiazepine derivative) reduces spasm of the anal sphincter, provides anti-inflammatory effect; lidocaine has